2012

Characterizing Dissolved Organic Matter and Cu2+, Zn2+, Ni2+, and Pb2+ Binding in Salt Water and Implications for Toxicity

Rachael L. Diamond
diam7900@mylaurier.ca

Characterizing Dissolved Organic Matter and Cu^{2+}, Zn^{2+}, Ni^{2+}, and Pb^{2+} Binding in Salt Water and Implications for Toxicity

Rachael L. Diamond

Bachelors of Science, Honours Chemistry, Wilfrid Laurier University, 2009

THESIS

Submitted to the Department of Chemistry

in partial fulfillment of the requirements for

Master of Science

Wilfrid Laurier University

© Rachael L. Diamond 2012

Abstract

The binding of metal to dissolved organic matter in aquatic environments is important in controlling the bioavailability and potential toxicity of metals such as Zn^{2+}, Pb^{2+}, Ni^{2+} and Cu^{2+}. The purpose of this research is to: (i) quantify binding capacity to different sources of marine organic matter at environmentally relevant concentrations; (ii) test fluorescence quenching and voltammetric method for use in seawater conditions and; (iii) compare predicted speciation parameters with toxicological observations in the same samples.

Information regarding the solubility of copper and copper compounds is important for risk assessment and can be used to set site specific criteria. Transformation/dissolution tests were completed to determine solubility of copper and cuprous oxide powder. The measured solution copper concentration values were compared to a copper solubility model which isolated the precipitate formation tenorite, malachite and copper hydroxide to be able to identify which precipitate would best describe the results obtained from the experiment. Tenorite underestimated solubility at 22 ppb while malachite and copper hydroxide overestimated copper solubility, 150 ppb and 600 ppb respectively. The experimental data point, 47.9 ppb was placed between the tenorite precipitation model and the malachite precipitation model still leaving questions about how to optimize the modeling of copper solubility.

Fluorescence spectroscopy was used to determine stability of natural organic matter (NOM) during storage and variability in the molecular nature of the NOM from different sources. The molecular differences in NOM will allow for the determination of

a source dependence on toxicity and whether or not it should be a factor considered in the BLM. Fluorescence Index (FI) was determined for all the NOM samples and had a range of 1.12 to 1.54 indicating that the fulvic acid within the samples was terrestrially derived. PARAFAC was used to determine the relative concentration of three components within the organic material determined to be tryptophan-like, humic and fulvic-like and tyrosine-like material. The comparison of the relative percents of each of these components showed a significant increase within the tryptophan-like material from 10% to 72% and a decrease in humic and fulvic-like material from 85% to 16% after storage, for a specific sample. The NOM did not remain stable and the quality of the sample changed during the storage procedure. This potentially was caused by the fractionation method used to collect the NOM samples.

Copper fluorescence quenching has been validated for marine systems. Experimental results agree with a tryptophan model and copper ion selective electrode results. The fluorescence quenching model did not agree with tryptophan model for lead, nickel and zinc and disagreed with lead toxicity data. The interaction of lead with a dissolved organic carbon (DOC) concentration of 2 mg C/L provided an EC_{50} of 738 (680-796) nM while a concentration of 12 mg C/L had an EC_{50} of 757 (680-830) nM for early lifestage development tests with blue mussel larvae. Binding capacity determined by fluorescence quenching suggested a dose dependence. Voltammetric methods demonstrated that a 2 and 12 mg C/L had similar binding capacity with an increase in by binding capacity by a factor of 1.1 consistent with the EC_{50} data. Voltammetric methods agree with lead toxicity data. Information on lack of dose dependence in seawater can be

implemented in a marine Biotic ligand model (BLM). More work is necessary to determine exact relationships.

Knowledge regarding salinity dependence and source dependence are important to implement a BLM. Binding capacities were determined for two different organic matter concentrations and three different salinities. Four different NOM sources were tested Nordic Reservoir, Pachena, Inshore Brazil and Bamfield. No significant differences were found within the NOM sources comparing salinities and concentrations. A statistically significant difference was found when comparing the four different sources of NOM to each other. The NOM with a lower humic and fulvic acid-like fraction was found to be significantly different from the NOM with a higher concentration of humic and fulvic-acid like component. The percent of fluorophore fraction was compared to the binding capacity to determine any potential trends. A strong trend was found for the humic and fulvic acid like fraction (R^2=0.9327), a slight trend for the tryptophan like fraction (R^2=0.7811) and no trend for the tyrosine like fraction (R^2=0.4436).

gone above and beyond in every aspect of our friendship. I am super lucky to have a best friend like you. Miss Amanda Johnston, whose surprise notes made the bad days so much better and always kept me smiling.

I would like to provide an additional thank you to Dr. Jelokhani and his lab for allowing ample access and use of the analytical balance. A final thank you goes to the funders: ICA (International Copper Association), CDA (Copper Development Association), ILZRO (International Lead and Zinc Research Organization), IZA (International Zinc Association), Teck Resources Inc., Vale Canada, Xstrata Zinc, NiPERA (Nickel Producers Environmental Research Association) and NSERC who allow for this research to be possible.

Table of Contents

List of Figures

List of Tables

List of Abbreviations and Symbols

NOM	**Natural Organic Matter**
POM	**Particulate Organic Matter**
DOM	**Dissolved Organic Matter**
DOC	**Dissolved Organic Carbon**
BLM	**Biotic Ligand Model**
EC$_{50}$	**Median Effective Concentration (required to induce a 50% effect)**
ASV	**Anodic Stripping Voltammetry**
EEM	**Excitation-Emission Matrix**
PARAFAC	**Parallel Factor Analysis**
L$_T$	**Binding Capacity**
logK	**Equilibrium Constant**
NIST Technology	**National Institute of Standards and**
SIMPLISMA	**SIMPLe-to-use Interactive Self-modeling Mixture Analysis**
SWASV	**Square Wave Anodic Stripping Voltammetry**
FI	**Fluorescence Index**
CEQG	**Canadian Environmental Quality Guidelines**
OECD	**Organisation for Economic Co-operation and Development**
SSIMs	**Sparingly soluble inorganic metal compounds**
PES	**Polyethersulfone**

ISE   **Ion selective electrode**

SI   **Saturation Index**

Chapter 1: Introduction and Background

Canada has the longest marine coastline of any country, the second largest continental shelf in the world, and a total offshore marine area equal to 40 percent of the Canadian land mass (Government of Canada, 2003). Meanwhile in the US, coastal areas are home to a wealth of natural and economic resources and are the most developed areas in the nation. The coastal region comprising 17 percent of the contiguous U.S. land area is home to more than half of the nation's population (DeWailley and Knap, 2006). Over 53% of the USA population is living along the coastal region (NOAA, 2004). Globally, over one billion people rely on fish and other seafood as their main source of animal proteins. Due to this high demand on seafood, there is an increasing alarm that seafood from the oceans is becoming contaminated with man-made pollutants.

There is a growing concern about pollution of the ocean from anthropogenic wastes including metals such as copper, lead, nickel and zinc. Trace amounts of certain metals, including copper and zinc, are present as natural components of the environment and at low concentrations are essential for life. Unfortunately, due to anthropogenic inputs, these trace metal concentrations are increasing and can potentially result in toxicity to organisms. This results in a need to monitor the levels and effects of these metals in marine systems and research toward appropriate regulatory criteria. For this research, four specific divalent metals are being investigated (Zn^{2+}, Pb^{2+}, Cu^{2+} and Ni^{2+}) in terms of their chemistry in saltwater systems and their potential for toxicity. Previous research has shown that natural organic matter (NOM) can potentially be protective due to its ability to reduce the bioavailability of metals. This study will focus on metal

speciation of zinc, lead and copper within salt water in the presence of NOM from variable sources.

1.1 Metals in the Environment

Copper, lead and nickel are among the metals of major environmental concern and are priority contaminants in water policy regulations (Wright and Welbourn, 2002; European Commission, 2001). This results in a need to monitor levels and effects of these metals in marine systems and research toward appropriate regulatory criteria.

1.1.1 Copper in Saltwater Systems

Copper is an essential trace nutrient for plants and animals and at low concentrations it is essential for life. Sources of mobile copper in the environment are due to waste disposal, agriculture and extraction operations including mining and smelting (Wright and Welbourn, 2002). Copper is deemed to be one of the most toxic metals to aquatic organisms (Solomon, 2009). The divalent form of copper is believed to be the most toxic form but copper hydroxide complexes ($CuOH^-$ and $Cu(OH)_2$) have demonstrated to be bioavailable and exert toxicity (Chakoumakos et al., 1979; Erickson et al., 1996; Paquin et al., 2002).

Copper is present at levels of 0.2 to 30ppb in freshwater (USEPA, 2007) and 0.001 to 0.1 ppb in open ocean (Bruland, 1980; Coale and Bruland, 1988; Sherrell and Boyle, 1992). In aquatic systems, copper can interact with the gills of organisms interfering with sodium channels resulting in electrolyte imbalances, ionoregulatory failure and death (Paquin et al., 2002; Grosell and Wood, 2002). The EC_{50} for copper in

Mytilus trossolus has been determined to be 9.6 µg/L and in the presence of 20 mg/L natural organic matter the EC_{50} increased to 39.0 µg/L (Nadella et al., 2009). EC_{50} is the concentration needed to affect 50% of the organisms. Thus, copper bioavailability is not dependent on total copper because organic matter is protective.

1.1.2 Lead in Saltwater Systems

Lead is a nonessential metal that is toxic at low doses in aquatic systems. In oceans, lead enters through surface water and decreases in concentration with depth due to settling of lead adhered particles and complexing with reduced species near the sediment. It is estimated that 50-70% of lead in the open ocean is organically bound, with inorganic compounds accounting for the vast majority of the rest (Reuer and Weiss, 2002).

In aquatic systems the majority of lead can be attributed to atmospheric deposition and combustion of fossil fuels. Total anthropogenic input of lead to aquatic ecosystems is estimated at 138000 tonnes/year (Nriagu and Pacyna, 1988).

Organisms including algae, invertebrates, fish and amphibians that suffer from lead toxicity can have side effects including muscular and neurological degeneration and destruction, growth inhibition, reproductive problems and mortality (Eisler, 1988). Within organisms, divalent lead has the ability to imitate calcium and interfere with calcium dependent physiological processes (Rogers and Wood, 2004). The EC_{50} for lead in seawater for embryo tests with *Mytilus trossolus* has been determined to be 99 µg/L (Nadella et al., 2009).

1.1.3 Zinc in Saltwater Systems

Zinc is essential to all cells in all known organisms. Zinc concentrations in aquatic systems vary greatly. In freshwater systems, zinc can range from 0.02 ppb to 1000 ppb near areas of mining (Eisler, 1993; Luoma and Rainbow, 2008). However, total zinc rarely exceeds 50 ppb in freshwater (Eisler, 1993; Bodar, 2005; Luoma and Rainbow, 2008). In open ocean the total zinc range is 1 to 60 ng/L (Eisler, 1993; Ellwood, 2004; Luoma and Rainbow, 2008). Combined global anthropogenic input of zinc has been estimated to be 226000 tonnes/year (Nriagu and Pacyna, 1988).

Zinc is required for the catalytic activity of nearly 100 enzymes and plays a role in protein synthesis, DNA synthesis, reproduction and cell division (Sandstead, 1994). Trace amounts of zinc supports normal growth and development for organisms. Zinc toxicity to organisms in aquatic systems is very similar to lead toxicity. Both work to imitate calcium and disrupt calcium dependent processes and offset the acid base balance within the organism (Spry and Wood, 1985). The EC_{50} for zinc in *Mytilus trossolus* has been determined to be 67 µg/L (Nadella et al., Appendix G: MS draft). Natural zinc in the environment is mobilized due to weathering of rock and soils. Zinc also enters into the environment through anthropogenic activities such as mining.

1.1.4 Nickel in Saltwater Systems

Nickel essentiality in animals has been difficult to establish because a nickel-containing biomolecule has not been isolated from tissues. Nickel essentiality in aquatic systems is circumstantial because nickel remains constant despite wide fluctuations in

environment nickel concentrations (Tjalve, 1988; Ray, 1990). In unpolluted freshwater, nickel concentration ranges from 0.1 to 10 ppb (Chau and Kulikovsky-Cordeiro, 1995) and 0.2 to 0.7 ppb in open oceans.

Nickel toxicity is associated with nickel-mediated oxidative damage to DNA and proteins and to inhibition of cellular antioxidant defenses (Rodriguez et al., 1996). The EC_{50} for nickel in *Mytilus trossolus* has been determined to be 150 µg/L (Nadella et al., 2009). Nickel enters the environment in much the same way as copper, zinc and lead through natural sources such as soil dust, forest fires and vegetation. However, 84% of atmospheric nickel is a result of anthropogenic effects including mining, smelting and refining activities (Eisler, 1998).

There has been very little research done on nickel in comparison to the other three metals. This is mainly due to nickel having a low gill binding affinity in comparison to the other metals (Niyogi and Wood, 2004). Nickel is also less toxic than copper and lead but is said to be equally as toxic as zinc (Pickering and Henderson, 1966).

1.2 Natural Organic Matter

Natural organic matter (NOM) contains many potential binding sites for available metals in marine systems. NOM is mainly comprised of the humic substances, humic acid and/or fulvic acid, together with carbohydrates, proteins and lipids (Thurman 1985). Fulvic and humic acids have been found to be most abundant in natural organic matter (Ericksen et al., 2001). Humic substances account for 5-25% of dissolved organic carbon (DOC) in the ocean surface (Benner, 2002). Meanwhile, fulvic acids are much more

abundant than dissolved humic substances in the water column (McKnight and Aiken, 1998). NOM is often divided into humin, humic acid and fulvic acids. These fractions are defined strictly on their solubility in either acid or alkali. Humin is insoluble in water and in alkali under any pH conditions (Ericksen et al., 2001). Humic acids are not soluble in water under acidic conditions but are soluble at higher pH values. Fulvic acids are soluble in water under all pH conditions (Thurman, 1985).

Section 4.1 in Chapter 4 provides greater detail on terrigenous, autochtonous and sewage derived NOM.

NOM has a high content of aromatic rings, carboxylic and phenolic groups which are mainly responsible for the metal complexing (Perdue, 1998; Tipping, 2002). Metals can bind to many functional groups present within NOM , with metal binding functional groups such as carboxyl (M-CO_2H), amino (M-NHR, [M-NH_2R]$^+$, phenolic (M-OAr), metal sulfides or thiols (M-SH) (Smith, 2002). NOM also has a polyelectrolyte nature. Polyelectrolytes are polymers carrying either positively or negatively charged ionizable groups. The properties of these polymers in solutions and at charged surfaces depend on the fraction of dissociated ionic groups, solvent quality for polymer backbone, solution dielectric constant, salt concentration, and polymer–substrate interactions. Its polyelectrolytic nature is dependent on size, carboxylic content and total acidity. Humic substances present within NOM tend to have a high negative charge at their outer surface (Buffle, 1984).

The colour of NOM is influenced by the molecular nature of the components within the sample. For example, humic acids are darkly coloured while fulvic acids are

light in colour (Gheorghiu et al., 2010). The specific absorption coefficient of the DOC at 340nm (SEC340) has been shown to be a simple effective predictor of protectivity. Terrigenous NOM with a dark colour and higher SAC340 tend to have a greater aromaticity and has the ability to bind metals with greater strength to the functional groups of the aromatic ring than the light colour autochtonous NOM with lower SAC340 values. It is because of this that it is generally assumed that terrigenous NOM will have a higher binding capacity and has a greater ability to reduce metal bioavailability (Gheorghiu et al., 2010).

NOM contains both dissolved organic matter (DOM) and particulate organic matter. Less than 5% of the organic matter in open ocean is particulate organic matter (POM) leaving the majority as dissolved organic matter (Benner, 1998). DOM is defined as the fraction of NOM that passes through a 0.45 μm filter. DOM concentration is measured based on its carbon content, dissolved organic carbon (DOC). In open ocean systems, organic matter content varies between 0.3 and 3 mg/L of carbon (Mota and Correia dos Santos, 1995).

Further information regarding marine NOM and affects of salinity or salt content can be found in section 5.1.

1.3 Biotic Ligand Model

For fresh water, the bioavailability of metals can be predicted based on bulk chemistry of water samples using the biotic ligand model (BLM). The BLM is based on equilibrium calculations of metal speciation and has a numerical scheme to predict toxic

metal concentrations (Santore et al., 2001). In addition to calculating chemical speciation, the BLM can also be used to predict the concentration of metal that would result in acute toxicity within a given aquatic system. The BLM is used to establish site specific criteria for a given location depending on its water chemistry parameters including temperature, pH, dissolved organic carbon, calcium, magnesium, sodium, sulfate, chloride, alkalinity and sulfide (Santore et al., 2001). The ability of the BLM to account for site-specific variations in the bioavailability and toxicity of copper has also lead the US EPA to develop a BLM-based approach for calculating the water quality criteria for copper (USEPA, 2007).

A diagram of the BLM can be found in Figure 1.1. The model assumes toxicity is proportional to the accumulation of the metal at the biotic ligand (the site of action). The bioavailable metal competes with cations (sodium, calcium, etc) for the active sites at the biotic ligand. Simultaneously, organic matter and inorganic matter can complex with the bioavailable metal decreasing its ability to accumulate at the biotic ligand. There are factors within marine system that can modify the bioavailability and potential toxicity of lead, zinc, nickel and copper to organisms. Some of these factors are pH, salinity, alkalinity, water hardness and NOM (Santore et al., 2001). Metal toxicity can be hindered by pH due to speciation of the metal.

The ocean has a pH of approximately 8, while seawater has a pH range of 7.5 to 8.4. At low pH, free metal tends to be most bioavailable and very toxic; however as pH increases the free metal can bind available anions or NOM in solution and decrease toxicity. Alkalinity, salinity and water hardness can hinder toxicity because the ions

present can out-compete the toxic metal for binding sites on the organism resulting in the decrease of toxic effects from the metal to this organism. Potentially, binding Cu^{2+}, Pb^{2+}, Ni^{2+} and Zn^{2+} to NOM can reduce metal bioavailability and reduce toxic effects.
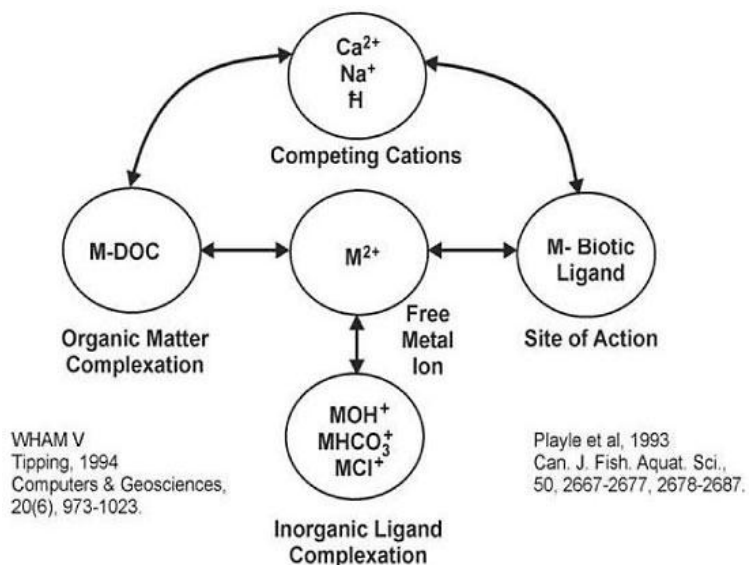
Figure 1.1: Biotic Ligand Model (Playle et al., 1993).

The BLM has been able to predict metal toxicity for a number of dissolved metals in freshwaters and has proven a very valuable asset and has been adopted by USEPA for freshwater criteria (US EPA, 2007). To date, regional risk assessments in the USA and Europe have employed BLMs for metals such as copper, nickel and zinc. The parameterization for an acute freshwater BLM for lead was recently completed (Mager et al., 2010b) and BLMs for other high-priority metals are currently in various stages of development (Wood et al., 2012). The freshwater BLM is based on a salt concentration of less than 0.05%. Meanwhile seawater has a salt concentration of 3.1 to 3.8%. The increase in salinity affects equilibrium constants and competition which are required for

an accurate prediction of bioavailability and toxicity. Due to the differences in freshwater and saltwater, there is a need for saltwater research in BLM.

1.4 Previous Research of Copper and NOM Toxicity

Depalma et al. (2011b) completed research on the molecular components of dissolved organic matter and its interaction with copper. The field based study showed that the quality or molecular composition of DOM does not appear to relate to its protectiveness in the environment (DePalma et al., 2011a; DePalma et al., 2011b). It was determined that DOC could be used as a prediction of EC_{50}. The EC_{50} equation determined by Arnold et al (2005), $EC_{50}=11.22x \ DOC^{0.6}$ was shown to be consistent, regardless of the natural organic matter quality and source. The increased amount of DOM affected protectiveness because it has an ability to act as a copper binding ligand and therefore, reduce bioavailability (Arnold et al., 2005). This has lead to the conclusion that DOC alone is sufficient to predict toxicity. These observations have lead to the expectation that the binding capacities of copper to the molecular components of the NOM will all be similar.

Nadella et al. (2009) has completed similar experiments with contradictory results. It was concluded that protective effects of dissolved organic matter did in fact vary depending on the source of natural organic matter. However, the organic matter used for these experiments was terrestrial organic matter and source dependence has been established for terrestrial organic matter (Schwartz et al., 2004).

There are numerous studies on the effects of metals in freshwater environments (Schwartz et al., 2004; De Schamphelaere et al., 2004; Glover et al., 2005), but very few available on the effects of lead, zinc and nickel with dissolved organic matter in marine systems (Franca et al., 2005; Kobayashi and Okamura, 2004; Radenac et al., 2001; Doig and Liber, 2007). In freshwater environments and the few marine papers cited above, there is evidence that NOM reduces bioavailability of the metals and ultimately decreases toxicity.

1.5 Anodic stripping voltammetry (ASV)

Anodic stripping voltammetry (ASV) is a non-destructive experimental technique that was used for this study. It is a direct method for the study of low concentration (10^{-8} to 10^{-11}M) trace metal speciation. ASV involves a deposition or pre-concentration step where the metals in solution are concentrated by plating them onto the electrode (usually a mercury drop). Initially, a purge step is applied for approximately 250 to 300 seconds to remove oxygen before the deposition step. Oxygen is electroactive and reduced in aqueous solutions which can mask signals from the metals in solution if not removed from the bulk solution (Riley and Watson, 1987). The electrode is then scanned linearly toward positive potentials so that the metals are stripped from the electrode and re-oxidized at a potential which is characteristic of each metal (Bott, 1995). For the electrical current to be generated, the bulk solution should be electrically conducting. This can be done by adding a supporting electrolyte solution, except for cases where the sample is already conducting.

Figure 1.2 shows the potential change and resultant current versus time that occurs to a sample while using ASV. In the deposition stage the ion is reduced to metal (1) that will form an amalgam with the mercury working electrode.

$$M^{n+} + ne- \rightarrow M \hspace{2cm} (1)$$

The next stage, allows for an equilibration time to let the solution rest and the metal to redistribute on the mercury drop. In the final stage, a potential scan towards more anodic values is applied, reoxidizing the metal (2) and stripping it into solution. The electron flow is detected as current and measured by the voltammeter.

$$M \rightarrow M^{n+} + ne- \hspace{2cm} (2)$$
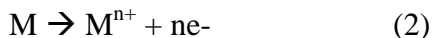
The peak potential of each metal is characteristic of the analyte and can be used to identify the metal. For example copper is found at -0.1V, lead at -0.38V and zinc at -0.98V versus a Ag/AgCl reference electrode. The height of each metal peak (i_p) is proportional to the concentration of the metal in the test solution (Scott, 1986).

Current (i)

$E_p = Cu = E^o$

$E_p = Cd = E^o$

i_p

+E

E_f

Potential

E_d $M^{n+} + ne- \rightarrow M$ $M \rightarrow M^{n+} + ne- \; M = E^o$

deposition step   linear sweep stripping

rest
period

-E
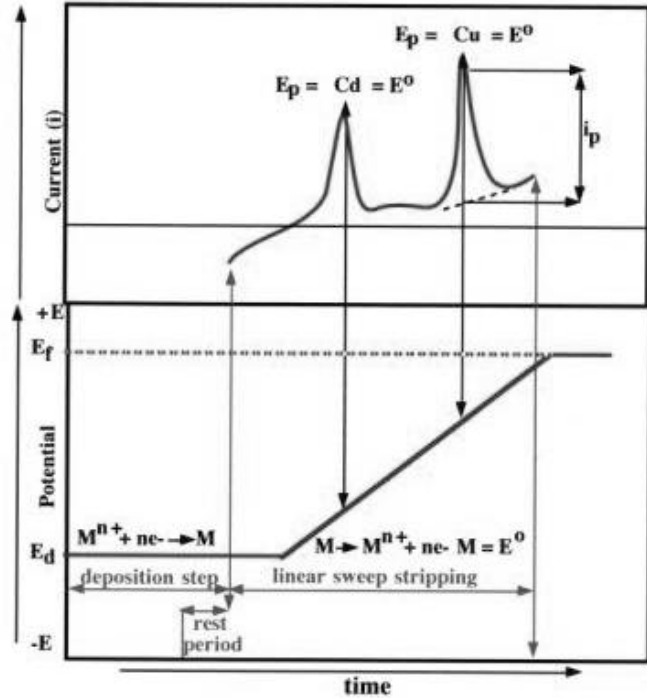
time

Figure 1.2: Linear voltage /time relationship for an ASV. Peaks are observed for the analytes, cadmium and copper (Scott, 1986).

1.5.1 ASV: Total Metal Analysis

Metal concentration for total metal analysis is generally determined by standard additions. Total metal analysis requires digestion of the samples to eliminate any strong complexes with the metal. Strong complexes are not detected by ASV because the ligand prevents the metal from accumulating at the mercury drop and being measured. NOM can be a strong ligand complex and must be UV digested to break down the NOM to allow for total analysis of the metal. The standard additions method uses several successive addition of analyte to an unknown analyte concentration. The original concentration of the analyte is found by fitting a line to the data and extrapolating to the x-intercept (Saxberg and Kowalski, 1979). A visual representation of standard additions can be

13

viewed in Figure 1.3. Spiked concentration c' can be found on the x-axis with the response signal, R on the y-axis. Linear regression to the x-axis provides c'$_o$, the initial concentration in the sample.

The reason for using the standard additions method is that the matrix may contain other components that interfere with the analyte signal causing inaccuracy in the determined concentration. The idea is to add analyte to the sample and monitor the change in instrument response. The change in instrument response between the sample and the spiked samples is assumed to be due only to change in analyte concentration.
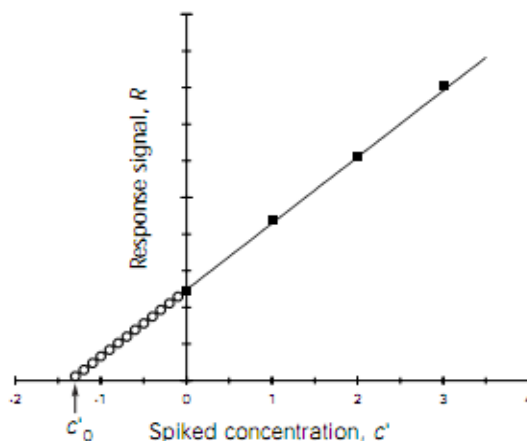
Figure 1.3: A representation of the standard additions method showing experimental data points and the extrapolated regression line, which intercepts the x-axis at –cx which equivalent to the concentration (Bruce and Gill, 1999).

1.5.2 ASV: Binding Capacity Determination

Binding capacity refers to the maximum amount of a sample that can be complexed to a molecule; in this case metal to NOM. Binding capacity is important because it allows for the determination of the potential protectivity of the NOM for specific metals. A higher binding capacity would have a higher protective effect because

14

it restricts the metals access to the biotic ligand, resulting in decreased toxicity from the metal. Rivera-Duarte et al. (2005) has related binding capacity of copper complexation with organic matter to toxicity results from three invertebrates, *Mytilus galloprovincialis* (Mediterranean mussel), *Dendraster excentricus* (sand dollar), and *Stronglyocentrotus purpuratus* (purple sea urchin). It was determined that the copper complex capacity of the San Diego Bay controlled toxicity by keeping the free divalent copper at non-toxic levels. Sanchez-Marin et al. (2011) made similar conclusions with lead and *Mytilus edulis*.

Binding capacity is usually done by the titration of the organic matter with metal additions. ASV techniques consider the metal organic matter complex to be inert and not reduced on the electrode. It is only the labile metal, free hydrated ions and mainly inorganic metal complexes that are able to be reduced at the electrode (Srna et al., 1980; Coale and Bruland, 1988). The current measurements at the peak potential versus the metal added result in a low slope for the initial data followed by steeper slope linear response at higher total metal. The small slope occurs because the NOM is binding the available metal while the steeper slope arises when the binding capacity for the NOM is exceeded. This method assumes that only inorganic complexes and free lead are detected at the electrode and strong organic matter complexes are not detected. Extrapolation of the linear data at high lead allows for estimation of the binding capacity at the x-intercept of the regression line.

1.6 Fluorescence Quenching

In natural waters dissolved organic matter fluorescence is potentially quenched in the presence of metals through formation of organo-metal complexes (Hood et al., 2005).

Quenching can occur by three different methods (Lakowicz, 2006). These methods are static, dynamic and apparent quenching. **Static quenching** results from a ground state interaction between the quencher and fluorescent species. **Dynamic quenching** occurs when the quenching species and the fluorescent compound collide, causing a non-radiative relaxation. **Apparent quenching** occurs when the quenching species absorbs the excitation or emission wavelength, making it appear as though the fluorescence has been suppressed (Lakowicz, 2006). It is assumed that the metals zinc, lead and copper will exhibit static quenching while binding to the fluorescent NOM which is tested in Chapter 4.

To assist in the visualization of the different types of quenching through electron transfer Figure 1.5 displays a Jablonski diagram illustrating ground state interaction, excited state interactions and non-radiative relaxation. The first step in Jablonski diagram is the transition of an electron from ground state to a higher energy level indicated by a straight arrow pointing up. This electron can be transferred through vibrational relaxation, internal conversion, fluorescence or phosphorescence. **Vibrational relaxation** occurs with the relaxation of the electron within vibrational levels. If vibrational energy levels strongly overlap electronic energy levels, a possibility exists that the excited electron can transition from a vibration level in one electronic state to another vibration level in a lower electronic state known as **internal conversion.** **Fluorescence** occurs with the emission of a photon. Finally, **phosphorescence** occurs after intersystem crossing of the electron from an excited singlet state to an excited triplet state and emission to the ground state.
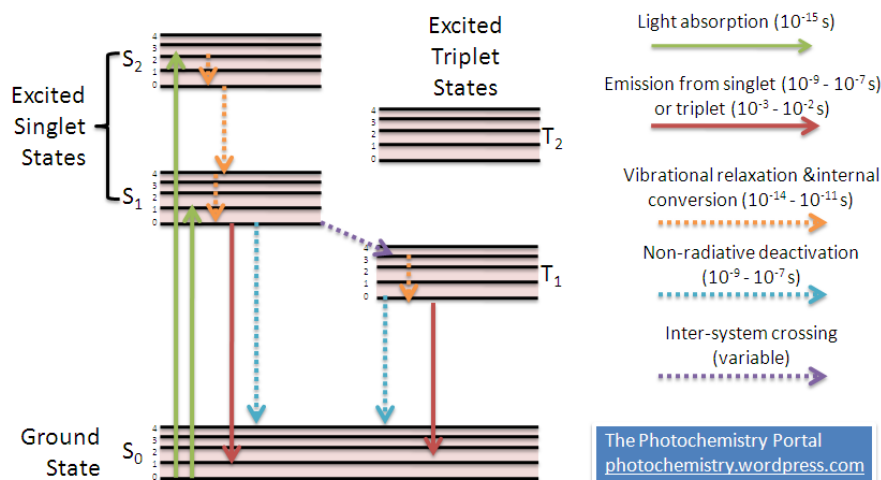
Figure 1.5: Jablonski Diagram. Radiative processes (those which are "vertical" in energy transfer) are shown in solid lines whereas non-radiative processes ("horizontal" energy transfer) are shown using dotted lines.

Previous marine organic matter copper quenching experiments have been able to solve for logK and binding capacity (Hernandez et al., 2006; Wu and Tanoe, 2001, and Dudal et al., 2006). Fluorescence quenching is a function of equilibrium binding parameters including logK, binding capacity (L_T) and proportionality constants for the ligand and metal ligand complexes. Hernandez et al. (2006) used fluorescence quenching to determine stability constants for copper and zinc with humic acids. They determined logK values for copper of 4.71-5.13 and a binding capacity of 1.01-2.84 mmol/g. Zinc and humic acid had a logK range of 4.24-4.49 and binding capacities of 0.066-1.86 mmol/g. Wu and Tanoe (2006) determined copper stability constants with varying molecular size fractions. This was done for CuL_1 and CuL_2 having a logK range of 7.98-9.56 and 7.05-8.78, respectively. Binding capacity range based on molecular size fraction was 8.19-19.88μM for CuL_1 and 25.44-32.94 μM for CuL_2. Dudal et al. (2006) used fluorescence quenching for coper, iron and nickel with low volume DOM samples but did

not solve for stability parameters. Fitting a fluorescence quenching curve with a Ryan Weber equilibrium model, equation (1), allows for the determination of logK and binding capacity for the NOM. By plotting fluorescence intensity versus total metal (C_M) added, a nonlinear regression analysis can be used to solve for K and C_L. I_{ML} is a limiting value below which the fluorescence will not continue to decrease due to metal addition.

$$I = \left(\frac{(I_{ML} - 100)}{2KC_L} \right) \left[(KC_L + KC_M + 1) - \sqrt{(KC_L + KC_M + 1)^2 - 4K^2 C_L C_M} \right] + 100$$

(1)

Freshwater fluorescence quenching has been validated for aluminum with salicylic acid and 2-hydroxy-3-napthoic acid by Smith et al. (1998). Copper fluorescence quenching was validated by its ability to predict free copper also by Smith et al. (2000). Experiments using model compounds with known stability constants for validation of the fluorescence quenching method for the metals copper, zinc, nickel and lead in marine systems were not discovered.

1.7 Matlab^{TM}: Solving for Chemical Equilibrium

Modeling of experimental data consists of simultaneously solving for the chemical equilibria in solution. A computerized model can be used to fit experimental data to chemical equilibrium binding constants by incorporating the constraints of mass balance and mass action. Matlab^{TM} was the program used to employ mass balance and mass action for solving chemical equilibrium represented by a tableau notation. The tableau notation defines the equilibrium problem and the entries in the columns are the stoichiometric coefficients required for the formation of each species (Smith, 2010). An example of a tableau can be viewed in Figure 1.6. Within the tableau the $CuOH^+$ species

18

is explained by stoichiometric coefficients of -1 H and 1 Cu. This can be explained by the formation of $CuOH^+$ which occurs from 1 copper and by removing 1 hydrogen from water, which is where the -1 H comes from. Additionally, if you multiply across the rows of the tableau it is possible to determine the species concentration and if you sum down the columns the total values (mass balance) can be recovered (Smith, 2010). Based on this tableau, it can be noted that the species are not independent of each other and components from the tableau can be selected to solve for the equilibria problem.

$$
\begin{bmatrix} H \\ 1 \\ 0 \\ -1 \\ -1 \\ TOTH \end{bmatrix}
\begin{bmatrix} Cu \\ 0 \\ 1 \\ 0 \\ 1 \\ Cu_T \end{bmatrix}
\begin{bmatrix} \log K \\ 0 \\ 0 \\ K_w \\ K_{Hydrolysis} \end{bmatrix}
\begin{bmatrix} Species \\ H^+ \\ Cu^{2+} \\ OH^- \\ CuOH^+ \end{bmatrix}
$$

Figure 1.6: Example Tableau. It is possible to determine species concentration if an individual multiplies across the rows. Mass balance can also be recovered and if the columns are summed.

The computerized code then creates four vectors. First a vector of species concentration labeled **C** is produced, and secondly a vector labeled **T** containing totals including TOTH and CuT. Next a vector summarizing the logK values are produced labeled **K** and finally a matrix of the stoichiometric coefficients for each of the components labeled **A**. Finally the Matlab code solves all these vector calculations by using the formula (3).

$$R=A'x(10^C)-T \text{ (3)}$$

To insert numerical values of C, the following equation (2) must be used (Smith, 2010).

$$C=10^{(K+A+X')} \text{ (2)}$$

1.8 Objective of Research

The purpose of this research is to:

1. Characterize different sources of NOM and their binding characteristics with copper, lead, zinc, and nickel in marine systems using fluorescence quenching and voltammetric methods.

2. Assess salinity dependence and NOM concentration dependence to determine their affect on binding capacity for lead with NOM.

3. Transformation/dissolution experiments will be completed to determine solubility of two copper compounds, copper and cuprous oxide, and ensure that they are within appropriate limits and regulations. A solubility model will be used to compare to experimental results, and conclusions will be made on which ones can effectively describe the experimental results obtained.

1. 9 Hypothesis

1. Source of organic matter will affect the binding capacities for the metals and will result in the magnitude of organic matter metal toxicity protection being source dependent.

2. An increase in DOM concentration will result in higher binding capacity and protectivity in marine samples.

3. An increase in salinity would result in similar binding capacity.

4. A solubility model based on NIST values will accurately predict copper solubility and match measured data.

1.10 Significance of study

The ability to characterize dissolved organic matter and its binding capacity with copper, lead, nickel and zinc in marine systems is important because the information can be used to expand the use of the Biotic Ligand Model (BLM) to marine systems.

The binding information for NOM and these metals in seawater will allow for the BLM to set guidelines and regulations for metal discharge in marine systems and accurately predict the effect of these metals on the organisms present. The setting of these regulations will appropriately protect marine organisms, prevent toxicity and allow for site specific discharge criteria.

Binding capacity comparison between different sources and concentration of NOM is essential to understand and characterize interaction of NOM with metals and apply it to research for the BLM. Binding capacity allows for information regarding the amount of metal the organic matter can hold. Equilibrium binding parameters allow for prediction of metal speciation and bioavailability for different bulk water chemistry allowing for site-specific regulatory criteria to be derived.

1.11 Thesis Road Map

Chapter 2: Transformation/Dissolution

Transformation/dissolution experiments are performed to determine the rate and extent to which metals and soluble metal compounds can produce soluble metal species in environmental conditions. Matlab^{TM} was used to create a copper solubility model. Parameters within in the model were adjusted to isolate individual precipitates and observe the changes in copper solubility.

Chapter 3: Sample Characterization by Fluorescence

Fluorescence spectroscopy is used to determine stability of NOM during storage and determine variability in molecular nature of NOM with different sources. PARAFAC was used to determine relative concentrations of three components humic and fulvic-like, tryptophan-like and tyrosine-like.

Chapter 4: Fluorescence Quenching Analysis for Copper, Nickel, Zinc and Lead in saltwater media

Fluorescence quenching was used to determine logK and L_T for NOM in seawater. The method was applied to NOM used in toxicity tests and did not provide measurements consistent with results. Tryptophan was used as a model ligand to validate fluorescence quenching method.

C.4 Matlab code for nickel

Appendix E: Competitive Ligand Exchange Method by Anodic Stripping Voltammetry

Competitive exchange experiments were completed on the voltammeter for copper with NOM Luther Marsh in artificial seawater and the competitive ligand, salicyladoxime. Binding capacities were determined.

Appendix F: Determination of Binding Capacity with Zinc

Zinc was measured using voltammetry to determine binding capacity. Resultant peak height versus total zinc were linear and binding capacity could not be determined.

Appendix G: Salinity and DOC variables that determine toxicity?

Nadella et al., Manuscript draft of toxicity results. Voltammetric results in chapter 5 comparing binding capacities for Nordic Reservoir at different NOM concentrations will be inserted into this paper.

1.12 References

Arnold, W.R., Santore, R.C., Cotsifas, J.S. Predicting Copper Toxicity in Estuarine and Marine waters using the Biotic Ligand Model. *Mar. Poll. Bulle.* **50**, 1634-1640. (2005).

Baker, A. Fluorescence excitation–emission matrix characterization of some sewage-impacted rivers. *Environ. Sci. Technol.*, **35**. 948–953. (2001)

Benner, R.H. Cycling of dissolved organic matter in the ocean. In: Hessen, D.O. and Tranvik, L.J. (Eds.) Aquatic Humic Substances. Ecology and biogeochemistry. Springer-Verlag, Berlin 1998.

Benner, R. Chemical composition and reactivity. In: Hansell, D.A., Carlson, C.A. (Eds.), Biogeochemistry of Marine Dissolved Organic Matter. Elsevier, USA, 59–90. 2002.

Bodar, C. W., Pronk, M. E., and Sijm, D. T. The European Union risk assessment on zinc and zinc compounds: the process and the facts. *Integr. Environ. Assess. Manag.* **1**, 301–319. (2005).

Bott, A.W. Voltammetric determination of trace concentrations of metals in the environment. *Curr. Sep.* **14**:1, 24-30. (1995).

Bruce, G and Gill, P. Estimates of Precision in a Standard Additions Analysis. J. Chem. Edu.**76**.805-807. (1999).

Bruland, K. W. Oceanographic distributions of cadmium, zinc, nickel, and copper in the North Pacific. *Earth Planet Sci. Lett.* **47**, 176–198. (1980).

Bruland K.W. and Coale K.H. Analysis of seawater for dissolved cadmium, copper and lead: an intercomparison of voltammetric and atomic absorption methods. *Mar. Chem.* **17**, 285-300. (1985).

Buck, K.N. and Bruland K.W. Copper speciation in San Francisco bay: A novel approach using multiple analytical windows. *Mar. Chem.* **96**, 185-198. (2005).

Buffle, J. Natural organic matter and metal-organic interactions in aquatic systems. In: Sigel, H. (Ed.) Metal ions in biological systems. Marcel Dekker, Inc. New York. 1984.

Chakoumakos, C., Russo, R. C., and Thurston, R. V. Toxicity of copper to cutthroat trout (*Salmo clarki*) under different conditions of alkalinity, pH and hardness. *Environ. Sci. Technol.* **13**, 219. (1979).

Chau, Y. K., and Kulikovsky-Cordeiro, O. T. R. Occurrence of nickel in the Canadian environment. *Environ. Rev.* **3**, 95–120. (1995).

Clifford, M and McGeer J. Development of a biotic ligand model for the acute toxicity of zinc to Daphnia pulex in soft waters. *Aquat Toxicol.* **91**(1):26-32.(2009).

Coale, K.H. and Bruland, K.W. Copper complexation in the Northeast Pacific. *Limnol. Oceanogr.* **33**. 1084-1101. (1988).

Coble, P.G. Characterization of marine and terrestrial DOM in seawater using excitation-emission matrix spectroscopy. *Mar. Chem.,* **51**. 325–346. (1996).

Coble PG, Green SA, Blough NV, Gagosian RB. Characterisation of dissolved organic matter in the Black Sea by fluorescence spectroscopy. *Nature*. **348**. 432-435. (1990).

DePalma S.G.S., Arnold W.R., McGeer J.C., Dixon, D.G., Smith, D.S. Variability in dissolved organic matter fluorescence and reduced sulphur concentration in coastal marine and estuarine environments. *App. Geochem.* **26.**394-404. (2011a).

DePalma S.G.S., Arnold W.R., McGeer J.C., Dixon, D.G., Smith, D.S. Protective effects of dissolved organic matter and reduced sulfur on copper toxicity in coastal marine environments. *Ecotox. And Environ. Saf.* **74**. 230-237. (2011b).

DePalma S.G.S., Arnold W.R., McGeer J.C., and Smith D.S. (2008). "Chemical Characterization of Saltwater Environments: Implications for Protective Effects on Copper Toxicity", 5[Th] SETAC World Congress, Sydney, Australia.

De Schamphelaere, K.A.C., Vasconcelois, F.M., Tack, F.M.G., Allen, H.E., Janssen, C.R. Effect of dissolved organic matter source on acute copper toxicity to Daphnia magna. *Environ. Toxicol. Chem.* **23**, 1248-1255. (2004).

DeWailly, E and Knap, A. Food from the Ocean and Human Health Balancing Risks and Benefits. *Oceanogr.***19**. 84-93. (2006).

Doig, L.E. and Liber, K. Nickel speciation in the presence of different sources and fractions of dissolved organic matter. *Ecotox. and Environ. Safety.* **66**. 169-177. (2007).

Dudal, Y., Holado, R., Maestri. G., Gullon, E., Dupont, L. Rapid screening of DOM's metal-binding ability using a fluorescence-based microplate assay. *Sci. of the Tot. Environ.* **354**. 286– 29. (2006).

Eisler, R. Lead hazards to fish, wildlife, and invertebrates: a synoptic review. *U.S. Fish Wildl. Serv. Biol. Rep.* **85**. 1.14. (1988).

Eisler, R. Nickel hazards to fish, wildlife, and invertebrates: a synoptic review. *Cont. Haz. Rev.* **34**. (1998).

Eisler, R. Zinc hazards to fish, wildlife and invertebrates: a synoptic review. In Contaminant Hazard Reviews Report (USA), Biological Report. Washington, DC: Fish and Wildlife Service. (1993).

Ellwood, M. J. Zinc and cadmium speciation in subantarctic waters east of New Zealand. *Mar. Chem.* **87**, 37–58. (2004).

Ericksen, R.S., Nowak. B. Van Dam, R. Copper Speciation and toxicity incontaminated Estuary. *Super. Sci. Rep.* **163**, 1-29. (2001).

Erickson, R. J., Benoit, D. A., Mattson, V. R., Nelson, H. P., Jr., and Leonard, E. N. The effects of water chemistry on the toxicity of copper to fathead minnows. *Environ. Toxicol. Chem.* **15**, 181–193. (1996).

European Commission (EC), 2001. Decision 2455/2001/EC of the European Parliament and of the Council of 20 November 2001, establishing the list of priority substances in the field of water Policy and amending Directive 2000/60/EC. Official Journal L331 of 15.12.2001.

Franca, S. Vinagre, C., Cacador, I., Cabral, H.N. Heavy metal concentrations in sediment, benthic invertebrates anf fish in three salt marsh areas subjected to different pollution loads in the Tagas Estuary (Portugal). *Mar. Poll. Bulle.* 50(9). 998-1003. (2005).

Gheorghiu, C., Smith, D.S., Al-Reasi, H.A., McGeer, J.C., Wilkie, M.P. Influence of natural organic matter (NOM) quality on Cu-gill binding in the rainbow trout (oncorhynchus mykiss). *Aqua. Tox.* **97**, 343-352. (2010).

Government of Canada. Water and Canada: Preserving a Legacy for People in the Environment. 2003.

Glover, C.N., Playle, R.C., Wood, C.M. Heterogeneity of natural organic matter amelioration of silver toxicity to Daphnia Magna: effect of source and equilibration time. Environ. *Toxicol. Chem.* **24**, 2934-2940. (2005).

Grosell.M., Wood, C.M. Copper uptake across a rainbow trout gills: Mechanisms of apical entry. *J. Exp. Biol.* **205**, 1179-1188. (2002).

Hernandez, D., Plaza, C., Senesi, N., Polo, A. Detection of copper(II) and zinc(II) binding to humic acid from pig slurry and amended soils by fluorescence spectroscopy. *Environ Pollut.* **143**(2). 212-20. (2006).

Hood, E., Williams, M.W., McKnight, D.M. Sources of Dissolved Organic Matter in a Rocky Mountain Stream using Chemical fractionation and Stable Isotopes. *Biogeochem.* **74**, 231-255. (2005).

Kobayashi, N and Okamura, H. Effects of heavy metals on sea urchin embryo development. 1. Tracing the cause by the effects. Chemosphere. 55 (10). 1403-1412. (2004).

Kogut M.B. and Voelker B.M. Strong copper binding behavior of terrestrial humic substances in seawater. *Environ. Sci. Technol.,* **35**, 1149-1156. (2001).

Lakowitz J.R. *In Principles of Fluorescence Spectroscopy.* Plenum Press; New York and London. 2000.

Luoma, S. N., and Rainbow, P. S. Metal Contamination in Aquatic Environments: Science and Lateral Management. Cambridge University Press, New York. (2008).

MacDonald, A., Silk, L., Schwartz, M., Playle, R. A lead–gill binding model to predict acute lead toxicity to rainbow trout (*Oncorhynchus mykiss*). *Compar. Biochem. and Phys. Part C: Tox. & Pharm.* 133, 227-242. (2002).

Mager, E. M., Esbaugh, A. J., Brix, K. V., Ryan, A. C., and Grosell, M. Influences of water chemistry on the acute toxicity of lead to *Pimephales promelas* and *Ceriodaphnia dubia*. *Comp. Biochem. Physiol*. **153**, 82–90. (2010b).

Mantoura,R. and Woodward M.Conservative behaviour of riverine dissolved organic carbon in the Severn Estuary: chemical and geochemical implications. *Geochim. Cosmochim. Acta*, **47**. 1293–1309. (1983).

McKnight, D.M. and Aiken, G.R. Source and age of aquatic humuc. In: Hessen, D.O. and Tranvik, L.J. (Eds.) Aquatic Humic substances:ecology and biogeochemistry. Springer-Verlag Berlin, 1998.

McKnight, D.M., Boyer, E.W., Westeroff, P.K., Doran, P.T., Kulbe T., Anderson, D.T. Spectrofluorometric characterization of dissolved organic matter for indication of precursor organic materials and aromaticity. *Limnol. Oceanogr*. **46**, 38-48. (2001).

Mota, A.M. and Corrieia dos Santos, M.M. Trace metal speciation of labile chemical species in natural waters: Electrochemical methods. In: Tesser, A., Turner, D.R. (Eds.) Metal speciation and bioavailability in aquatic systems. John Wiley and Sons Ltd., Chisester, UK. 1995.

Nadella, S.R., Fitzpatrick, J.L., Franklin, N., Bucking, C.P., Smith, S., Wood, C.M. Toxicity of dissolved Cu, Zn, Ni and Cu to developing embryos of the blue mussel (mytilus trossolus) and the protective effect of dissolved organic carbon. *Comp. Biochem. Physiol.* **149**, 340-348. (2009).

Niyogi, S., and Wood, C. M. Biotic ligand model, a flexible tool for developing sitespecific water quality guidelines for metals. *Environ. Sci. Technol.* **38**, 6177–6192. (2004).

NOAA. Population trends along the coastal united states: 1980–2008. Technical report, National Oceanic and Atmospheric Administration, National Ocean Service. (2004).

Nriagu, J. O., and Pacyna, J. M. Quantitative assessment of worldwide contamination of air, water and soils by trace metals. *Nature*. **333**. 134–139. (1988).

Paquin, P.R., Gorsuch, J.W., Apte, S., Batley, G.E., Browles, K.C., Campbell, P.G.C., Dloes, C.G., Di Toro, D.M., Dwyer, R.I., Galvez, F., Gensemer, R.W., Goss, G.G., Hogstrand, C., Janssen, C.R., McGeer, J.C., Naddy, R.B., Playle, R.C., Santore, R.C., Schneider, U. Stubblefield, W.A., Wood, C.M., Wu, K.B. The biotic ligand model: a historical overview. *Comp. Biochem. Physiol. C.* **133**, 3-36. (2002).

Perdue, E.M. Chemical composition, structure, and metal binding properties. In: hessen, D.O. and Tranvik, L.J. (Eds). Aquatic Humic substances:ecology and biogeochemistry. Springer-Verlag Berlin, 1998.

Pickering, Q. H., and Henderson, C. The acute toxicity of some heavy metals to different species of warmwater fishes. *Air Wat. Pollut. Int. J.* **10**, 453–463. (1966).

Radenac, G., Fichet, D., Miramand, P. Bioaccumulation and toxicity of four dissolved metals in Paracentrotus lividus sea urchin embryo. *Mar. Environ. Resea.* **51** (92).151-166. 2001.

Ray, D., Banerjee, S. K., and Chatterjee, M. Bioaccumulation of nickel and vanadium in tissues of the catfish Clarias batrachus. J. Inorg. Biochem. 38, 169–173. (1990).

Reuer, M. K., and Weiss, D. J. Anthropogenic lead dynamics in the terrestrial and marine environment. *Philos. Trans. A Math. Phys. Eng. Sci.* **360**. 2889–2904. (2002).

Riley, T. and Watson, A. Polarography and other voltammetric methods. Analytical chemistry by open earning. John Wiley & Sons. Chichester. 1987.

Rivera-Duarte, I., Rosen, G., LaPota, D., Chadwick, D.B., Kear-Padilla, L., Zirino, A. Copper Toxicity to Larval Stages of Three Marine Invertebrates and Copper Complexation Capacity in San Diego Bay, California. *Environ. Sci. Technol.* **39**. 1542-154. (2005).

Rodriguez, R. E., Misra M., Diwan, B.A., Riggs, C.W., and Kasprzak, K.S.. Relative susceptibilities of C57BL/6X, (C57BL/6 X C3H/He)F1, and C3H/He mice to acute toxicity and carcinogenicity of nickel subsulfide. Toxicology 107:131-140. (1996).

Rogers, J. Characterization of branchial lead-calcium interaction in the freshwater rainbow trout Oncorhynchus mykiss. *J. Exp. Bio.* **207**: 5, 813-825. (2004).

Sanchez-Marin, P., Bellas, J., Mubiana, V.K., Lorenzo, J.I., Blust, R., Beiras, R. Pb Uptake by the marine mussel *Mytilus* sp. Interactions with dissolved organic matter. *Aqua. Tox.* **102**. 48-57. (2011).

Sandstead H.H. Understanding zinc: recent observations and interpretations. *J. Lab. Clin. Med.* **124**, 322-327. (1994).

Santore, R.C., Di Toro, D.M., Paquin, P.R., Allen, H.E., Meyer, J.S. Biotic Ligand Model of the Acute Toxicity of Metals. 2. Application to Acute Copper Toxicity in Freshwater Fish and Daphnia. *Environ. Toxic. And Chem.* **20**, 10, 2391-2402. (2001).

Saxberg, B.E.H., Kowlaski, B.R. Generalized standard addition method. *Anal. Chem.* **51**, 1031-1038.(1979).

Schwartz, M.L., Curtis, P.J., Playle, R.C. Influence of natural organic matter source on acute copper, lead, and cadmium toxicity to rainbow trout oncorhynchus mykiss. *Environ. Tox. and Chem* **23**, 2889-2899. (2004).

Sherrell, R. M., and Boyle, E. A. The trace metal composition of suspended particles in the oceanic water column near Bermuda. *Earth Planet. Sci. Lett.* **111**, 155–174. (1992).

Smith, D.S., Bell, R.A., Kramer, J.R. Review: Metal Speciation in Natural Waters with Emphasis on Reduced Sulfur groups as Strong Binding Sites. *Comparative Biochem.and Phys. Part C.* 133, 65-74. (2002).

Smith, D.S., Kramer, J.R. Fluorescence analysis for multi-site aluminum binding to natural organic matter. *Environ. Internat.,* **25**. 295–306. (1999).

Smith, D. S., and Kramer, J. R. Multi-site aluminum speciation with natural organic matter using multiresponse fluorescence data. *Anal. Chim. Acta.* **363**. 21-29. (1998).

Smith, D.S., Kramer, J.R. Multisite Metal Binding to Fulvic Acid Determined Using Multiresponse Fluorescence. *Anal. Chim. Acta.* **416**, 211–222. (2000).

Smith, D.S. Solution of Simultaneous Chemical Equilibria in Heterogeneous systems:implementation in Matlab. Wilfrid Laurier University, 2010. <http://www.wlu.ca/documents/24984/matlab_speciation_calculation.pdf>.

Spry D.J., Wood C.M. Ion flux rates, acid-base status and blood gases in rainbow trout, Salmo gaidneri, exposed to toxic zinc in natural softwater. *Can. J. Fish. Aquat. Sci.* **42**, 1332-1341. (1985).

Srna, R.F., Garret, K.S., Miller, S.M., Thum, A.B. Copper complexation capacity of marine water samples from southern California. *Environ. Sci. Technol.* **14**, 1482-1486. (1980).

Stedmon, C.A. and Bro, R. Characterizing dissolved organic matter fluorescence with parallel factor analysis: a tutorial. *Limnol. Oceanog. Methods*, **6**. 572–579. (2008).

Stedmon, C.A. and Markager, S.Resolving the variability in dissolved organic matter fluorescence in a temperate estuary and its catchment using PARAFAC analysis. *Limnol. Oceanog.,* **50**. 686–697. (2005).

Thurman E.M. Organic geochemistry of natural waters, Martinus Nijhof/Dr. W. Junk Publishers, Dordrecht (1985).

Tipping, E. Cation binding by humic substances. Cambridge University press, Cambridge, UK, 2002.

Tjalve, H., Gottofrey, J., and Borg, K. Bioaccumulation, distribution and retention of $^{63}Ni^{2+}$ in the brown trout (*Salmo trutta*). *Wat. Res.* **22**, 1129–1136. (1988).

USEPA. Aquatic Life Ambient Freshwater Quality Criteria – Copper. EPA-822-R-07-001,2007 revision. Washington, DC: US Environmental Protection Agency. (2007).

Wright, D.A. and Welbourn, P. Environmental Toxicology, Cambridge University Press, Cambridge, UK, 2002.

Wood, C.M., Farrell, P., and Brauner C.J. Homeostasis and Toxicology of Non-Essential Metals: Fish Physiology V31B. Academic Press, 2012.

Wu, F.C., Evans, R.D., and Dillon, P.J. Separation and characterization of NOM by high-performance liquid chromatography and on-line three-dimensional excitation emission matrix fluorescence detection. *Environ. Sci. Technol.,* **37**. 3687–3693. (2003).

Wu, F and Tanoue, E. Geochemical characterization of organic ligands for copper(II) in different molecular size fractions in Lake Biwa, Japan. *Org. Geochem.* 32, 1311-1318. (2001).

Xie,W.H., Shiu, W.Y., and Mackay, D. A review of the effect of salts on the solubility of organic compounds in seawater. *Mar. Environ. Res.*, **44**. 429–444. (1997).

Chapter 2: Transformation/Dissolution

2.1 Introduction

Copper solubility is an important piece of information needed for many companies that manufacture copper containing products. At low copper concentrations copper is essential but at increased concentrations copper can become toxic to organisms and harmful to the environment. Therefore, it is very important for manufacturers to know that the amount of copper that can potentially be released into the environment from their products or waste is not an amount that can be harmful or exceed any regulatory requirements. If a compound is found to be highly soluble, a greater environmental impact is expected. Conversely, insoluble copper compounds are less likely to have a negative environmental impact. There is a need for solubility assessment in marine environments where high salinity can influence solubility.

Copper solubility is extremely important to antifouling paint companies. Antifouling paint is used to counteract or prevent the buildup of deposits on underwater structures. It is added to the hull of a boat and is designed to slow the growth of organisms that would attach to the hull and affect performance and durability. This paint contains such compounds as copper powder and cuprous oxide, and can flake off into the seawater. It is extremely important to know the solubility of copper and ensure that it is within appropriate limits and regulations. Harbour environments have a higher concentration of boats in a designated area and therefore have a greater likelihood of having an environmental impact.

Transformation/dissolution experiments are performed to determine the rate and extent to which metals and soluble metal compounds can produce soluble metal species in environmental conditions. These experiments have been completed for 100 mg/L of copper and cuprous oxide powder following OECD (Organisation for economic cooperation and development) protocols. Both powders undergo oxidation while dissolving into solution. The solubilization of copper powder can be seen in equation (1) while the solubilization of cuprous oxide can be viewed in equation (2).

$$Cu_{(s)} \rightarrow Cu^{2+} + 2e^- \qquad (1)$$

$$Cu_2O(s) + 2H^+ \rightarrow 2Cu^+ + H_2O \qquad (2)$$
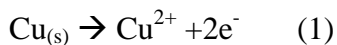
The OECD work with governments to understand what drives economic, social and environmental change. They use data to predict future trends and set international standards on a range of things including the safety of chemicals. The OECD protocols are the accepted means to determine safe thresholds on solid substances. The solubility results can be used to evaluate the short and long term aquatic toxicity of the metal. The test guidance applied is the outcome of an international effort under the OECD to develop an approach for the toxicity testing and data interpretation of metals and sparingly soluble inorganic metal compounds (SSIMs).

Copper solubility modeling has been based on the precipitate tenorite (CuO) which cannot be located within the national institute of standards and technology's (NIST) standard reference database. However, other precipitates that are included in the copper solubility modeling, including malachite ($Cu_2(OH)_2CO_{3(s)}$), copper hydroxide

33

$(Cu(OH)_2)$ and copper carbonate $(CuCO_3)$, can be found in the NIST database. This has led to the discussion of which is the most reliable solid phase for dissolution equilibrium modeling.

2.2 Experimental Details

2.2.1 Transformation/Dissolution

A standard laboratory transformation/dissolution protocol, Annex 10 following OECD standards, was applied to seawater sample agitation of 100 mg/L of cuprous oxide (Cu_2O) and copper (Cu) powder in a pH buffered aqueous medium (OECD, 2001; Annex 10, 2007). The chemical composition of the marine medium can be found in Table 2.1.

Table 2.1: Chemical Composition of Marine Medium used for Transformation/Dissolution.

Chemical	mg/L
NaF	3
$SrCl_2\ 6H_2O$	20
H_3BO_3	30
KBr	100
KCl	700
$CaCl_2\ 2H_2O$	1470
Na_2SO_4	4000
$MgCl_2,6H_2O$	10780
NaCl	23500
$Na_2SiO_3\ 9H_2O$	20
$NaHCO_3$	200

The marine medium was added to three vessels and allowed to equilibrate for 24 hours before the addition of the 100 mg/L metal powder. Enough headspace was maintained in each vessel to keep the dissolved oxygen concentration above 70%. The solutions were agitated by a radial impeller at 200 rpm and the vessels were kept closed. Controls were taken from each vessel before the addition of the metal powder. Every 24 hours, temperature, pH and dissolved oxygen was measured to ensure experimental conditions were met. Temperature had to remain between 20 and 25ºC, without varying more than 2ºC. The pH had to remain constant at +/-0.2 pH units and dissolved oxygen above 70%. After the measurements were recorded, two subsamples were taken from each vessel. They were filtered through a 0.2µm polyethersulfone (PES) membrane syringe filter and acidified with 1% HNO_3. The volume removed from each vessel was replaced by fresh marine medium. Sampling and analyzing of the solutions occurred at 24 hour intervals for 7 days to determine the concentration of total dissolved metal.

2.2.2 Total Soluble Copper Analysis

Copper concentrations were measured with a voltammeter following the Metrohm No. 231/2e method. A KCl-sodium acetate solution was prepared by dissolving 55.9 g KCl, 25 mL 30% by weight NaOH and 14.2 mL acetic acid up to 500mL of Milli-Q water. 10mL of the collected sample and 1 mL of the KCl-sodium acetate solution were placed in the voltammeter vessel and the pH was tested to ensure it was at 4.6+/-0.2. The voltammeter was run with the following parameters: purge time 300 seconds, deposition potential -1.15 V, deposition time 90 seconds, equilibration time 10 seconds, scan range

of -1.15 to 0.05 V, voltage step of 0.006 V and voltage step time of 0.1 seconds. The concentration was determined by standard additions.

The copper concentrations for the copper and cuprous oxide powder samples (+/-standard deviation) were determined to be 47.9 ± 3.48 μg/L and 46.0± 5.56 μg/L, respectively. Figure 2.1 illustrates the results collected by the transformation/dissolution protocol as described above.
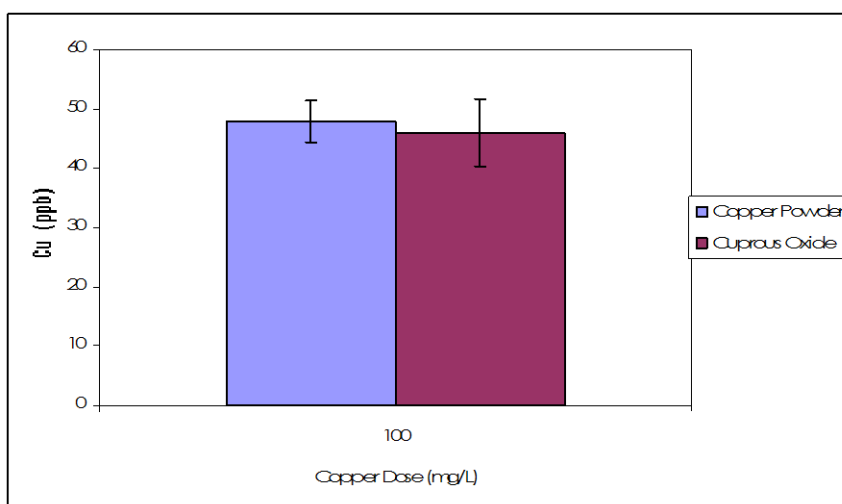
Figure 2.1: Copper analysis and standard deviation for 100 mg/L of copper powder and cuprous oxide powder in standard marine medium.

2.2.3 Modeling

Matlab^{TM} was used to create a copper solubility model. Parameters within the model were adjusted to isolate individual precipitates and observe the changes in copper solubility accordingly. Based on the modeling completed with Matlab^{TM}, conclusions were made on the acceptability of current precipitates used in the models and which ones can effectively describe the experimental results obtained.

2.3 Aquatic and Solid Tableaus

The seawater used for the transformation/dissolution protocol in Table 2.1 has a distinct recipe that needs to be followed. The species within the recipe that can directly bind to copper are hydroxide, chloride, carbonate and sulfate. The species within this recipe that were placed within a tableau for aquatic species can be found in Table 2.1. The matlab script used can be found in Appendix A.

Species	H	Cu	CO_3	Cl	SO_4	log K
H	1	0	0	0	0	0
Cu	0	1	0	0	0	0
CO_3	0	0	1	0	0	0
Cl	0	0	0	1	0	0
SO_4	0	0	0	0	1	0
OH	-1	0	0	0	0	log K_W
CuOH	-1	1	0	0	0	log Kh_1
Cu_2OH_2	-2	2	0	0	0	log Bh_{22}
HCO_3	1	0	1	0	0	pKa_2
H_2CO_3	2	0	1	0	0	$pKa_2 + pKa_1$
$CuCO_3$	0	1	1	0	0	log $KCuCO_3$
$Cu(CO_3)_2$	0	1	2	0	0	log $KCu(CO_3)_2$
$CuHCO_3$	1	1	1	0	0	log $KCuHCO_3$
CuCl	0	1	0	1	0	log KCuCl
$CuSO_4$	0	1	0	0	1	log $KCuSO_4$
HSO_4	1	0	0	0	1	log $KHSO_4$

Table 2.2: Aquatic species tableau used for matlab copper solubility modeling containing species name, number of H, Cu, CO_3, Cl and log K values. Log K values can be found in the NIST standard reference database and were corrected for ionic strength.

The tableau for the precipitates can be found in Table 2.2. There is a need for a separate solid tableau because it requires an additional residual involving saturation index (SI). The SI is used to predict the ability of the solution to form a precipitate. It is defined as the log of the ion activity product divided by K_{sp}. The tenorite equation can be used to explain how the tableau is created. The formation of tenorite can be described by this equation (3).

$$Cu^{2+} + H_2O \rightarrow CuO_{(s)} + 2H^+ \qquad (3)$$
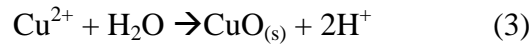
From this it can be seen that 1 copper is present as the reactant and 2 hydrogens are present as products, thus expressed as -2 reactants. The activity corrected logKsp value for an ionic strength of 0.7 of tenorite is 7.89 but because the way tableaus are written requires formation constants, not dissolution constants, the logK value becomes -7.89.

Species	H	Cu	CO₃	Cl	SO₄	log K
$CuOH_2$	-2	1	0	0	0	log Ksp + 2 log Kw
$CuCO_3$	0	1	1	0	0	log $KCuCO_3$
Malachite	-2	2	1	0	0	log $K_{malachite}$ +2 log Kw
Tenorite	-2	1	0	0	0	log $K_{tenorite}$ + 2 log Kw

Table 2.3: Precipitate tableau. LogK values were corrected for ionic strength by using the extended Debye Huckel equation.

2.4 Activity Corrections

All logK values present within the tableau were corrected for ionic strength. The ionic strength of the OECD seawater used is 0.7M which was calculated based on the concentrations of each compound used to prepare the seawater medium, as seen in equation 4. Here C_i is the molar concentration in mol/L and Z_i is the charge number of that ion.

$$\mu = \frac{1}{2} \sum_{i=1}^{n} C_i Z_i^2$$

(4)

This means that the logK values collected must be corrected for this ionic strength. Two methods were applied to adjust for the ionic strength. The first method is applied with multiple measured stability constants at different salinities. It involves an interpolation method of measured logK values at different ionic strengths. Data was taken from NIST (Martell and Smith, 2001). The measured values are plotted against salinity and an interpolation is done to find the measured logK for the specific salinity of the solution. This uses the known data points to estimate the logK at the salinity of interest. A representation of the interpolation for hydroxide can be found in Figure 2.2. The additional interpolations can be found in Appendix B.
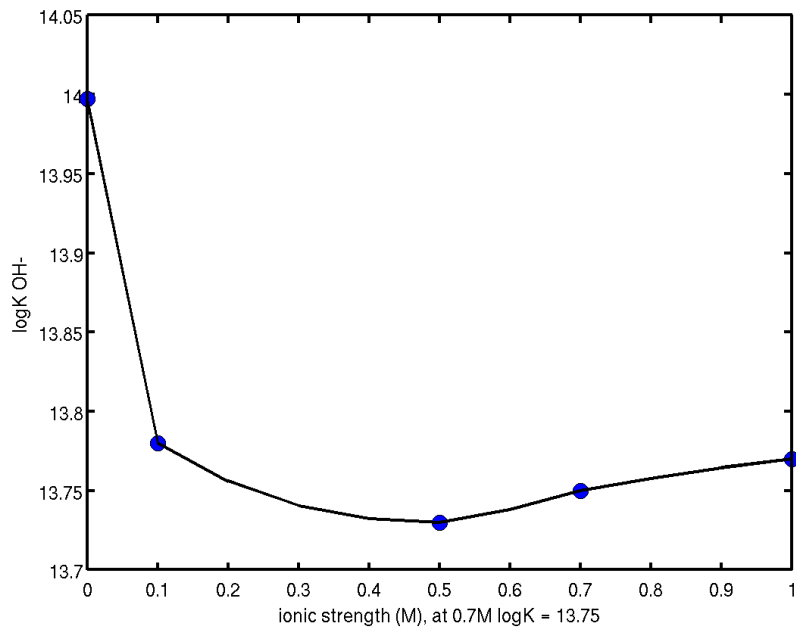
Figure 2.2: Interpolation of logK for hydroxide at an ionic strength of 0.7 M.

The second method, using the extended Debye Huckel equation, was applied to the logK values that could not be interpolated within Matlab because multiple ionic strength data was lacking. The extended Debye Huckel equation (5) is used for this correction. Here z is the charge, μ is the ionic strength and α is the radius in pm in an aqueous solution.

$$\log \gamma = \frac{-0.51z^2\sqrt{\mu}}{1+(\alpha\sqrt{\mu/305})} \qquad (5)$$

Based on reaction (6) the fixed ionic strength concentration K value (K_{conc}) can be defined as seen in (7).

$$aA + bB \rightarrow cC + dD \qquad (6)$$
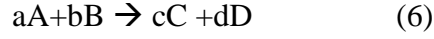
$$K_{conc} = \frac{[C]^c [D]^d}{[A]^a [B]^b} \qquad (7)$$

Activity is defined in equation (8). The activity of species A is its concentration multiplied by its activity coefficient (γ). The activity coefficient measures the deviation of behavior from ideality.

$$A = \gamma_A [A] \qquad (8)$$

The equilibrium constant can be adjusted to the thermodynamic constant which is based on activities (9).

$$K_{thermo}(K_{activity}) = \frac{\gamma_C^c [C] \gamma_D^d [D]}{\gamma_A^a [A] \gamma_B^b [B]} \qquad (9)$$

Rearrangement of this equation results in (10).

$$K_{thermo} = \frac{\gamma_C^c \gamma_D^d}{\gamma_A^a \gamma_B^b} \frac{[C]^c [D]^d}{[A]^a [B]^b} \qquad (10)$$

The simplified equation can be written as (11) where β is a constant which is a function of ionic strength.

$$K_{thermo} = \beta K_{conc} \qquad (11)$$

Then the activity correction for the K values can be completed using (12).

$$K_{conc} = \frac{K_{thernmo}}{\beta} \qquad (12)$$

2.5 Copper Solubility Diagram

The Matlab^{TM} program containing the aquatic and precipitate tableau found in Appendix A produced the solubility diagram in Figure 2.3. The sum of soluble copper species was determined by the difference between total and precipitates as defined by equation (13) where CuT was set to 5.0×10^{-5} M to ensure super saturation.

$$Cu_{soluble} = Cu_T - (2*[malachite] + [tenorite] + [Cu(OH)_{2(s)}] + [CuCO_{3(s)}] \qquad (13)$$

In this diagram at a pH of 8, which is roughly the pH in seawater, and the exact pH in the transformation/dissolution experiments, the soluble copper is approximately 22 ppb. This value is lower by about half than the 47.9 +/- 3.48 ppb and 46.0 +/- 5.56 ppb measured in the experiment.
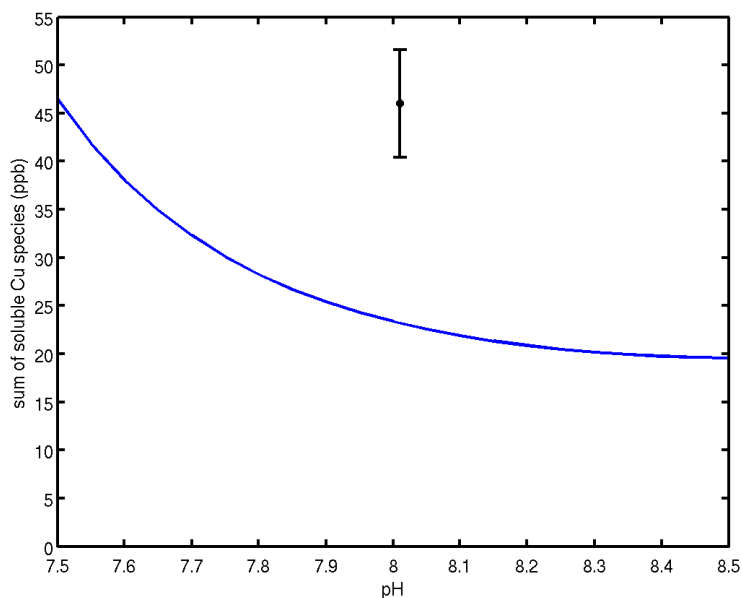
Figure 2.3: Copper solubility diagram with precipitates malachite, tenorite, copper hydroxide and copper carbonate. The blue data point is the amount in ppb with standard deviation measured within the transformation/dissolution experiments.

The next step taken with the Matlab[TM] program was to isolate the precipitate formation to be able to identify which precipitate would best describe the results obtained from the experiment. Three solid phases: tenorite, malachite and $Cu(OH)_{2(s)}$ were systematically tested and solubility versus pH was compared to measured values. The next model had only one precipitate present in the model, tenorite. However, it is identical to the figure 2.3. Indicating that tenorite is the most stable precipitate and dominates in the original copper solubility model. This value still underestimates compared to the experimentally measured value.

The next precipitate to isolate in the modeling is malachite. Figure 2.4 shows the copper solubility allowing only malachite formation as the stable mineral phase. At a pH

of eight, the copper solubility is predicted to be approximately 150 ppb. This overestimates the copper solubility based on the experimentally collected results.
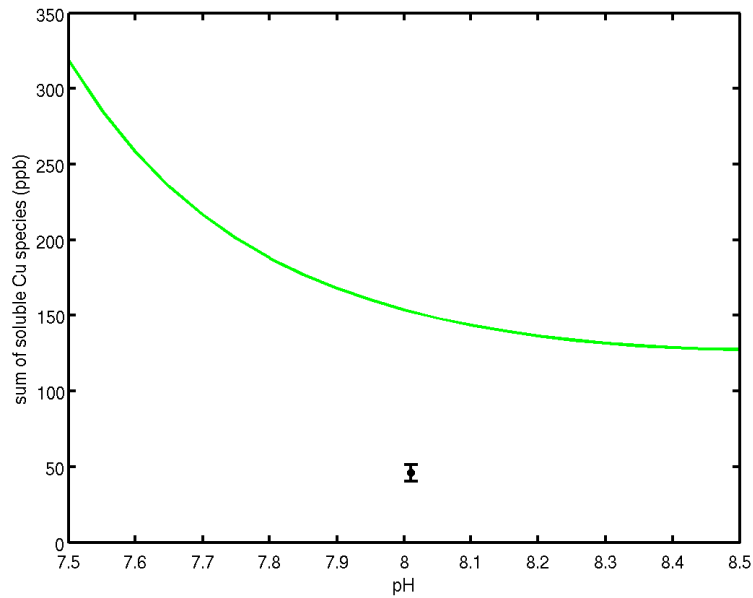
Figure 2.4: Copper solubility model with malachite as the only precipitate present. The blue data point is the amount measured in ppb with standard deviation within the transformation/dissolution experiments.

The copper solubility diagram for only the copper hydroxide solid can be found in figure 2.5. At a pH of eight, the copper solubility is predicted to be approximately 600 ppb which overestimates the soluble copper found in the system.
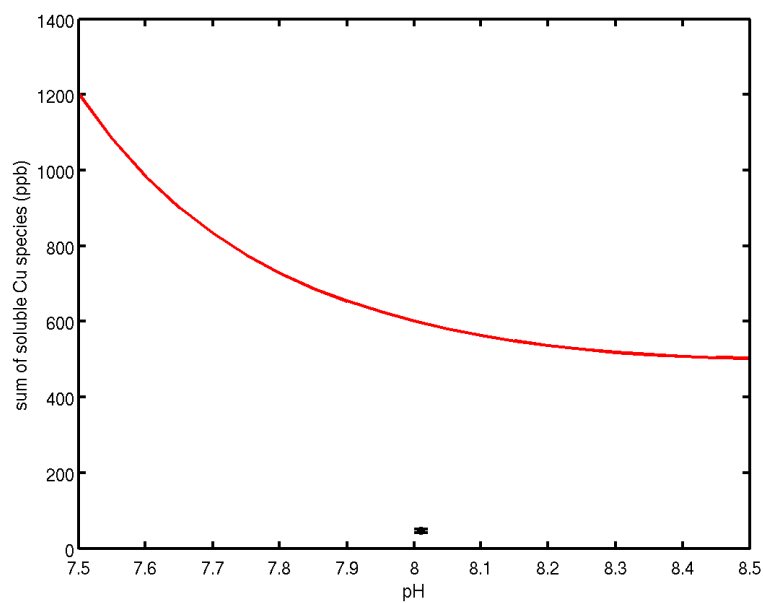
Figure 2.5: Copper solubility model with copper hydroxide as the only precipitate present. The blue data point is the amount measured in ppb with standard deviation within the transformation/dissolution experiments.

Finally, Matlab^{TM} was used to accumulate figures 2.3-2.5 to give an idea of which precipitate could be used to best model copper solubility in figure 2.6.

45
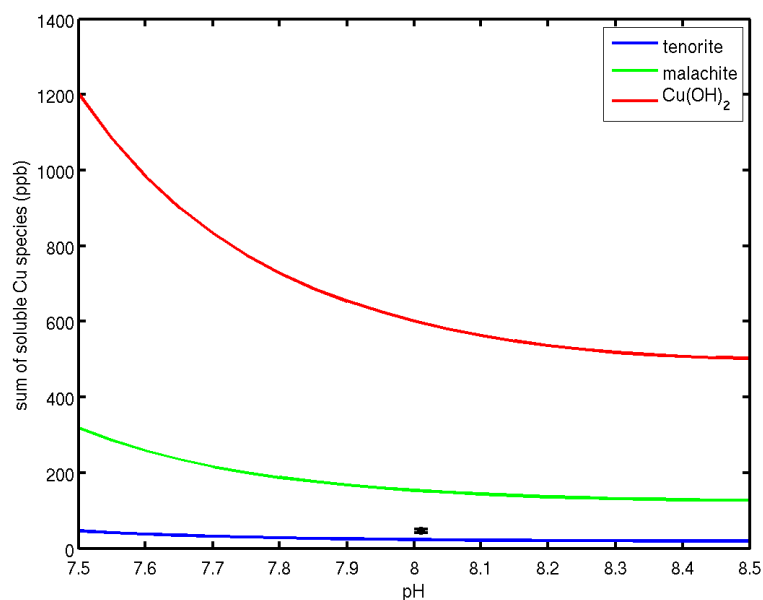
Figure 2.6: Copper solubility model with copper hydroxide as the only precipitate present (red line). Copper solubility model with malachite as the only precipitate present (green line). Copper solubility model with tenorite as the only precipitate present (blue line). The overall copper solubility model including tenorite, malachite, copper hydroxide and copper carbonate is directly blue the tenorite only model. The blue data point is the amount in ppb with standard deviation measured within the transformation/dissolution experiments.

2.6 Discussion

Tenorite precipitation underestimates the copper solubility but it most closely matches the measured data. This disagreement could be due to kinetics. It is important to note that the logK value assumes that the tenorite precipitate is at equilibrium. Research regarding the length of time it takes for tenorite to reach an equilibrium state has yet to be determined. Therefore, tenorite may actually be a good precipitate representation for the copper solubility model but it cannot be accurately observed because the logK value is for the precipitate at equilibrium and, in fact, the compound may not be there yet.

Copper hydroxide solid seriously overestimates copper solubility so is also not a reasonable precipitate to be used for modeling. The malachite precipitate overestimates the value of copper solubility at 150 ppb compared to 47.9 +/-3.48 ppb and 46.0 +/- 5.56 ppb. The tenorite solubility model provides closer values than the malachite solubility model but from a toxicity standpoint the malachite model could be more conservative.

The Canadian Environmental Quality Guidelines (CEQG) for copper is currently based on total copper concentrations that are considered 'safe' copper levels in both fresh and marine water. The Canadian freshwater copper criteria range from 2 to 4 µg/L depending on water hardness, and the saltwater criteria state a limit of 3 µg/L (CCME, 2007). The total soluble copper of the copper powder and cuprous oxide was found to be 47.9 and 46.0 µg/L, respectively and exceeds the limits set by the CEQG.

Mytilus are among the most copper sensitive taxa in the USEPA ambient seawater copper criteria document (Arnold et al., 2009). The EC_{50} for copper in *Mytilus trossolus* was determined to be 9.6 µg/L without the presence of NOM (Nadella et al., 2009). The solubility of these compounds, if used for antifouling agents, could be very hazardous to the *Mytilus* genus because the solubility is almost five times higher than the EC_{50} and greater than ten times the regulatory guidelines. In comparison, blue crab (*Callinectes sapidus*) is a very copper tolerant species with an EC_{50} of 3367.9 µg/L (Martins et al., 2011) so the solubility of these copper compounds would not affect them.

2.7 Conclusions

With the use of modeling using chemical stability constants corrected for ionic strength of seawater, a greater understanding of modeling of copper solubility was established. Tenorite precipitation underestimates the copper solubility in comparison to the solubility seen in experimental testing, but agrees more closely than any of the other precipitates. However, it is possible that the tenorite precipitate is not at equilibrium and given long time periods, may be a reasonable precipitate to use for modeling. More information regarding the precipitate is required before an appropriate decision can be made. Copper hydroxide solid seriously overestimates measured copper solubility via dissolution so is also not a reasonable precipitate to be used for modeling. The malachite precipitate overestimates the copper solubility but appears to be more reasonable than the copper hydroxide model. Ultimately, the experimental data point was placed between the tenorite precipitation model and the malachite precipitation model, still leaving questions about how to optimize the modeling of copper solubility. Only divalent copper precipitates were used in the solubility model because the copper powders undergo oxidation reactions. These models can be used as an estimate but much more work is needed to produce an accurate copper solubility model. It is also important to model precipitation of copper and not just the dissolution to get a complete picture of copper solubility in marine systems.

The solubility values measured were almost five times more concentrated than the EC_{50}'s for *Mytilus trossolus*, and greater than ten times the regulatory guidelines indicating that, if used as an antifouling paint, it may have toxicity effects in marine systems.

2.8 References

Annex 10: Guidance on transformation/dissolution of metals and metal compounds. United Nations, 2007.

Arnold, R. W., Cotsifas, J. S., Smith, D. S., LePage, S., and Gruenthal, K. M. A Comparison of the copper sensitivity of two economically important saltwater mussel species and a review of previously reported copper toxicity data for mussels: important implications for determining future ambient copper saltwater criteria in the USA. *Environ. Tox.* **24**. 618-628. (2009).

CCME, December 2007. Canadian water quality guidelines for the protection of aquatic life. Canadian Council of Ministers of the Environment, 6th Edition.

Martell, A., Smith, R. (2001). Critically selected stability constants of metal complexes, NIST database 46 version 6. NIST, Gaithersburg, MD 20899.

Martins, C.D.M.G., Barcolli, I.F., Giacomin, M.M., Wood, C.M., Bianchini., A. Acute toxicity, accumulation and tissue distribution of copper in the blue crab callinectes sapidus accimilated to different salinities: In vivo and in vitro studies. Aqua. Toxic. 101. 88-99. (2011).

Nadella, S.R., Fitzpatrick, J.L., Franklin, N., Bucking, C.P., Smith, S., Wood, C.M. Toxicity of dissolved Cu, Zn, Ni and Cu to developing embryos of the blue mussel (mytilus trossolus) and the protective effect of dissolved organic carbon. *Comp. Biochem. Physiol.* **149**, 340-348. (2009).

OECD environment health and safety publications, series on testing and assessment No. 29 Environment Directorate, organization for economic cooperation and development, April 2001.

Santore, R.C., Di Toro, D.M., Paquin, P.R., Allen, H.E., Meyer, J.S. Biotic Ligand Model of the Acute Toxicity of Metals. 2. Application to Acute Copper Toxicity in Freshwater Fish and Daphnia. *Environ. Toxic. And Chem.* **20**, 10, 2391-2402. (2001).

Smith, S. Solution of simultaneous chemical equilibria in heterogenous systems: implementation in matlab. Preprint submitted to *Elsevier*. October 2010.

Chapter 3: Sample Characterization by Fluorescence

3.1 Introduction

Fluorescence spectroscopy can be used to provide a molecular fingerprint of the molecular nature (related to source) of NOM and determine the stability of fluorophores in NOM during storage. Fluorescence spectroscopy is a highly selective and sensitive technique that was used for characterization of NOM. Fluorescence spectroscopy resolves fluorophores based on different fluorescent properties. NOM is particularly useful for fluorescence and fluorescence quenching because of the presence of aromatic structural groups. The concentration and chemical composition of NOM influences the intensity and shape of the fluorescence spectra allowing for different fractions of the NOM pool to be distinguished using detailed spectral fluorescence measurements (Coble et al. 1990; Coble 1996). DOM fluorescence has a broad excitation between 250 and 400 nm and a broad emission from 350 to 500 nm. The location of the excitation and emission peaks varies with the composition of DOM (Stedmon and Bro, 2008).

Terrigenous NOM can be detected in the excitation and emission ranges of 300–350 nm, 400–450 nm and 250–390 nm, 460–520 nm, suggesting the presence of terrestrially derived fulvic and humic material, respectively (Smith and Kramer, 1999; McKnight et al., 2001; Wu et al., 2003; Stedmon and Markager, 2005).

Autochthonous NOM can be detected by the excitation and emission peaks of 225–275 nm, 350 nm and 225–275 nm, 300 nm identifying microbially derived tryptophan-like and tyrosine-like fractions (Baker, 2001; Stedmon and Markager, 2005). An example of an Excitation-Emission Matrix (EEM) for a marine NOM, Nordic Reservoir, can be seen in Figure

3.1. Nordic Reservoir has high fulvic and humic acid-like fractions and low tryptophan and tyrosine-like fractions.
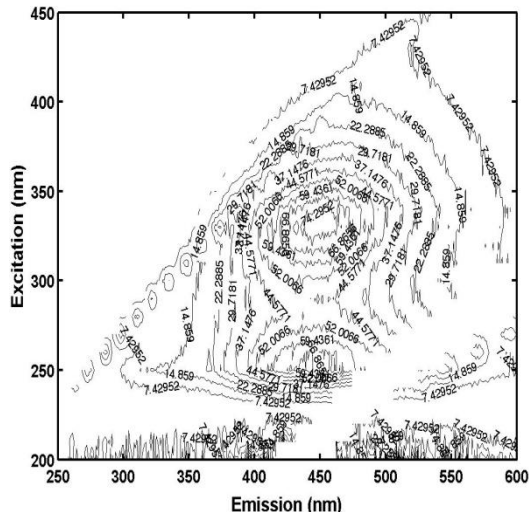
Figure 3.1: Nordic Reservoir NOM in seawater. EEM shows a high humic and fulvic like fraction with a low tryptophan and tyrosine-like fraction.

To quantify humic-, fulvic-, tryptophan-, and tyrosine-like fractions observed by fluorescence, parallel factor analysis (PARAFAC) is used. Through spectral deconvolution of a 'stack' of fluorescent EEMs, PARAFAC quantifies a minimum number of fluorescent components to describe each EEM in a set of related samples (Depalma et al., 2011b).

Natural organic matter (NOM) is mainly comprised of the humic substances, humic acid and/or fulvic acid, together with carbohydrates, proteins and lipids (Thurman 1985). Fulvic and humic acids have been found to be most abundant in NOM (Ericksen et al., 2001). Aquatic systems usually contain a mixture of terrigenous and autochtonous natural organic matter (NOM) (McKnight et al., 2001). Terrigenous NOM is terrestrially derived and is composed of organic matter from decomposition of plants (mostly lignin oxidation), containing carboxylic and phenolic functional groups attached to aromatic rings. The presence of the many aromatic

51

structural groups within NOM, as seen in Figure 3.2, allows for its fluorescent nature. Autochtonous NOM is composed from the organic matter from microorganisms and bacteria and is generated within the water column, containing proteinaceous functional groups including amines. The chemical structure of tryptophan and tyrosine can be viewed in Figure 3.3 and Figure 3.4. Sewage derived organic matter is also common and contains intermediate properties between terrigenous and autochtonous NOM.
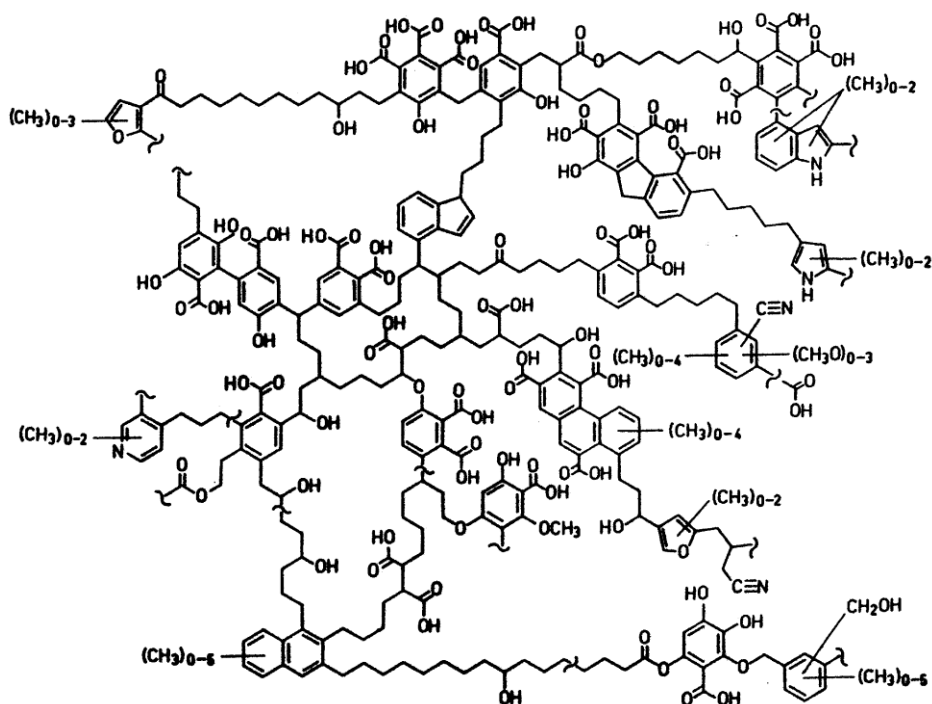
Figure 3.2: A proposed structure of a humic acid molecule containing carboxylic and phenolic functional groups attached to aromatic rings (Schulten et al., 1993).
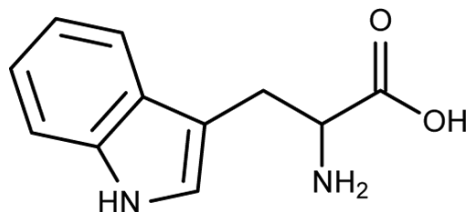
Figure 3.3: Tryptophan molecule. Trytophan-like components are present within NOM representing proteinacious material containing amine groups attached to aromatic rings.
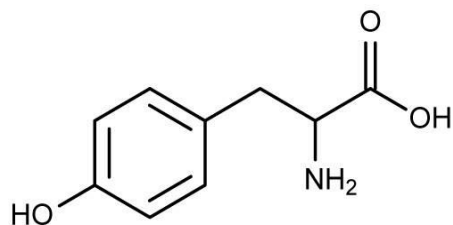
Figure 3.4: Tyrosine molecule. Tyrosine-like components are present within NOM representing proteinacious material containing amine groups attached to aromatic rings.

There is a lack of information regarding the molecular composition of marine NOM. Ocean profiles exist for two components, amino acids and carbohydrates. Amino acids account for 1-3% of the ocean pool while carbohydrates account for 2.5-7% of the DOC, leaving 90% of DOC uncharacterized (Benner, 2002).

3.2 Method

Fluorescence spectra of the NOM samples were collected using a Varian Cary fluorescence spectrophotometer with 1cm pathlength quartz cuvettes. A table of the NOM samples containing source, location and method of collection can be viewed in Table 3.1.

Table 3.1: NOM samples source, year collected and collection method.

NOM	Source	Year Collected	Collection Method
Bamfield	British Columbia. Collected deep into the Bamfield marine station inlet.	2010	Rodriguez and Bianchini, 2007
Pachena	Collected at the point where a river meets the Pacific ocean (bamfield, B.C.).	2010	Rodriguez and Bianchini, 2007
Offshore	Collected far off the coast of Bamfield, B.C.	2010	Rodriguez and Bianchini, 2007
Rio Grande	Extracted from water far off the coast in the Southern Atlantic	2010	Rodriguez and Bianchini, 2007
Harbour	Bamfield Harbour. Lots of boating activity.	2010	Rodriguez and Bianchini, 2007
Nordic Reservoir	IHSS substance	N/A	N/A
Inshore	Brazil	2009	Rodriguez and Bianchini, 2007

The fluorescence spectra were measured by using excitation wavelengths from 200 to 450nm using 10nm increments. The emission wavelengths were measured in the range of 250 to 650nm for every 1nm increment. The EEMs are plotted as contours to identify the fluorescing components. Parallel Factor Analysis (PARAFAC) was used to identify and quantify the component peaks in the EEMs, as implemented in the PLS toolbox (Eigen-vectors Research Inc, WA, USA). Each matrix contains fluorescence information for specific excitation/emission wavelength pairs. PARAFAC resolves this information into component spectra and relative component concentrations (Gheorghiu et al.,2010; Nadella et al., 2009; Depalma et al., 2011b).

3.3 Fluorescence Scans

The fluorescence scans before and after storage for each NOM can be found below in figures 3.5 to 3.11.

Seven different sources of organic matter were measured using fluorescence to determine quality and stability during storage time of a year and a half. The NOM samples were filtered through a 0.45 μm filter, acidified and stored in a fridge at 4ºC. Every NOM was diluted to a concentration of 10 mg C/L before fluorescence analysis. Each NOM sample source potentially contains a range of terrigenous, autochtonous and sewage derived organic matter. This can be quantified by determination of the fluorescence index (FI), equation (1).

$$FI_{EX370} = \frac{Em450}{Em500} \qquad (1)$$

An FI of ~1.9 indicates a microbially derived fulvic acid (autochtonous) and a FI of ~1.4 is a terrestrially derived fulvic acid (terrigenous) (McKnight et al., 2001). Bamfield and Harbour contain terrigenous and autochtonous organic matter. Pachena and Nordic Reservoir are solely terrigenous organic matter. Inshore Brazil is a mixture of terrigenous and sewage derived organic matter. Finally, Offshore and Rio Grande are solely autochtonous organic matter based on location.

(a)   (b)
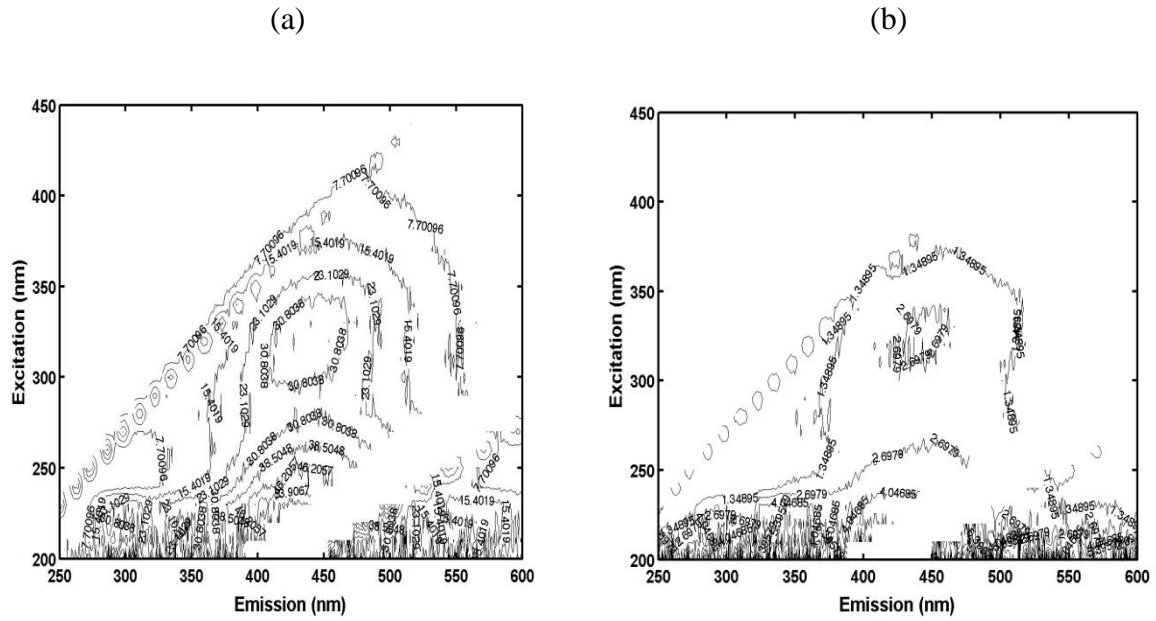
Figure 3.5: Fluorescence fingerprint of Bamfield NOM containing terrigenous and autochtonous NOM (a) before storage and (b) after storage.

(a)   (b)
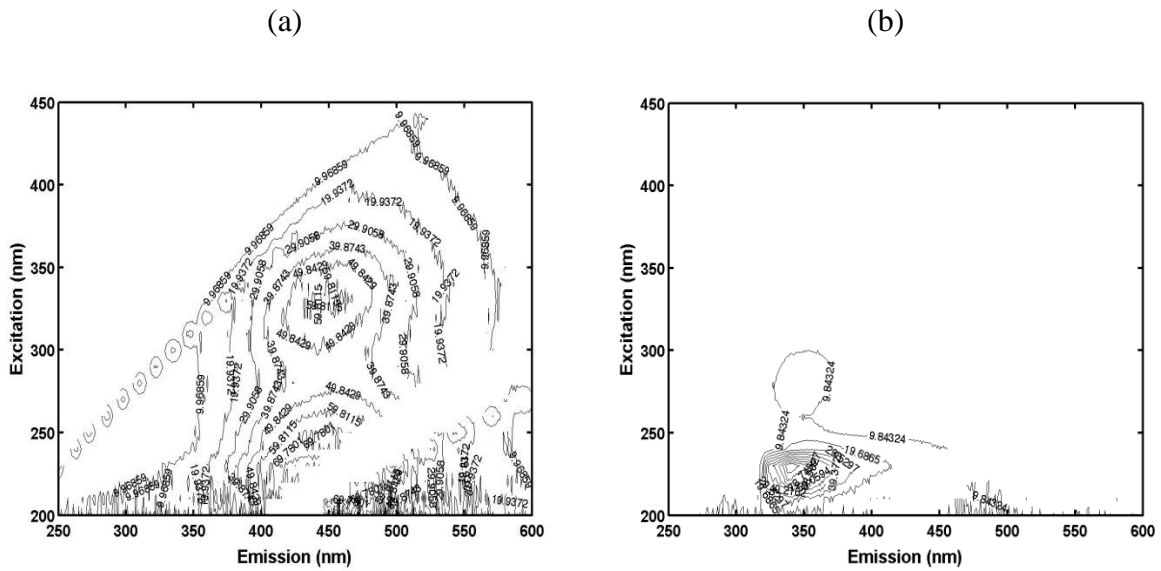
Figure 3.6: Fluorescence fingerprint of Pachena NOM containing terrigenous NOM (a) before storage and (b) after storage.
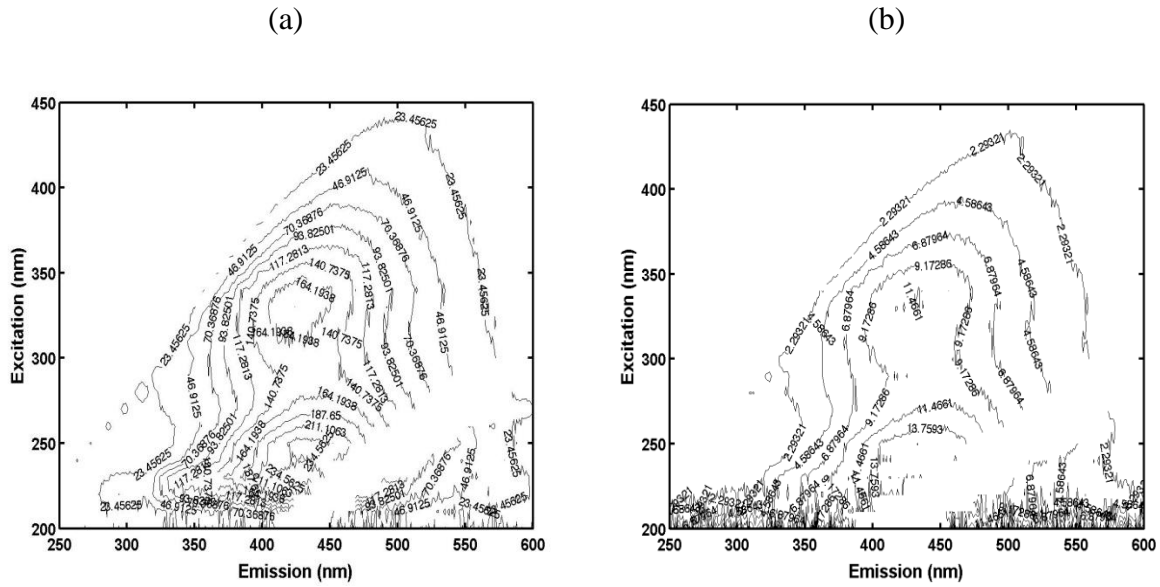
Figure 3.7: Fluorescence fingerprint of Inshore Brazil NOM containing sewage and terrigenous NOM (a) before storage and (b) after storage.

(a)

(b)
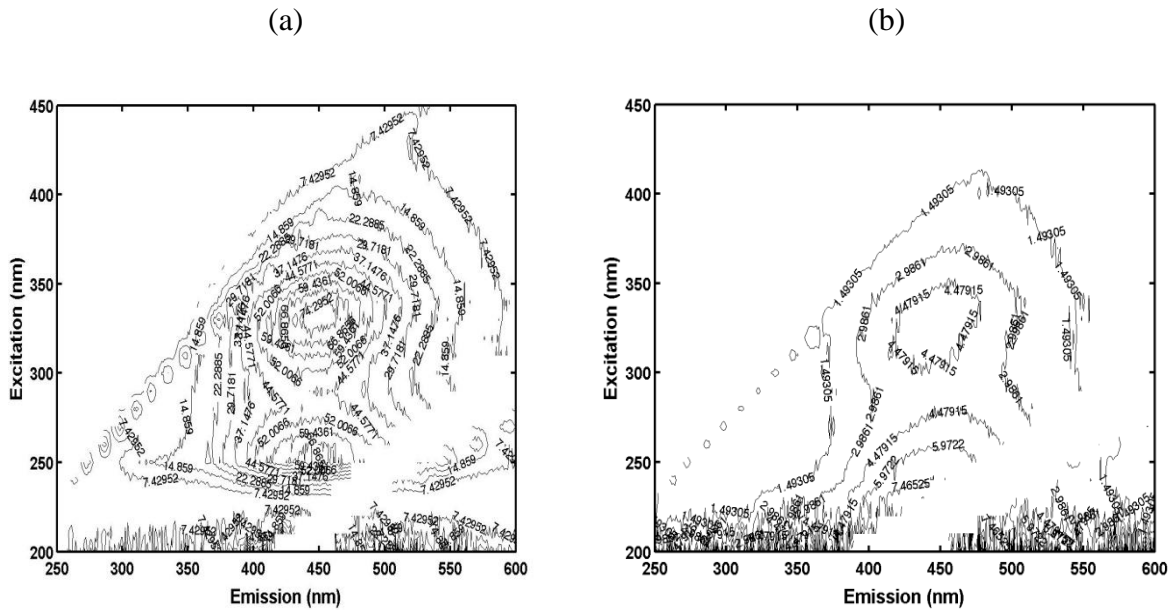
Figure 3.8: Fluorescence fingerprint of Nordic Reservoir NOM containing terrigenous NOM (a) before storage and (b) after storage.

(a)   (b)
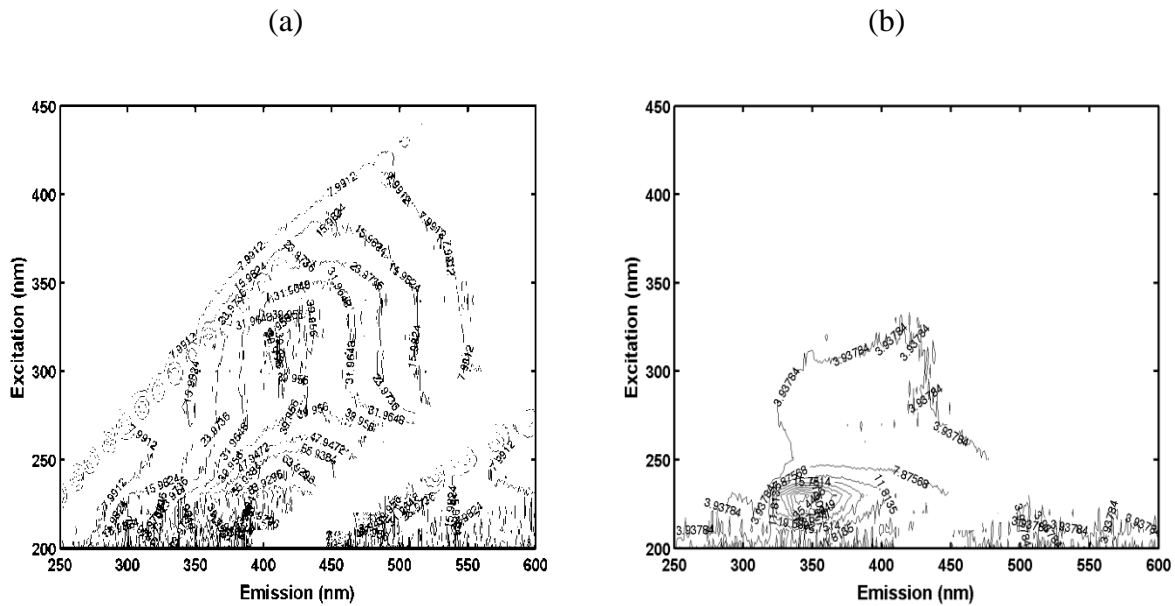
Figure 3.9: Fluorescence fingerprint of Rio Grande NOM containing autochtonous NOM (a) before storage and (b) after storage.

(a)   (b)
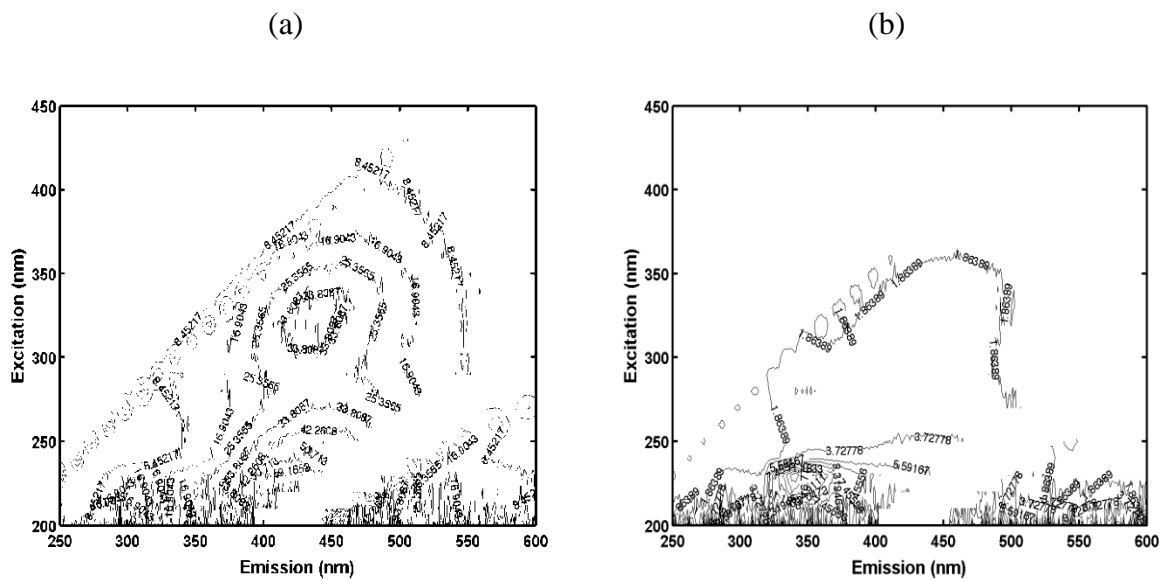
Figure 3.10: Fluorescence fingerprint of Harbour NOM containing terrigenous and autochtonous NOM (a) before storage and (b) after storage.
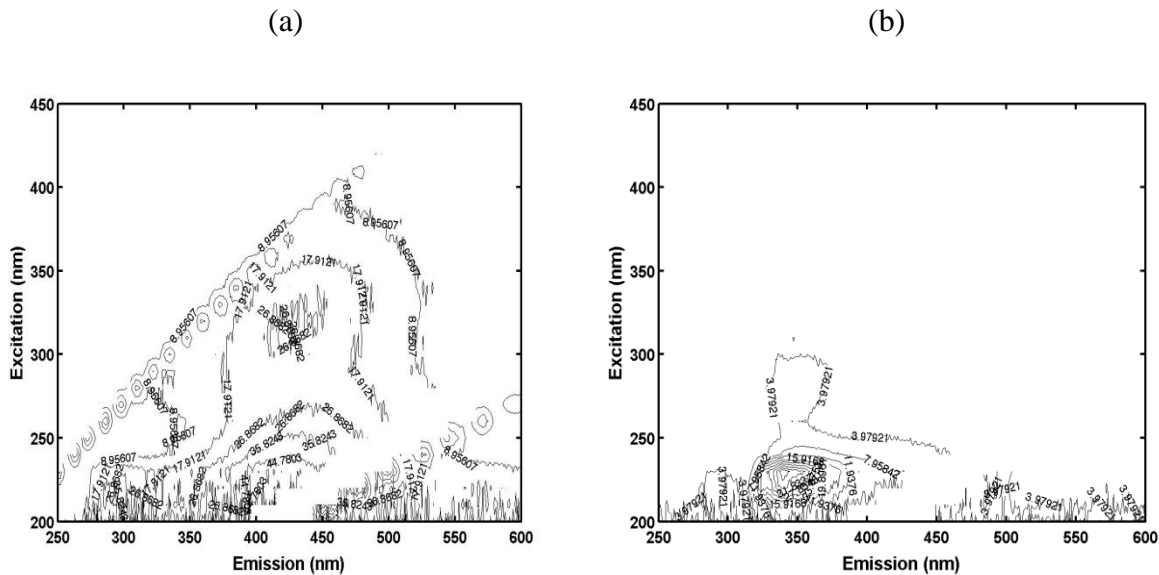
Figure 3.11: Fluorescence fingerprint of Offshore NOM containing autochtonous NOM (a) before storage and (b) after storage.

While analyzing the fingerprints before and after a storage period, significant changes can be viewed in the humic and fulvic acid quality in Figure 3.6 Pachena, Figure 3.9 Rio Grande, Figure 3.10 Harbour and Figure 3.11 Offshore NOM. In each of these figures there is a significant decrease or even absence of the humic and fulvic acid like components in the after storage found at an excitation of 360-390, 265nm and 320-340, 230nm with emission at 460-520nm and 400-450nm. A component analysis was performed on each fluorescent EEM using PARAFAC to determine the percent of each component before storage and after storage.

3.4 PARAFAC

Parallel Factor Analysis (PARAFAC) was used to identify and quantify the component peaks in the EEMs. PARAFAC was set to determine three resolved fluorescence components with 95.802 % of variability of the data explained by the three fluorophore model. The results for the three component fit in Figure 3.12 contain tryptophan-like at 280 nm and 230 nm

excitation, 340-350 nm emission, humic and fulvic-like at 360-390, 400-450 nm or 265 nm excitation, and 320-340 nm, 460-520 nm emission, and tyrosine-like at 280 and 230 nm excitation and emission at 300 nm.
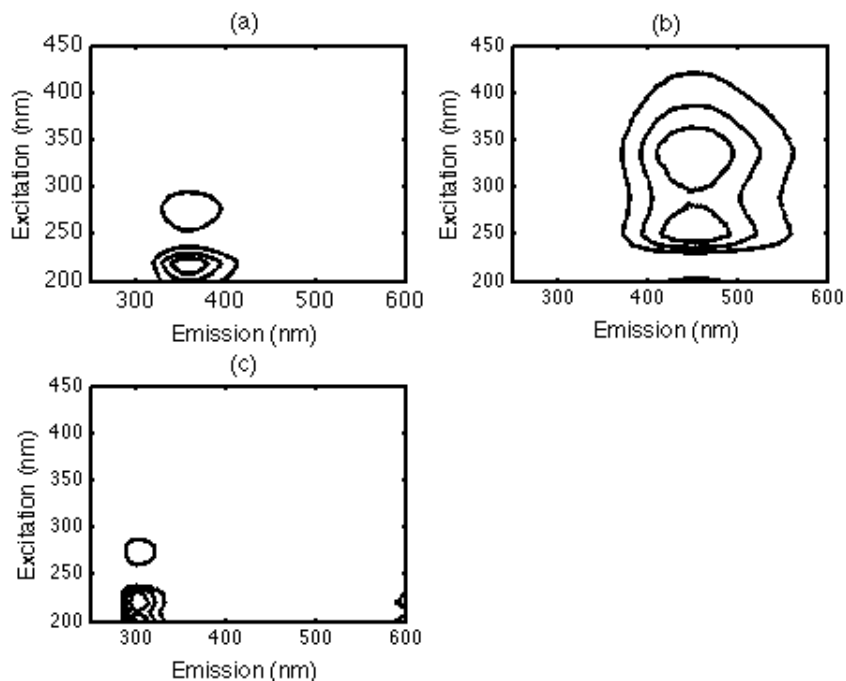
Figure 3.12: Parallel Factor Analysis (PARAFAC) results showing the three resolved fluorescence components of each NOM isolate (a) Tryptophan-like component (b) Humic and Fulvic-like component (c) Tyrosine-like component.

The fluorescence index (FI) was calculated using equation (1) for each NOM source and compared to determine whether the fulvic acid was microbially derived (~1.9) or terrestrially derived (~1.4). These results can be found in Table 3.2.

Table 3.2: Fluorescence Indices for NOM sources before and after storage.

Source	FI (Before, After)	Classification
Bamfield	1.21, 1.20	Terrestrial Fulvic Acid
Pachena	1.23, 1.12	Terrestrial Fulvic Acid
Offshore	1.68, 1.37	Terrestrial Fulvic Acid
Rio Grande	1.45, 1.41	Terrestrial Fulvic Acid
Harbour	1.18, 1.23	Terrestrial Fulvic Acid
Nordic Reservoir	1.35, 1.41	Terrestrial Fulvic Acid
Inshore	1.52, 1.54	Terrestrial Fulvic Acid

The relative concentration of each of the three components in the different NOM sources were converted to percent in equation (2) and plotted in a bar graph.

$$\%Fluorophore_{component1} = \frac{[component\ 1]}{[Total\ Component]} * 100 \qquad (2)$$

Figure 3.13 displays the percent of components present within the organic matter before storage. Each source of organic matter has a different ratio of tryptophan-like, humic and fulvic-like and tyrosine-like components. Pachena and Nordic Reservoir which were both terrigenous NOM had extremely similar ratios of components; above 80% humic and fulvic acid with less than 10% each of tryptophan and tyrosine. Offshore and Rio Grande were both classified as autochtonous NOM and both contain less of the humic and fulvic acid like component and more of the proteinacious materials (tryptophan and tyrosine-like). Inshore Brazil was a mix of terrigenous and sewage derived NOM, the ratio appears very similar to the solely terrigenous

NOM of Pachena and Nordic Reservoir except with a higher fraction of tryptophan-like component. Finally Bamfield and Harbour were classified as a mixture of terrigenous and autochtonous NOM and do have a relatively high amount of tryptophan and tyrosine-like components, 20% and 15-20% respectively, with the rest being humic and fulvic-like material.
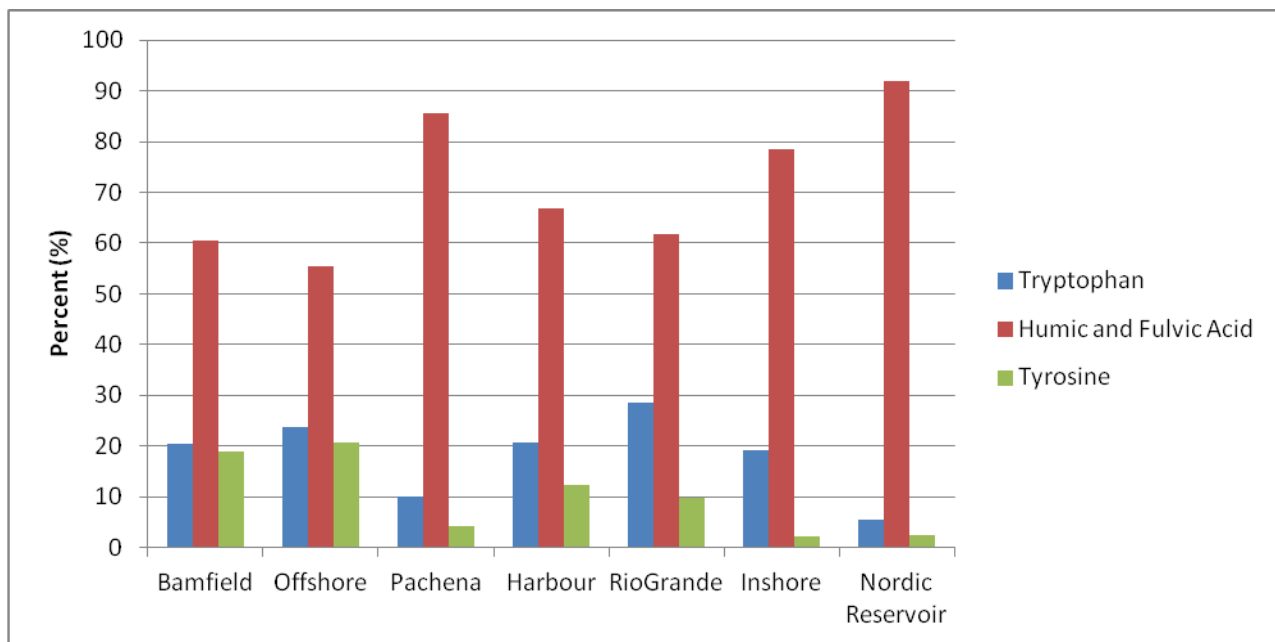
Figure 3.13: Percent of tryptophan-like, humic and fulvic-like, and tyrosine-like organic material present within each NOM sample before storage.

Figure 3.14 displays the relative percent of each component after storage. It appears that for certain NOM sources, the humic and fulvic-like material decreased during storage and the tryptophan-like material increased with tyrosine-like material staying relatively the same. Pachena had tryptophan-like material increase from 10.1% before storage to 72.2% after storage, with a humic and fulvic-like decrease from 85.1% to 16.1%. The same trend can be seen with Harbour and Rio Grande. Harbour had 20.7% tryptophan-like material and 66.9% humic and fulvic-like material before storage, which changed to 51.7% and 35.1% after storage. Rio Grande

had a tryptophan-like material change of 28.6% to 62.3% and a humic and fulvic-like change of 66.9% to 25.2%. A possible reason for this change is that the humic and fulvic-like material is precipitating out of solution during storage. The Pachena DOM had an obvious precipitate formation in the solution after storage; sonication did not redissolve the precipitate.
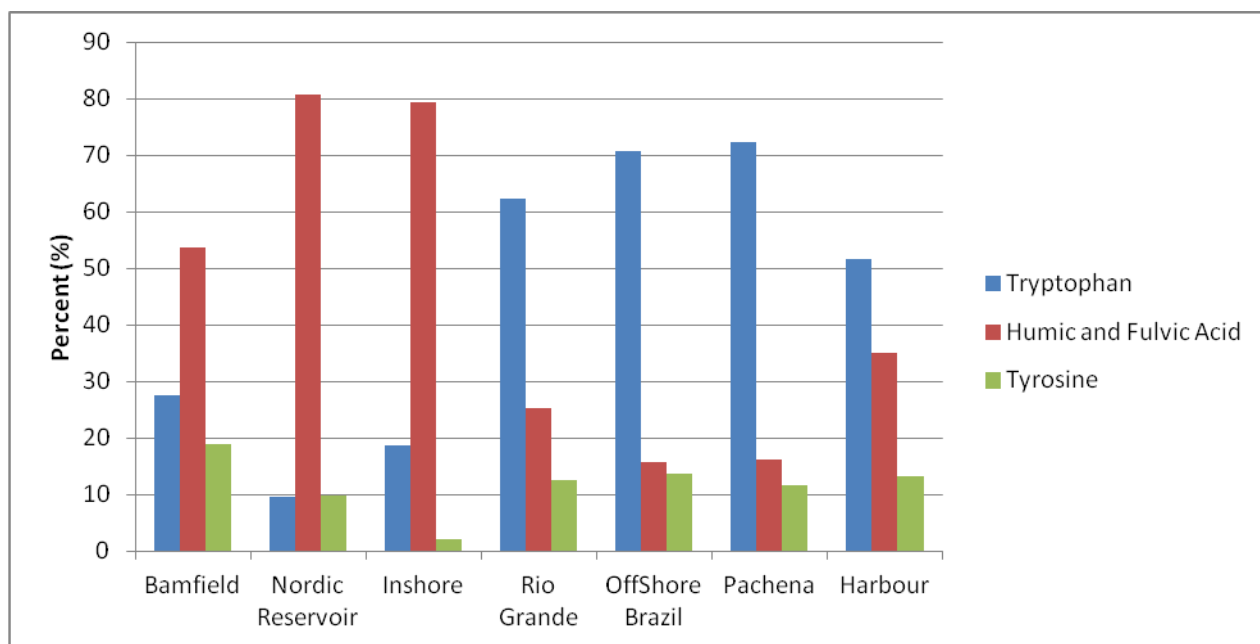
Figure 3.14: Percent of tryptophan-like, humic and fulvic-like, and tyrosine-like organic material present within each NOM sample after storage.

The percent of each component before storage and after storage were plotted against each other and compared to a 1:1 line to determine whether the changes with the quality of NOM were significant (Figure 3.15). The tryptophan-like material does not scatter around the 1:1 line as would be expected for a systematic change within the system but is consistently above the line. The humic and fulvic-like material, similar to the tryptophan-like material does not scatter around the line but is consistently below it. The tyrosine-like material scatters closely around the line.
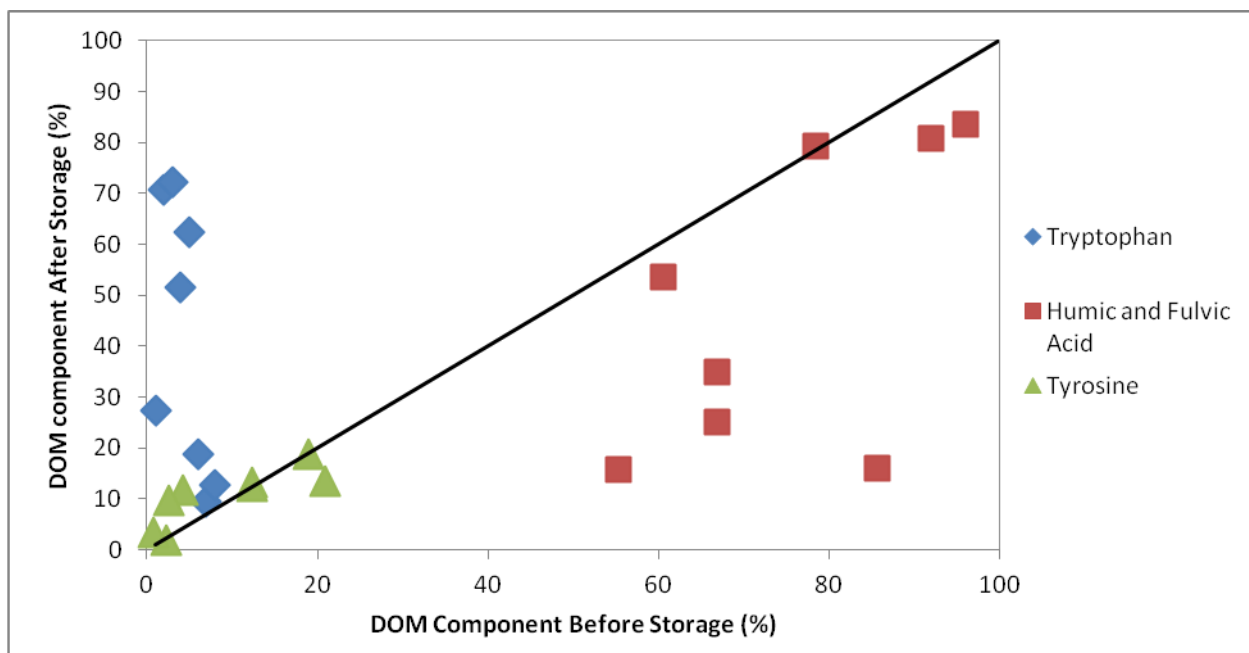
Figure 3.15: NOM component of Tryptophan-like material, humic and fulvic-like material and tyrosine-like material before storage versus after storage against a 1:1 line.

Depalma (2009) showed that NOM fluorescence did not change over storage. The change in fluorescence after storage demonstrated within this chapter could be attributed to the difference in the collection method. The method used to collect the samples was Rodriguez and Bianchini (2007). This process involves filtration with 1 and 0.5 μm mesh filters, acidification to a pH of 2 with HCl, passage through PPL cartridges (to remove highly polar species), remove the salts from the resin before elution of DOM, DOM elution with methanol, lyophylization, DOM solution prepared with Milli-Q water, and storage in the dark at 4ºC. This process may not leave the NOM as stable as was seen by Depalma (2009).

3.5 Conclusion

Fluorescence spectroscopy provided EEM's which were used as fingerprints for each of the different DOM sources before and after storage. FI was determined for all the NOM samples

and had a range of 1.12 to 1.54 indicating that the fulvic acid within the samples was terrestrially derived. PARAFAC was used to determine the relative concentration of three components within the organic material determined to be tryptophan-like, humic and fulvic-like and tyrosine-like. The NOM samples with similar classifications, solely terrigenous or solely autochtonous had very similar ratios of each component before storage. Comparison of the relative percents of each of these components showed significant changes within the tryptophan-like material and the humic and fulvic-like material after storage. The DOM did not remain stable and the quality of the sample changed during the storage procedure. This potentially was caused by the method used to collect the NOM samples.

3.6 References

Baker, A. Fluorescence excitation–emission matrix characterization of some sewage-impacted rivers. *Environ. Sci. Technol*., **35**. 948–953. (2001).

Coble, P.G. Characterization of marine and terrestrial DOM in seawater using excitation-emission matrix spectroscopy. *Mar. Chem.,* **51**. 325–346. (1996).

Coble PG, Green SA, Blough NV, Gagosian RB. Characterisation of dissolved organic matter in the Black Sea by fluorescence spectroscopy. *Nature*. **348**. 432-435. (1990).

DePalma S.G.S., Arnold W.R., McGeer J.C., Dixon, D.G., Smith, D.S. Protective effects of dissolved organic matter and reduced sulfur on copper toxicity in coastal marine environments. *Ecotox. And Environ. Saf.* **74.** 230-237.(2011b).

Depalma, S.G.S and Smith, D.S. Characterization of dissolved organic matter and reduced sulphur in coastal marine and estuarine environments: Implications for protective effects on acute copper toxicity. A thesis submitted to Department of Biology. University of Waterloo. 2009.

Ericksen, R.S., Nowak. B. Van Dam, R. Copper Speciation and toxicity incontaminated Estuary. *Super. Sci. Rep.* **163**, 1-29. (2001).

Gheorghiu, C., Smith, D.S., Al-Reasi, H.A., McGeer, J.C., Wilkie, M.P. Influence of natural organic matter (NOM) quality on Cu-gill binding in the rainbow trout (oncorhynchus mykiss). Aqua. Tox. 97, 343-352. (2010).

McKnight, D.M., Boyer, E.W., Westeroff, P.K., Doran, P.T., Kulbe T., Anderson, D.T. Spectrofluorometric characterization of dissolved organic matter for indication of precursor organic materials and aromaticity. *Limnol. Oceanogr*. **46**, 38-48. (2001).

Nadella, S.R., Fitzpatrick, J.L., Franklin, N., Bucking, C.P., Smith, S., Wood, C.M. Toxicity of dissolved Cu, Zn, Ni and Cu to developing embryos of the blue mussel (mytilus trossolus) and the protective effect of dissolved organic carbon. *Comp. Biochem. Physiol.* **149**, 340-348. (2009).

Rodrigues, S.C. and Bianchini, A. Extraction and concentration of Freshwater-seawater-derived dissolved organic matter for use in aquatic toxicological studies. *J. Braz. Soc. Ecotoxicol.* **2.** 275-281. (2007).

Schluten, H.R. A state of the art dtructural concept for humic substances. *Naturwissenschaften.* **80**, 29-30. (1993).

Smith, D.S., Kramer, J.R. Fluorescence analysis for multi-site aluminum binding to natural organic matter. *Environ. Internat.,* **25**. 295–306. (1999).

Stedmon, C.A. and Bro, R. Characterizing dissolved organic matter fluorescence with parallel factor analysis: a tutorial. *Limnol. Oceanog. Methods*, **6**. 572–579. (2008).

Stedmon, C.A. and Markager, S.Resolving the variability in dissolved organic matter fluorescence in a temperate estuary and its catchment using PARAFAC analysis. *Limnol. Oceanog.,* **50**. 686–697. (2005).

Thurman E.M. Organic geochemistry of natural waters, Martinus Nijhof/Dr. W. Junk Publishers, Dordrecht (1985).

Wu, F.C., Evans, R.D., and Dillon, P.J. Separation and characterization of NOM by high-performance liquid chromatography and on-line three-dimensional excitation emission matrix fluorescence detection. *Environ. Sci. Technol.,* **37**. 3687–3693. (2003).

Chapter 4 Fluorescence Quenching Analysis for Copper, Nickel, Zinc and Lead in saltwater media

4.1 Introduction

Trace amounts of metals are present as natural components of the environment and at low concentrations, many metals including copper and zinc are essential for life. Unfortunately, due to anthropogenic inputs, trace metal concentrations are increasing. This increase can potentially result in toxicity to organisms and there is a need to monitor the levels and effects of these metals in aquatic systems. In seawater systems, there are many components including increased salinity and NOM that can compete or bind bioavailable metal and decrease toxicity.

For freshwater systems the Biotic Ligand Model (BLM) has been successful in predicting metal toxicity as a function of water chemistry. The BLM has become an excellent tool for regulatory and risk assessment purposes. For saltwater systems, such as estuaries and ocean environments, BLMs have not been as extensively developed. A requirement for BLM development in salt water is an understanding of metal interactions (speciation) in saltwater environments.

Aquatic systems usually contain a mixture of terrigenous and autochthonous natural organic matter (McKnight et al. 2001). Terrigenous DOM is terrestrially derived and is comprised of organic matter from decomposition of plants (mostly lignin oxidation products), containing carboxylic and phenolic functional groups attached to aromatic rings. Autochthonous DOM is composed from the organic matter from microorganisms and bacteria and is generated within the water column, containing proteinaceous functional groups including amines. Sewage derived organic matter contains intermediate properties between terrigenous and autochthonous DOM.

The BLM has been adopted by the USEPA for prediction of metal toxicity for a number of dissolved metals in freshwaters. The BLM is based on equilibrium calculations of metal speciation and has a numerical scheme to predict toxic metal concentrations and establish site specific criteria for a given location depending on its water chemistry parameters (Santore et al., 2001). Although well developed for freshwater, there is a need for saltwater research for a marine BLM. The purpose of this research is to characterize dissolved organic matter and its binding characteristics with divalent metal cations, Cu^{2+}, Zn^{2+}, Pb^{2+} and Ni^{2+} in marine systems using fluorescence spectroscopy.

4.2 Experimental Methods

Fluorescence spectra of the NOM samples were collected using a Varian Cary fluorescence spectrophotometer with 1cm pathlength quartz cuvettes at an excitation of 275nm and emission range of 300 to 600nm. Luther Marsh NOM collected from southern Ontario (43°54′N, 80°26′W) was dissolved in OECD synthetic seawater recipe in Chapter 2, at a concentration of 5 mg C/L and maintained at a constant pH of 7.802 +/-0.002. The NOM was titrated with each metal individually and allowed for a 15 to 20 minute equilibration time or until the scan stabilized.

Additionally, 10μM tryptophan (>98% Sigma-Aldrich, USA) prepared with OECD synthetic seawater was titrated with each of the metals at a constant pH of 7.802 +/-0.002 to validate the method.

4.3 Fluorescence Quenching to Determine Binding Capacity and logK

Fluorescence quenching has been used previously to determine equilibrium constants and binding capacity with great success in freshwater applications (Smith and Kramer, 2000). In natural waters, dissolved organic matter fluorescence is quenched in the presence of metals

through formation of organo-metal complexes. The natural organic matter (NOM) is a fluorescent compound due to the presence of the aromatic structural groups within it as discussed in Chapter 3. As the metals bind to the NOM, it produces a less fluorescent compound (M-NOM) and results in fluorescence quenching seen in equation (1) and log K expression in (2). Fluorescence is based on a single or a combination of fluorescence species multiplied by its proportionality constant as seen in expression (3). The quenching is seen because the proportionality constant for the M-NOM is lower than for the NOM.

$$M^{2+} + NOM \rightarrow M\text{-}NOM \qquad (1)$$

$$K = \frac{[M-NOM]}{[M^{2+}][NOM]} \qquad (2)$$

$$F = k_{NOM}[NOM] + k_{M\text{-}NOM}[M\text{-}NOM] \qquad (3)$$

4.4 Results: Luther Marsh Titration in Seawater

This spectroscopic technique was applied for copper, lead, nickel and zinc with a freshwater isolate, Luther Marsh, in artificial seawater. Figure 4.1 displays an example of the fluorescence spectra quenching for nickel additions of 0 to 188 ppb. It can be observed that with each addition of nickel, the fluorescence intensity decreases because the fluorescent Luther Marsh dissolved organic matter is binding to the nickel and becoming less fluorescent. It is assumed that static quenching is occurring when the metal and NOM interact. There is no spectral shifting present in the fluorescence spectra which means that only one fluorophore is present within the system. If more than one fluorophore was present under the peak then, as the metal bound to one or the other, the fluorescence spectra would shift accordingly.
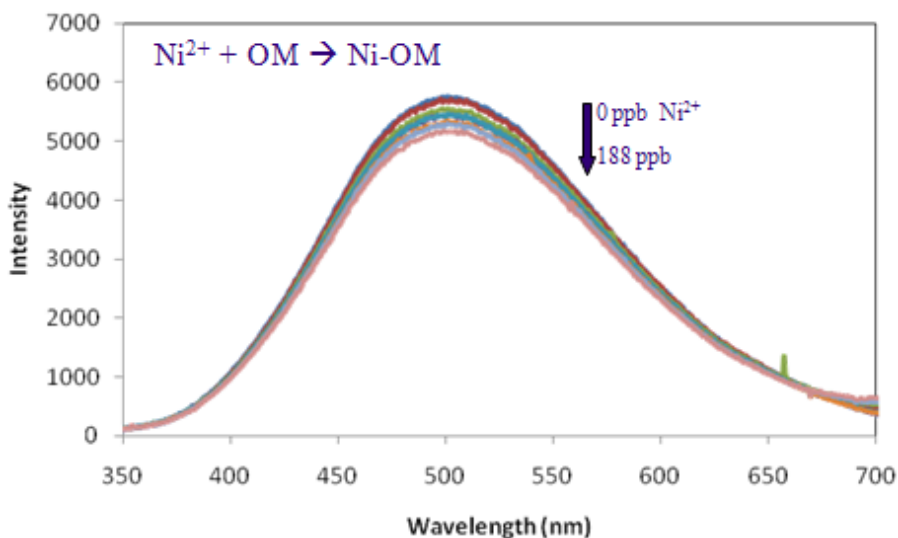
Figure 4.1: Fluorescence quenching spectra of Luther Marsh dissolved organic matter with nickel additions ranging from 0 to 128 ppb.

This fluorescence quenching method was repeated with lead (0 to 50ppb), zinc (0 to 129 ppb) and copper (0 to 120 ppb) and the freshwater isolate luther marsh in OECD synthetic seawater. Fluorescence quenching is a function of equilibrium binding parameters including logK equation (2), binding capacity (L_T) and proportionality constants for the ligand and metal ligand complexes equation (3). Fitting a fluorescence quenching curve with a Ryan Weber equilibrium model, as discussed in section 1.6 in Chapter 1, allows for the determination of logK and binding capacity for the NOM.

Figure 4.2 displays fluorescence quenching curves for Luther Marsh NOM with nickel, copper, lead and zinc fit to Ryan Weber equilibrium curve to solve for logK and binding capacity. As the total metal concentration for each metal is increased, the fluorescence is decreased due to the formation of a less fluorescent metal organic matter complex. Table 4.1 displays equilibrium constants and binding capacities for the complexation of these metals and

71

the freshwater isolate were obtained. Equilibrium constants (LogK) obtained from fluorescence quenching curves fit to a modified Ryan-Weber model showed a binding strength order of $Zn^{2+}>Pb^{2+}>Ni^{2+}>Cu^{2+}$. The Irving-Williams series shows the binding strength as $Ni^{2+}<Cu^{2+}>Zn^{2+}$ with no placement for lead and does not agree. Binding capacity ($LogL_T$) for each of the metals was found to range from 10.0 to 17.8 nmol/mg C. This indicates that the metals are binding to the same average site on the freshwater NOM and that the Luther Marsh NOM has a similar binding capacity for each of the metals. Based on these results, it appears as though fluorescence quenching can be used to quantify organic matter Pb, Zn, Cu and Ni interactions. These results imply that NOM is predicted to be protective at the EC_{50} region of the metal with the Luther Marsh freshwater isolate. The utility of fluorescence quenching has to be validated for model systems and the underlying assumption of static quenching occurring must be confirmed.
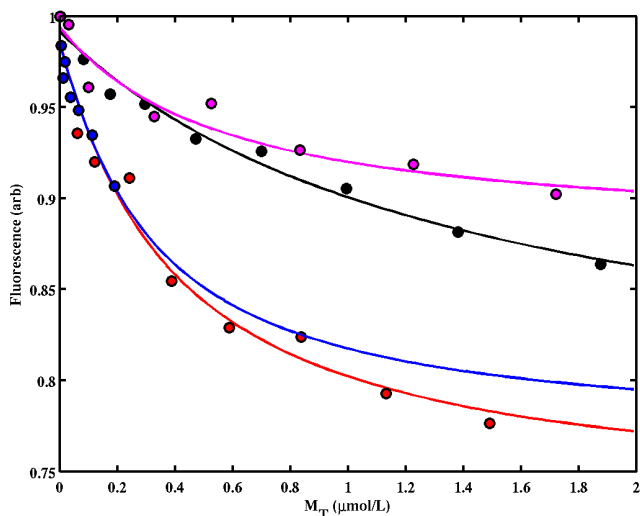
Figure 4.2: Fluorescence quenching curves from nickel, copper, lead and zinc fit to Ryan Weber equilibrium curve to solve for logK and binding capacity for nickel (pink), copper (black), lead (blue) and zinc (red).

72

Table 4.1: LogK and L_T values from equilibrium fitting of fluorescence quenching with metals are arranged from most toxic to least toxic. EC_{50} for *Mytilus trossolus* embryo toxicity test (Nadella et al., 2009).

Metals	EC_{50} (nmol/L)	LogK	L_T (nmol/mg C)
Copper	0.151	5.9	12.6
Lead	0.965	6.6	17.8
Zinc	1.51	6.7	15.8
Nickel	2.56	6.3	10.0

4.5 Fluorescence Quenching Testing

Due to the great promise of this technique for seawater applications, the fluorescence quenching method was applied to a raw sample from Jimbo Bayou in Miami FL, USA. The sample was held at a constant pH of 7.67 and DOC concentration of 3.47 mg C/L while fluorescence scans were taken at increasing additions of copper. Figure 4.3 shows the fluorescence quenching and equilibrium model fittings for the Jimbo Bayou Miami sample. As copper concentration is increased from 0 ppb to 231 ppb, the fluorescence intensity decreases due to the formation of less fluorescent copper organic matter complexes. The fluorescence scan shows multiple fluorophores present in the sample. Specifically, the wavelength shifting observed within the box indicates that more than one fluorophore is present under that broad peak. Fluorescence for multiple combinations of NOM can be described by equation (4). The fluorescence spectra contains multiple fluorescent NOM and the decreased fluorescent copper bound to the NOM. Spectra with different emission maxima have a different response to the copper and result in spectral shifts which were seen in the Jimbo Bayou sample. This is because one NOM would bind copper more efficiently than the other.

$$Fspec = Spec_{NOM1}[NOM1] + Spec_{CuNOM1}[CuNOM1] + Spec_{NOM2}[NOM2] + Spec_{CuNOM2}[NOM2] \quad (4)$$
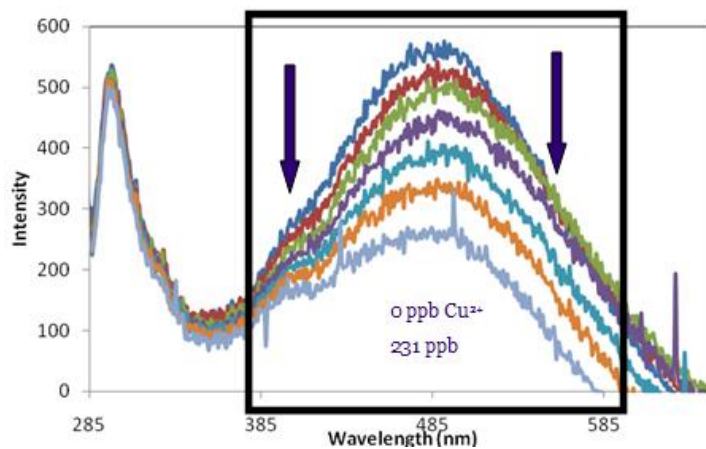
Figure 4.3: Fluorescence of Jimbo from a Miami Bayou with copper. This sample shows multiple fluorophores, the wavelength shifting within the box indicates more than one fluorophore present under the peak.

SIMPLISMA (SIMPLe-to-use Interactive Self-modeling Mixture Analysis), a spectral resolution technique, was used to determine the minimum number of fluorophores present within the sample of DOM using the method Windig and Guilment (1991). This method involves selecting variables that are proportional in intensity to one of the components in the mixture. Once this has been identified, a matrix equation is solved to determine the pure spectra and concentrations of each component. This is done using least squares fitting. Negative concentrations were prevented by modifying the SIMPLISMA code (Appendix D) so that constrained non-negative least squares optimization was used to solve the matrix equation. Figure 4.4 displays the spectral deconvolution of the peak within the box. This shows the presence of two fluorophores, an autochtonous organic matter (green line) and terrigenous organic matter (blue line). The autochtonous organic material was classified by its low emission wavelength due to fulvic-like organic material while the terrigenous organic material was classified by its higher emission wavelengths due to high humic-like components.

74
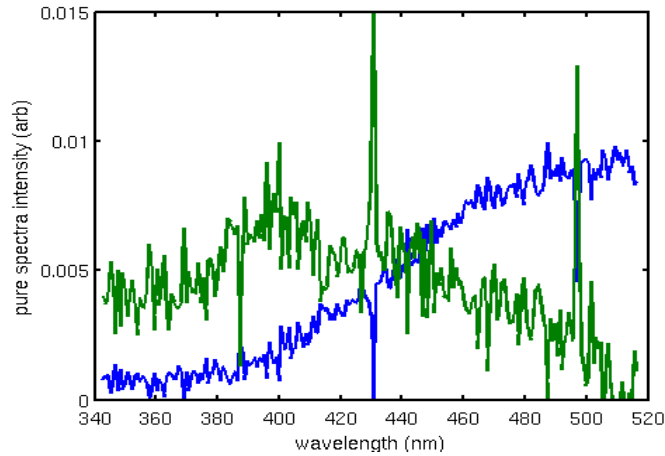
Figure 4.4: Uncorrected Resolved Spectra. Spectral deconvolution of the peak shows the presence of two fluorophores. The green line represents autochtonous organic matter (mainly proteinaceous material) while the blue line represents terrigenous organic matter.

A binding site model was used to interpret the fluorescence quenching results with each fluorescent component representing a binding site. To do this a multi-site Ryan-Weber model was employed (Smith and Kramer, 1999). Fluorescence at any excitation and emission wavelength pair is a function of concentration of the fluorescence species as seen in equation (5).

$$F(M_T) = \sum_{j=1}^{m} (e_j c_j(M_T)) + \xi \qquad (5)$$

Where e_j and c_j are proportionality constants and c_j is a function of M_T and ξ is an experimental variation assumed to have a Gaussian distribution. The equation can be rewritten in matrix form for p additions of metal seen in equation (6).

$$F = CE + \Xi \qquad (6)$$

Here F=pxq where column is length p for q different sets of fluorescence observations and C=pxm where there is a column of concentrations for each of the m fluorescent species. E=mxq containing a proportionality constant for each species at each set of observation wavelengths. The calculation is simplified by assuming that each wavelength pair can be found for each

75

component at which fluorescence depends on the speciation only at that component. The fluorescence of component n, of a total of N components, can be written as equation (7).

$$F_n = C_n(\theta)E_n + \Xi_n \qquad (7)$$

Linear components are contained in matrix E_n and correspond to the fluorescence of free ligand and metal bound ligand. The parameters are common to all N sets of observations and are collected in the vector θ. The parameters include N conditional stability constants (K') and N ligand concentrations (L'_T) (Smith and Kramer, 1999).

Figure 4.5 displays the resolved fluorescence quenching curves for each of the fluorophores under the peak. While both seem to bind the copper added to the system, the blue points, representing the terrigenous organic matter, appear to have a higher capacity for copper and continue to quench past 1-1.5 µmol/L. The logK and L_T parameters can be found in Table 4.2. The results indicate that the autochtonous OM has a larger logK value but binds less copper per mg of carbon. Meanwhile, terrigenous OM binds less strongly then autochtonous but has an increased binding capacity by a factor of eleven.
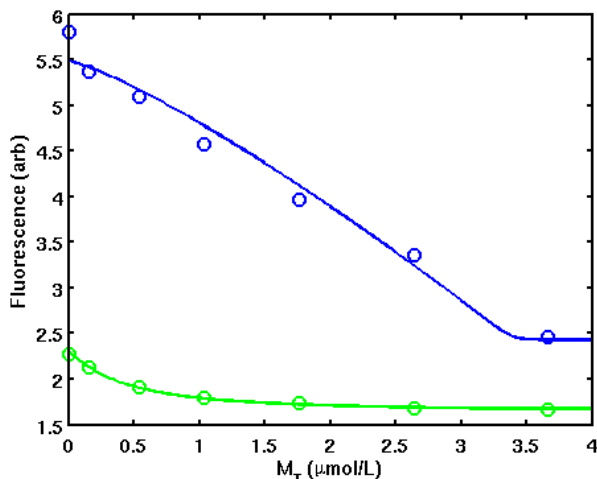
Figure 4.5: Fluorescence quenching for the resolved fluorophores under the peak in the Raw Miami Bayou sample.

Table 4.2: logK and L$_T$ binding parameters for Jimbo Bayou with copper.

Organic Matter Component	logK	L$_T$ (μmol/mg C)
Autochtonous OM	10.38	0.078
Terrigenous OM	9.20	0.89

Additionally, the Jimbo Bayou was analyzed with copper ion selective electrode (ISE) by another masters student using the method from Ericksen et al (1999). The comparison can be found in Figure 4.6. The solid line is the speciation model from the fluorescence quenching, the data points are ISE measurements and the dashed line is the 1:1 free copper to copper total. The two methods agree indicating a working fluorescence quenching method for copper.
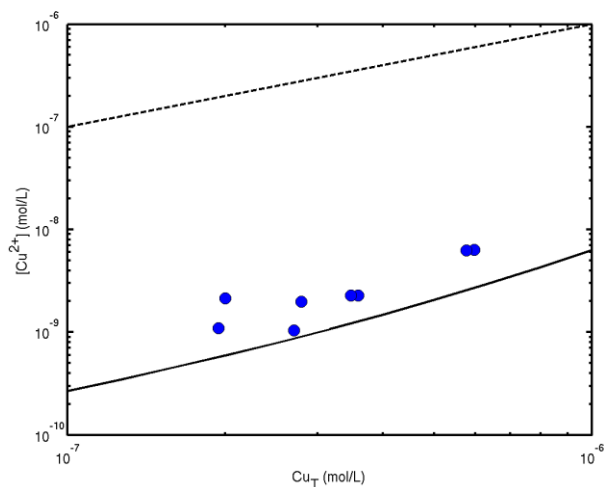
Figure 4.6: Fluorescence quenching speciation solid line comparison to copper ion selective electrode (blue data points) measurements. Dashed line is the 1:1 free copper to total copper.

4.6 Fluorescence Quenching comparison to Toxicity Tests

Based on the results from the Luther Marsh isolate and fluorescence quenching results, the method was applied to a Nordic Reservoir DOC for comparison of logK and L$_T$ by fluorescence quenching to lead and zinc toxicity development embryo tests. The lead EC$_{50}$

results showed that the DOC is protective for lead but an increase in DOC did not show greater protection. A DOC concentration of 2 mg C/L provided an EC_{50} of 738 nM while a concentration of 12 mg C/L had an EC_{50} of 757 nM. The EC_{50}'s demonstrate that the Nordic Reservoir DOC protection displays no dose dependence. This was surprising because it was assumed that an increased amount of DOC would have an increased number of binding sites and provide further protection for lead.

Table 4.3 demonstrates that the fluorescence quenching results do not agree with the conclusions of the lead toxicity tests. The fluorescence quenching parameter indicates an increase in the DOC concentration resulted in an increased binding capacity for lead by a factor of five. This indicates that there should be dose dependence by the DOC with lead in protection because according to the fluorescence quenching results, at a higher DOC there are more available binding sites for the metal.

Table 4.3: Binding Capacity for Nordic Reservoir organic matter concentrations of low and high DOC with comparison to EC_{50} values for *Mytilus galloprovincialis* in seawater. 95% confidence values indicated by ranges of values.

Nordic Reservoir	EC_{50} (nmol/L) *Mytilus galloprovincialis*	FQ Binding Capacity (nM)
0 mg C/L	304.04 (173-453)	---
2 mg C/L NR	738.38 (680-796)	6.35
12 mg C/ NR	757.69 (680-830)	32.34

4.7 Testing of Fluorescence Quenching Method

The contradiction between the chemistry and the biological observations suggested the need for a validation of the fluorescence quenching method. The fluorescence quenching method was tested in model systems where speciation can be calculated. Tryptophan was chosen because it was necessary to pick a test ligand for which certified equilibration constants exist as in National Institute of Standard and Technologies (NIST) (Martell and Smith, 2001).

Figure 4.7 displays the measured quenching for lead, copper, zinc and nickel. The data points are measured fluorescence quenching and lines are theoretical fluorescence quenching model based on NIST equilibrium constants and calculated speciation. Interpolation graphs used to determine corrected logK values can be found in Appendix B. The measured logK values are plotted versus salinity as described in Chapter 2. The measured points are connected by a curve or line depending on the trend in the data and the value for a salinity of 0.7 is taken from that line.

Theoretical fluorescence at each point in the titration is calculated by determining the speciation of the system using equilibrium constant values from NIST (Martell and Smith, 2001). With known calculated speciation, equation (8) can be used to calculate predicted fluorescence. In particular, the HTrp term is calculated with added metal at a fixed pH of 7.8. The equation assumes that HTrp is the only fluorescent species. kHTryp is a proportionality constant determined by the fluorescence response in the absence of metal (first data point). There are no adjustable parameters within the calculation. Matlab codes used for calculation of the theoretical fluorescence can be found in Appendix C.

$$F = k_{HTryp}[HTryp] \qquad (8)$$
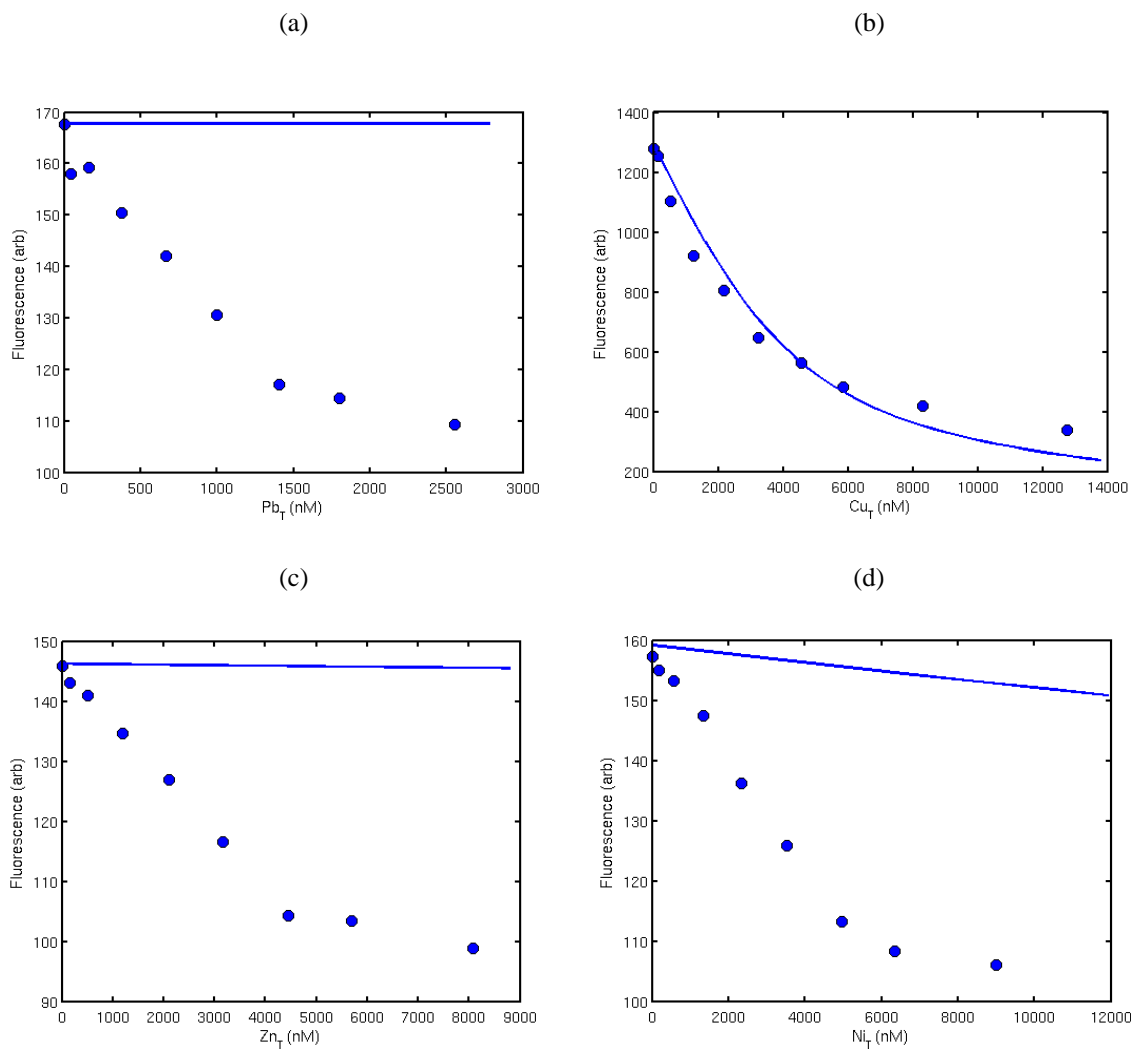
Figure 4.7: Model ligand tryptophan in synthetic seawater with metals (a) lead (b) copper (c) zinc (d) nickel. Data points are measured fluorescence quenching and lines are theoretical fluorescence quenching model based on NIST equilibrium constants and calculated speciation.

Fluorescence quenching measurements for copper agree well with the theoretical model. Lead, nickel and zinc data demonstrate excessive quenching compared to the predicted model. It appears as though the assumption that static quenching is occurring might be incorrect. For the fluorescence quenching technique to work, the decrease in fluorescence is assumed to be a result of the formation of a less fluorescent metal-ligand complex (static quenching). Alternatively fluorescence can be quenched by collisional deactivation in the excited state (dynamic

80

quenching). It appears that fluorescence quenching for lead, zinc and nickel is predominantly dynamic and thus the fluorescence quenching method, although it yields quenching curves, is not suitable for application in marine systems.

Additional experiments can be completed to confirm the presence of dynamic quenching. Stern-Volmer plots can be used to determine whether the quenching is solely one type of quenching (static or dynamic) or a combination of the two. If the plot is linear then further analysis needs to be completed to differentiate static quenching from dynamic quenching. This can be done through two possible methods. The first would be to complete the fluorescence quenching experiments at a higher temperature. Higher temperatures will result in larger diffusion coefficients which will result in an increased quenching constant (an increased slope in the Stern-Volmer plot) if it is dynamic quenching. However, for static quenching the increased temperature will result in a decreased stability of the complexes formed and lower the quenching constant. A smaller slope will be seen in the Stern-Volmer Plot in comparison to the room temperature one (Lakowicz, 2006).

Another method to differentiate static from dynamic quenching would be to examine the absorption spectra of tryptophan. Dynamic quenching only affects the excited state of the fluorophore which should result in no change to the absorption spectra. Static quenching occurs due to the formation of complex and can result in changes to the absorption spectra. Individually or in combination these experiments should be done to ensure that the quenching that is being viewed is dynamic.

These techniques could also be applied to the Luther Marsh results in section 4.3 to determine the type of quenching that was measured for those experimental tests.

4.8 Discussion

Fluorescence quenching measurements for copper agree with predictions in a model system and agree with copper ion selective electrode results done on the same sample. Lead, nickel and zinc display excessive quenching and disagreed with the theoretical model. Thus, fluorescence quenching seems to be a viable technique for copper speciation in marine systems but not for the other metal cations tested.

Fluorescence quenching is a very popular technique and has been validated for aluminum with salicylic acid and 2-hydroxy-3-napthoic acid by Smith et al. (1998) in freshwater. Copper fluorescence quenching was validated by its ability to predict free copper also by Smith et al. (2000). Since copper has been validated in freshwater and seawater, it is not believed that the salinity is preventing the fluorescence quenching method from working. Fluorescence quenching validation for the three other metals (Ni^{2+}, Zn^{2+} and Pb^{2+}) in freshwater or seawater was not found during an in depth literature search, indicating that the metals themselves maybe the reason the fluorescence quenching method did not provide accurate results.

4.9 Conclusions

Fluorescence quenching showed great promise for determining equilibrium binding parameters and provided results for Luther Marsh with Cu^{2+}, Ni^{2+}, Pb^{2+} and Zn^{2+} and Jimbo Bayou organic matter with Cu^{2+}. Copper ion selective electrode results for the Jimbo Bayou with copper give consistent results. Fluorescence quenching comparison with lead EC_{50} developmental toxicity tests did not agree. Results showed an increased predicted binding capacity as DOC is increased. Fluorescence quenching measurements for copper agree with predictions in a model system but lead, nickel and zinc display excessive quenching and

disagreed with the theoretical model. Fluorescence quenching seems to be a viable technique for copper speciation in marine systems but not for the other metal cations tested.

4.10 References

Eriksen, R.S., Mackey, D.J., Alexander, P., De Marco, R., Wang, X.D. Continuous flow methods for evaluating the response of a copper ion selective electrode to total and free copper in seawater. *J. Environ. Monit*. **1(5)**. 483-487. (1999).

Martell, A., Smith, R., (2001). Critically selected stability constants of metal complexes, NIST Database 46 version 6. NIST, Gaithersburg, MD 20899.

McKnight, D.M., Boyer, E.W., Westeroff, P.K., Doran, P.T., Kulbe T., Anderson, D.T. Spectrofluorometric characterization of dissolved organic matter for indication of precursor organic materials and aromaticity. *Limnol. Oceanogr.* **46**, 38-48. (2001).

Nadella, S.R., Fitzpatrick, J.L., Franklin, N., Bucking, C.P., Smith, S., Wood, C.M. Toxicity of dissolved Cu, Zn, Ni and Cu to developing embryos of the blue mussel (*mytilus trossolus*) and the protective effect of dissolved organic carbon. Comp. *Biochem. Physiol. Part C.* **149**, 340-348. (2009).

OECD Environment, Health and Safety Publications Series on Testing and Assessment. No. 29 "Guidance Document on Transformation/Dissolution of Metals and Metal Compounds in Aqueous Media" ENV/JM/MONO(2001)9. April (2001).

Ryan, D.K. and Weber, J.H. Fluorescence quenching titration for determination of complexing capacities and stability constants of fulvic acid. *Anal. Chem.* **54**, 986-990. (1982).

Sanchez-Marin, P., Bellas, J., Mubiana, V.K., Lorenzo, J.I., Blust, R., Beiras, R. Pb Uptake by the marine mussel *Mytilus* sp. Interactions with dissolved organic matter. *Aqua. Tox*. **102**. 48-57. (2011).

Santore, R.C., Di Toro, D.M., Paquin, P.R., Allen, H.E., Meyer, J.S. Biotic Ligand Model of the Acute Toxicity of Metals. 2. Application to Acute Copper Toxicity in Freshwater Fish and Daphnia. *Environ. Toxic. And Chem.* **20**, 10, 2391-2402. (2001).

Smith, D.S., Bell, R.A., Kramer, J.R. Review: Metal Speciation in Natural Waters with Emphasis on Reduced Sulfur groups as Strong Binding Sites. *Comparative Biochem.and Phys. Part C*. **133**, 65-74. (2002).

Smith, D.S., Kramer, J.R. Fluorescence analysis for multi-site aluminum binding to natural organic matter. *Environ. Internat.,* **25**. 295–306. (1999).

Smith, D. S., and Kramer, J. R. Multi-site aluminum speciation with natural organic matter using multiresponse fluorescence data. *Anal. Chim. Acta.* **363**. 21-29. (1998).

Smith, D.S., Kramer, J.R. Multisite Metal Binding to Fulvic Acid Determined Using Multiresponse Fluorescence. *Anal. Chim. Acta.* **416**, 211–222. (2000).

Windig, W and Guilment, J. Interactive self-modeling mixture analysis. *Anal Chem.* **63**, 1425-1432. (1991).

Chapter 5 Natural Organic Matter Source and Salinity Dependence on Binding of Lead in Saltwater Media

5.1 Introduction

There is a lack of information regarding the molecular composition of marine NOM. Ocean profiles exist for two components, amino acids and carbohydrates. Amino acids account for 1-3% of the ocean pool while carbohydrates account for 2.5-7% of the DOC; this leaves 90% of DOC uncharacterized (Benner, 2002). Fluorescence can be used to determine number of fluorophores present within the NOM. Humic-like fluorescence is derived from a mixture of fluorophores which varies between freshwater and marine environments. There is the presence of a protein or amino acid component in marine surface water. Coble (1996) determined that there were specific marine humic-like materials which are shifted towards shorter wavelengths in comparison to unconcentrated non-marine samples.

NOM can be affected by salinity or salt content. Salt content is known to decrease solubility and increase the activity coefficient resulting in a salting out effect. The salting out effect refers to a decrease in solubility with an increase in ionic strength (Xie et al., 1997). It has been observed with organic molecules in a NaCl medium (Xie et al., 1997) and with DOM in natural estuarine and marine coastal waters (Mantoura and Woodward, 1983).

As mentioned in Chapter 1, lead toxicity is a concern due to anthropogenic outputs into saltwater systems. Embryo-Larval toxicity tests are often done to monitor pollutants in marine systems (Nadella et al., Appendix G). Early life stages of aquatic invertebrates are considered more sensitive than adults as they respond to subtle chemical and physical changes in the environment (His et al., 1999).

In fish, acute lead toxicity is due to respiratory asphyxiation in extreme concentrations. Under environmentally relevant concentrations, lead toxicity it attributed to ionoregulatory homeostasis (Wood et al., 2012). Chronic lead toxicity results in neurological dysfunction because the lead substitutes for calcium and possibly other essential divalent cations including iron and zinc.

Mechanisms of lead toxicity to fish in seawater have received very little attention in comparison to freshwater toxicity tests. Hypocalcemia may contribute to lead toxicity in seawater because the calcium uptake mechanism is similar in freshwater and marine organisms (Wood et al., 2012). The high alkalinity and calcium content of seawater does limit lead solubility and bioavailability which could potentially prevent the ionic divalent lead fraction from reaching the levels sufficient to inhibit calcium flux (Wood, Farrell and Brauner, 2012).

The purpose of this project is to use voltammetric methods to determine binding capacities of different concentrations and sources of NOM with lead in different salinities. These results will be compared to toxicological observations.

5.2 Experimental Method

DOM sources Bamfield, Inshore Brazil, Pachena and Nordic Reservoir were dissolved in OECD synthetic seawater (sample details given in Table 2.1 in section 2.2.1) at two different nominal concentrations of 2 and 12 mg C/L to determine if binding capacity was dependent or independent of NOM concentration. Table of sources can be found in Table 3.1 in section 3.2. Additionally, the 2 mg C/L NOM concentration was measured for each organic matter source at three different salinities 3, 15 and 30 ppt. The solutions were held at a constant pH of 7.765+/-

0.02, left to equilibrate for 24 hours and repeated in triplicate. Lead additions were made up to 900ppb.

Fluorescence was used as a molecular fingerprint for each of the NOM sources. Fluorescence spectra of the NOM samples were collected using a Varian Cary Fluorescence spectrophotometer with 1cm pathlength quartz cuvettes. The fluorescence spectra were created by using excitation wavelengths from 200 to 450nm using 10nm increments. The emission wavelengths were measured in the range of 250 to 650nm for every 1nm increment. The excitation-emission matrices (EEMs) are plotted as contours to identify the fluorescing components. Parallel Factor Analysis (PARAFAC) was used to identify and quantify the component peaks in the EEMs, as implemented in the PLS toolbox (Eigen-vectors Research Inc, WA, USA). Each matrix contains fluorescence information for specific excitation/emission wavelength pairs. PARAFAC resolves this information into component spectra and relative component concentrations (Gheorghiu et al., 2010; Nadella et al., 2009; Depalma et al., 2011b). Fluorescence EEMs and PARAFAC results can be found for the NOM sources in Chapter 3. Binding capacities determined correspond to the EEMs after storage.

Anodic stripping voltammetry (ASV) was used for determination of binding capacity. A Metrohm Autolab instrument with a 663 VA stand was used with the NOVA 1.7 software to obtain scans and peak height. Electrochemically labile lead was measured using square wave anodic stripping voltammetry (SWASV) with a deposition potential of -0.65 V, a deposition time of 30 seconds, equilibration time of 5 seconds, voltage scanning (-0.65 to -0.25V), amplitude of 25 mV, frequency of 25 Hz, and a scan increment of 2mV. This corresponds to the method of Sánchez-Marín et al. (2011). After each scan and lead addition, the peak height is

recorded at the lead potential and used to determine the binding capacity. An example of the peak heights can be found in Figure 5.1. Peak height increases with standard addition of lead.
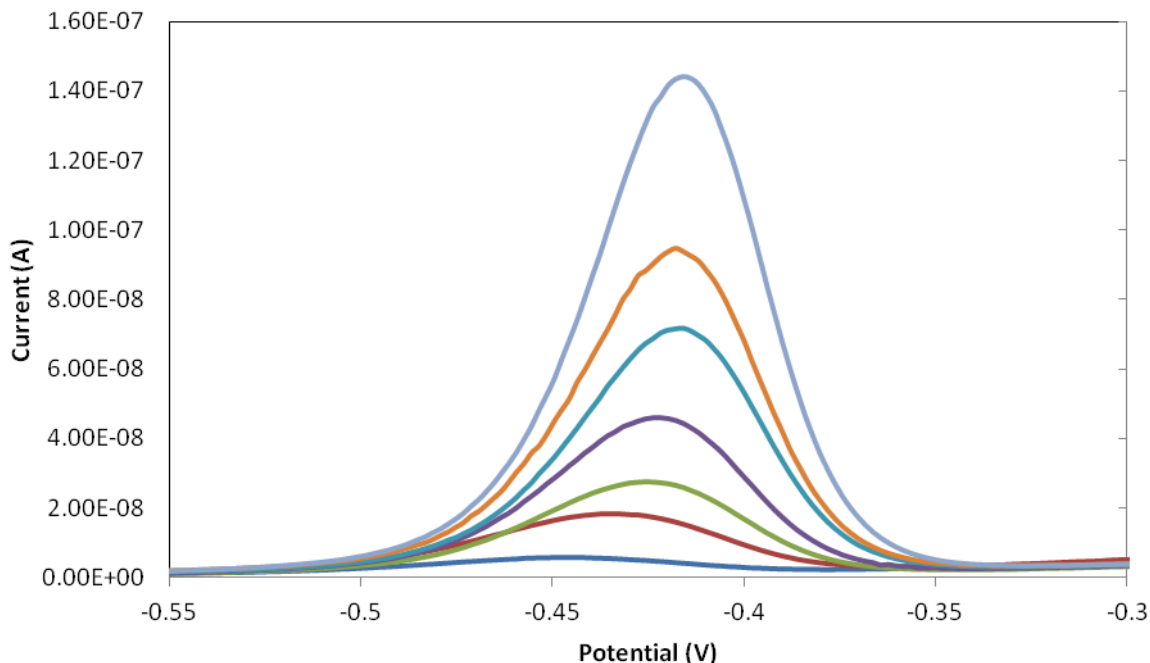
Figure 5.1: Voltammetric spectra. Scan of peak height versus potential as total lead is increased.

The current measurements at the peak potential versus the lead added result in a low slope for the initial data followed by steeper slope linear response at higher total lead. The small slope occurs because the NOM is binding the available lead while the steeper slope arises when the binding capacity for the NOM is exceeded. This method assumes that only inorganic complexes and free lead are detected at the electrode and strong organic matter complexes are not detected. Extrapolation of the linear data at high lead allows for estimation of the binding capacity as the x-intercept of the regression line. An example of this can be viewed in Figure 5.2.
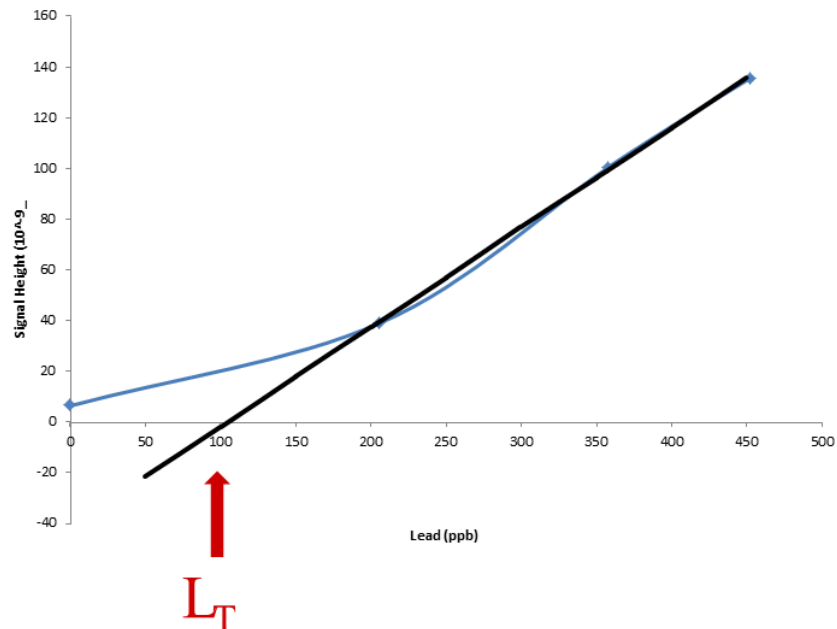
Figure 5.2: Lead speciation for Nordic Reservoir (2 mg C/L) measured by Anodic stripping voltammetry (ASV). Voltammetric results lead addition (nM) vs. height of lead peak and linear regression to obtain binding capacity (L_T).

Statisical comparisons of binding capacities were computed by a two-way ANOVA followed by the Student-Newman-Keuls post-hoc test when required. These methods were used for all pairwise comparisons of means among the different treatment groups. The limit of $P<0.05$ was used to indicate significance.

A competitive ligand method for determining copper binding capacity was also completed and can be found in Appendix E. Binding capacity for zinc was also attempted and results can be found in Appendix F.

5.3 Determination of Binding Capacity

The lead speciation results for the Nordic Reservoir organic matter in synthetic seawater agrees more closely than fluorescence results with the observed lead toxicity in the same system.

The results of binding capacity for the lead determination with ASV can be viewed in Table 5.1. Voltammetry demonstrates that an increased amount of DOC does not bind significantly more lead. The 2 mg C/L Nordic Reservoir had a binding capacity of 320 nM while the 12 mg C/L had a binding capacity of 347 nM. This represents a binding capacity increase by a factor of 1.1, which supports the EC_{50} data indicating similar EC_{50} values resulting from similar binding capacities. Binding capacity results for zinc with Nordic Reservoir can be viewed in Appendix E.

Table 5.1: Binding Capacity for Nordic Reservoir organic matter concentrations of low and high DOC with comparison to EC_{50} values for *Mytilus galloprovincialis* in seawater. 95% confidence values indicated by ranges of values.

Nordic Reservoir	EC_{50} (nmol/L) *Mytilus galloprovincialis*	Voltammetry Binding Capacity (nM)
0 mg C/L	304 (173-453)	---
2 mg C/L NR	738 (680-796)	320 (206-434)
12 mg C/ NR	758 (680-830)	347 (279-415)

5.4 Organic Matter Source Effects

Organic matter concentrations were confirmed by TOC analysis. The results can be found in Table 5.2. Bamfield, Pachena and Nordic Reservoir NOM had a TOC concentration much less than the nominal amount while Inshore Brazil was very close to expected. The actual TOC, as a percent of nominal values, was 49.1% and 44.7% for the Bamfield 2 and 12 mg C/L respectively. Inshore Brazil was 129% and 100%, Pachena was 43.3% and 45.1%, and Nordic Reservoir was 59.2% and 35.7% for the 2 and 12 mg C/L solutions. The nominal concentration was originally calculated to have an increase in NOM concentration between the two solutions by a factor of 6.

The actual NOM concentration factor was 5.46 for Bamfield, 4.65 for Inshore Brazil, 6.26 Pachena and 3.62 for Nordic Reservoir.

Table 5.2: Measured TOC compared to nominal concentration for each of the NOM sources.

Organic Matter Source	Nominal Concentration (mg C/L)	Measured TOC (mg C/L)
Bamfield	2	0.982
	12	5.363
Inshore Brazil	2	2.587
	12	12.030
Pachena	2	0.865
	12	5.416
Nordic Reservoir	2	1.184
	12	4.288

Lead binding capacity was measured at different concentrations of DOC. Table 5.3 displays the binding capacity results for 2 and 12 mg C/L in 30ppt OECD seawater for each NOM source. It can be seen that an increase in DOM concentration does not result in a significantly increased binding capacity for lead.

Table 5.3: Binding capacities for 2 and 12 mg C/L for each of the different NOM sources in 30ppt OECD seawater. Binding capacity in nmol/mg C is based on measured TOC values.

Organic Matter Source	Nominal Concentration (mg C/L)	Lead Binding Capacity (nM)	Lead Binding Capacity (nmol/mg C)
Bamfield	2	428.4 (+/-53.5)	436.2 (+/-54.5)
	12	378.9 (+/-86.2)	70.7 (+/-16.1)
Inshore Brazil	2	300.6 (+/-25.6)	116.2 (+/-9.9)
	12	295.7 (+/-32.5)	24.58 (+/-2.7)
Pachena	2	464.9 (+/-48.7)	537.5 (+/-56.3)
	12	485.6 (+/-10.7)	89.7 (+/-0.02)
Nordic Reservoir	2	320.2 (+/-161.2)	270.4 (+/-136.1)
	12	347.4 (+/-96.2)	81.0 (+/-22.4)

5.5 Salinity

Binding capacities were determined at a constant organic matter concentration of 2 mg C/L but at seawater salinities of 3, 15 and 30 to determine if salinity affects binding capacity. Table 5.4 displays the binding capacities for each NOM at salinities of 3, 15, and 30 ppt. Similarly to the increase in organic matter concentration, no significant increase in binding capacity was seen for the NOM at the different salinities.

Table 5.4: Binding Capacities for each NOM at salinities of 3, 15, and 30 ppt in OECD seawater. Binding capacity in nmol/mg C is based on measured TOC values.

Organic Matter Source	Salinity (ppt)	Lead Binding Capacity (nM)	Lead Binding Capacity (nmol/mg C)
Bamfield	3	350.7 (+/-145.9)	357.1 (+/-148.6)
	15	413.1 (+/-17.4)	420.7 (+/-17.7)
	30	428.4 (+/-53.5)	436.25 (+/-54.5)
Inshore Brazil	3	339.0 (+/-62.6)	131.0 (+/-24.2)
	15	292.7 (+/-22.6)	113.1 (+/-8.7)
	30	300.6 (+/-25.6)	116.2 (+/-9.9)
Pachena	3	381.9 (+/-35.8)	441.5 (+/-41.4)
	15	412.8 (+/-67.0)	477.2 (+/-77.5)
	30	464.9 (+/-48.7)	537.5 (+/-56.3)
Nordic Reservoir	3	306.7 (+/-87.1)	259.0 (+/-73.6)
	15	313.7 (+/-12.67)	264.9 (+/-10.7)
	30	320.2 (+/-161.2)	270.4 (+/-136.1)

5.6 Binding Capacity Comparisons and Statistics

The binding capacities for the NOM at different salinities and concentration can be viewed in Figure 5.3. No significant differences were found using a two-way ANOVA within the NOM sources comparing salinities and concentrations. The average binding capacity for Bamfield, Inshore Brazil, Pachena and Nordic Reservoir were 392.8 nM, 307.0 nM, 436.4 nM and 322.0 nM, respectively. A statistically significant difference was found when comparing the

different sources of NOM to each other. Pachena was found to be significantly different from

Inshore Brazil and Nordic Reservoir but not the Bamfield sample. Differences are reasonable

given that fluorescence scans for the Pachena EEM are significantly different from the Inshore

Brazil and Nordic Reservoir samples (Chapter 3, Figure 3.6, 3.7 and 3.8). Pachena is lacking in

the humic and fulvic acid component that is present in the Inshore Brazil and Nordic Reservoir

EEM's.
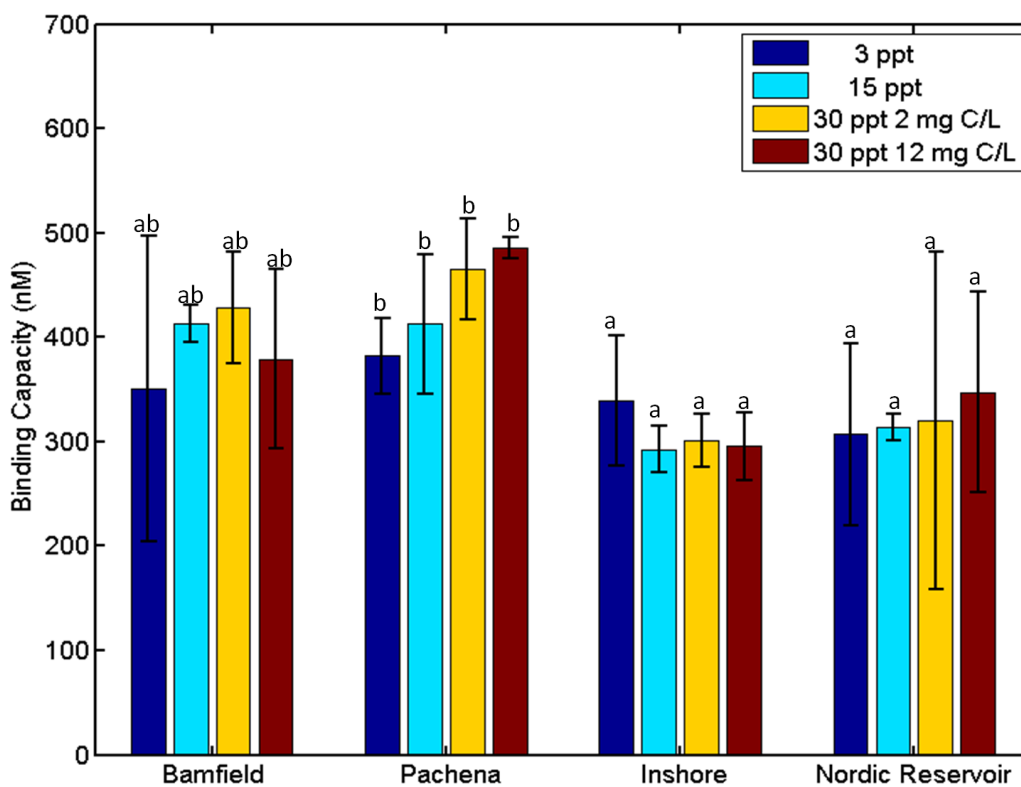
Figure 5.3: Comparison of binding capacities for each NOM source at different salinity and organic matter concentration. Error bars are standard deviations. All bars labelled a are statistically the similar while bars labelled b are statistically similar determined by a two-way ANOVA.

These results indicate that there is a source dependence on binding capacity of lead to

NOM and source needs to be taken into account when predicting bioavailability and toxicity of

metals in the presence of NOM. It was also determined that an increase in DOC did not bind more lead. No dose dependence was seen. It is possible that the ionic strength effect of the samples cause the lack of dose dependence of lead-DOM complexation and DOC protectivity. At low DOC concentrations, the ligand is free to interact with lead cations. As DOC concentrations are increased, DOC-DOC interactions predominate due to salting out effects and salt induced colloid formation. This information can be incorporated into the BLM to accurately predict toxicity and bioavailability of metals based on the source and dose of NOM.

5.7 Fluorophores and Lead Binding Capacity

Binding capacity for each NOM source was compared to the percent fluorophore determined in chapter 3. The percent fluorophore from after storage was used for the comparison because that was the state of the NOM before lead binding titration. Figure 5.4 displays the correlation between the humic and fulvic acid-like component and the binding capacity. The trendline fit to the data shows a strong correlation between the fluorphore percent and binding capacity with an R^2 value of 0.9327. This correlation shows that a decrease in humic and acid-like fraction resulted in a higher binding capacity. The highest binding capacity with the lowest percent of the humic and fulvic-like acid was Pachena which was found to be the most statistically different from Inshore Brazil and Nordic Reservoir. These are the two present with the lowest binding capacity and highest amount of humic and fulvic–like material. The data point in between these two is Bamfield which was found to be statistically similar to all the NOM sources in section 5.6. The error bars present on the data points do overlap which indicates that this correlation may not be as strong as the R^2 value indicates.

Figure 5.4: Humic and Fulvic-like Acid Fraction versus Binding capacity, error bars are standard deviation. A strong correlation between the two is observed with an R^2 value of 0.9327.

Figure 5.5 displays the tryptophan-like fraction compared to the binding capacity for each of the NOM sources. A slight trend was seen with an R^2 value of 0.7811, indicating that a higher tryptophan percentage resulted in a higher binding capacity. Pachena is the data point with the highest binding capacity and highest percent tryptophan, while Nordic Reservoir and Brazil Inshore are at the low end with Bamfield in the middle.

95

Figure 5.5: Tryptophan-like Acid Fraction versus Binding capacity. Error bars are standard deviation. A slight correlation between the two is observed with an R^2 value of 0.7811.

Finally, a comparison between the tyrosine-like acid fraction and the binding capacity was completed in figure 5.6. No correlation was seen with an R^2 value of 0.4436.
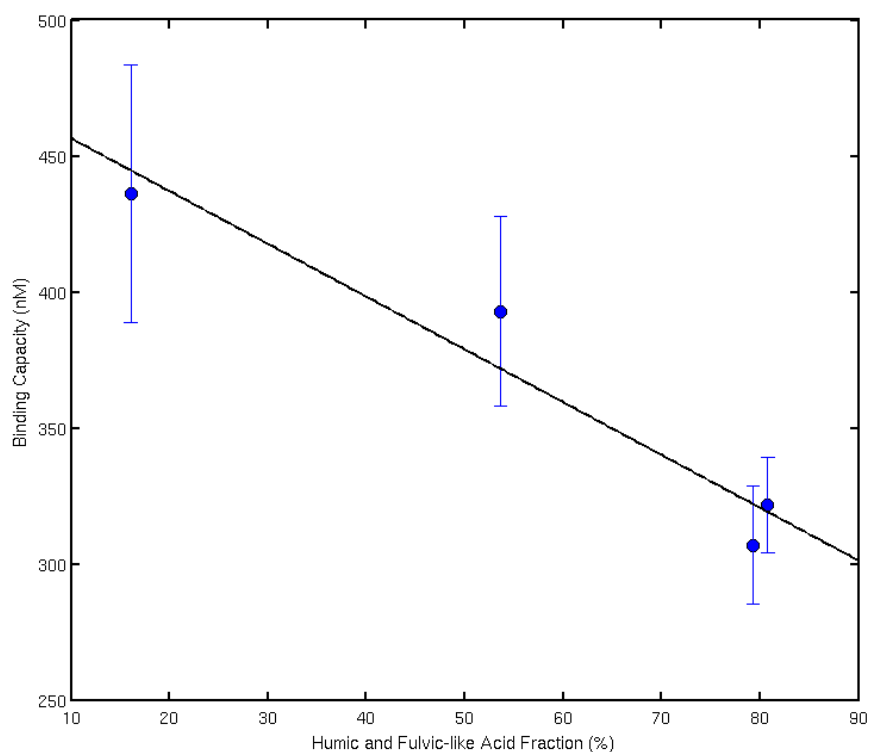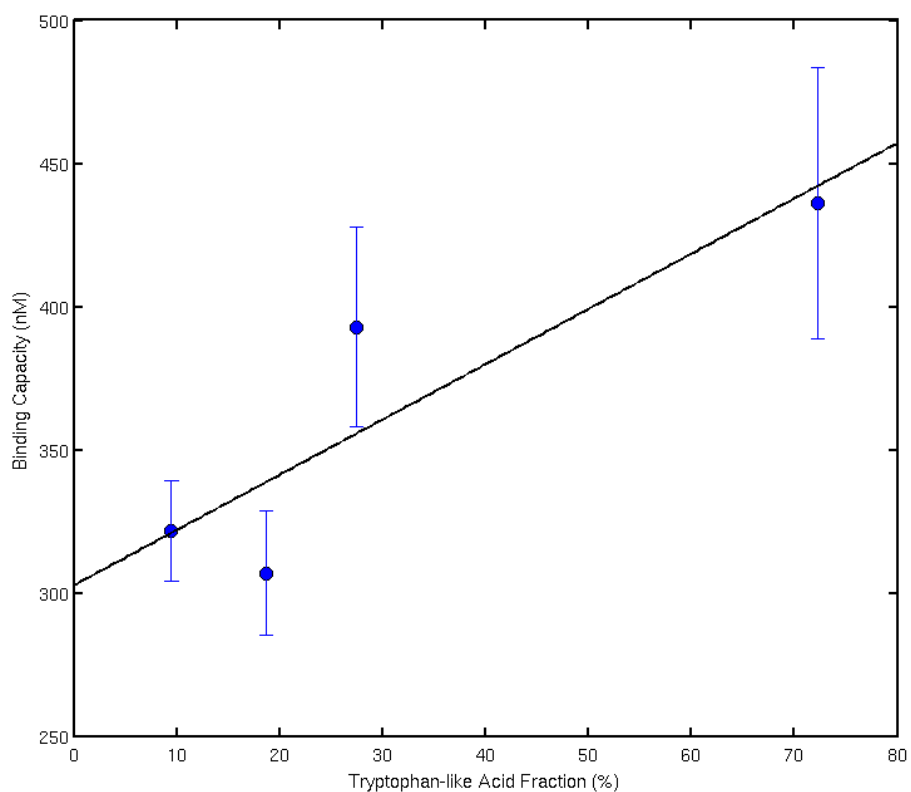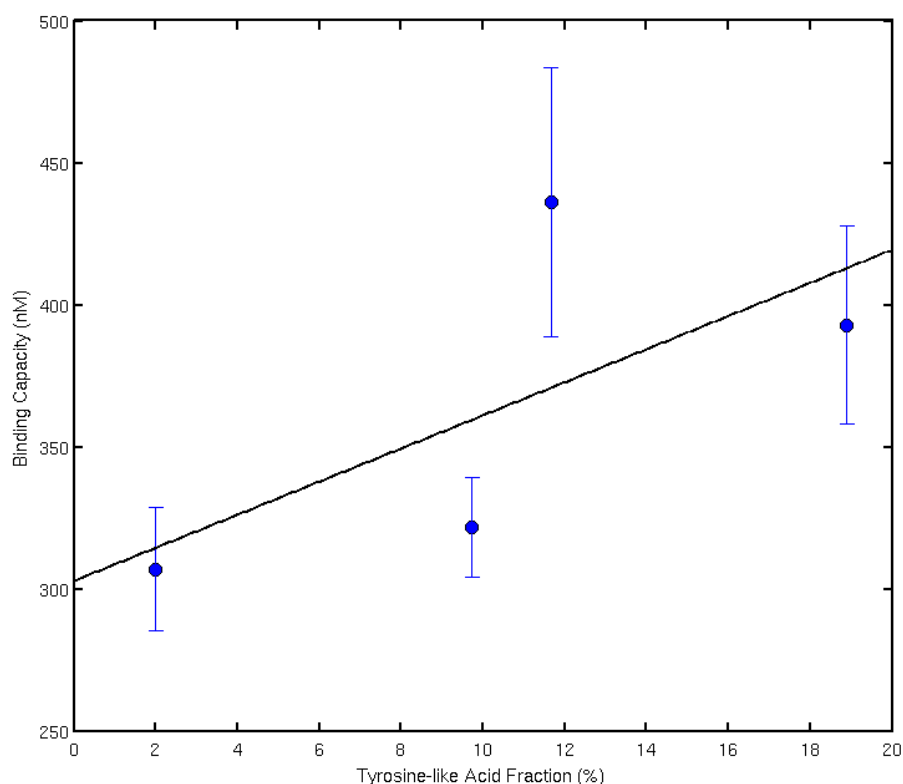
Figure 5.6: Tyrosine-like Acid Fraction versus Binding capacity. Error bars are standard deviation. A slight correlation between the two is observed with an R^2 value of 0.4436.

R^2 values alone indicate that quality of NOM affects binding capacity and in turn protectivity of lead. However, some of the error bars do overlap, decreasing the confidence in the correlation between the molecular components and binding capacity. This signifies that there might be a requirement for a BLM quality factor but further research on NOM with varying molecular components is required to confidently determine this. There is much disagreement about the requirement of a BLM quality factor. Depalma et al. (2011b) determined that a source dependent quality factor should not be necessary to use equilibrium models to predict site specific EC_{50} values, at least not for the low levels of copper where toxicity is observed for *Mytilus*. Al-Reasi et al. (2012) argue the need for a quality indicator using SAC340.

Gheorghiu et al. (2010) also argue the need for a quality indicator due to a disconnect between the effects of NOM quality on Cu–gill binding and Cu toxicity studies which demonstrate clear effects of NOM quality on toxicity. Gheorghiu et al. (2010) suggests that this discrepancy is likely the result of direct NOM effects on the gills, which are quality dependent, and that this possibility needs to be considered in future investigations of the inter-relationships between NOM quality, metal–gill binding and toxicity in fishes exposed to metals.

Experiments displayed in this chapter indicate that a lower amount of humic and fulvic-like fraction resulted in an increased binding capacity and greater protection while there is evidence that a greater amount of humic acid decreases toxicity (Ryan et al., 2004; Al-Reasi et al., 2012). Al-Reasi et al. (2012) saw a positive correlation between the humic like component and copper LC_{50}s but a negative correlation correlation between fulvic-like component concentration and copper LC_{50}.

PARAFAC results only allowed for a three component fit. If a four component fit had been possible it would have allowed the fulvic-like and humic-like fraction to be separated and possibly allow for a correlation between the binding capacities that agrees with previous literature.

5.8 Conclusions

Binding capacities were determined for two different organic matter concentrations and three different salinities. No significant differences were found within the NOM sources comparing salinities and concentrations. The average binding capacity for Bamfield, Inshore Brazil, Pachena and Nordic Reservoir were 392.8 nM, 307.0 nM, 436.4 nM and 322.0 nM, respectively. A statistically significant difference was found when comparing the different

sources of NOM to each other. Pachena was found to be significantly different from Inshore Brazil and Nordic Reservoir but not the Bamfield sample.

These results indicate that there is a source dependence on binding capacity of lead to NOM and source needs to be taken into account when predicting bioavailability and toxicity of metals in the presence of NOM. It was also determined that an increase in NOM did not bind more lead and no dose dependence was seen. This is potentially because the ionic strength effect of the seawater causes DOC-DOC interactions at higher NOM concentrations due to salting out affects and salt induced colloid formation.

The percent of fluorophore fraction was compared to the binding capacity to determine any potential trends. A strong trend was found for the humic and fulvic acid like fraction, a slight trend for the tryptophan-like fraction and no trend for the tyrosine like fraction. However, error bars on data points did overlap, decreasing the confidence in this trend.

5.9 References

Al-Reasi, H.A., Smith, D.S., Wood, C.M. Evaluating the ameliorative effect of natural dissolved organic matter (DOM) quality on copper toxicity to Daphnia Magna: Improving the BLM. *Ecotox*. **21**. 524-537. (2012).

Benner, R. Chemical composition and reactivity. In: Hansell, D.A., Carlson, C.A. (Eds.), Biogeochemistry of Marine Dissolved Organic Matter. Elsevier, USA, 59–90. 2002.

Coble, P.G. Characterization of marine and terrestrial DOM in seawater using excitation-emission matrix spectroscopy. *Mar. Chem.,* **51**. 325–346. (1996).

DePalma S.G.S., Arnold W.R., McGeer J.C., Dixon, D.G., Smith, D.S. Protective effects of dissolved organic matter and reduced sulfur on copper toxicity in coastal marine environments. *Ecotox. And Environ. Saf.* **74**. 230-237. (2011b).

Gheorghiu, C., Smith, D.S., Al-Reasi, H.A., McGeer, J.C., Wilkie, M.P. Influence of natural organic matter (NOM) quality on Cu-gill binding in the rainbow trout (oncorhynchus mykiss). *Aqua. Tox.* 97, 343-352. (2010).

His, E., Beiras, R., Seaman, M.N.L.1999. The assessment of marine pollution-bioassays with bivalve embryos and larvae. In: Southward, A.I., Tyler, P.A., Young, C.M. (Eds.), Advances in Marine Biology, vol. 37. Academic Press, London, pp. 1–178.

Mantoura,R. and Woodward M.Conservative behaviour of riverine dissolved organic carbon in the Severn Estuary: chemical and geochemical implications. *Geochim. Cosmochim. Acta*, **47**. 1293–1309. (1983).

Ryan, A.C., Van Genderen, E.J., Tomasso, J.R., Klaine, S.J. Influence of natural organic matter source on copper toxicity to larval fathead minnows (Pimephales promelas): implications for the biotic ligand model. *Environ Toxicol Chem*. **2**3. 1567–1574. (2004).

Wood, C.M., Farrell, P., and Brauner C.J. Homeostasis and Toxicology of Non-Essential Metals: Fish Physiology V31B. Academic Press, 2012.

Xie,W.H., Shiu, W.Y., and Mackay, D. A review of the effect of salts on the solubility of organic compounds in seawater. *Mar. Environ. Res.*, **44**. 429–444. (1997).

Chapter 6 Conclusion and Future Work

6.1 Conclusions

Objective 1: Characterize different sources of NOM and their binding characteristics with copper, lead, zinc, and nickel in marine systems using fluorescence quenching and voltammetric methods.

Fluorescence spectroscopy provided EEM's which were used as fingerprints for each of the different DOM sources before and after storage in Chapter 3. PARAFAC was used to determine the relative concentration of three components within the organic material determined to be tryptophan-like, humic and fulvic-like and tyrosine-like. The comparison of the relative percents of each of these components showed significant changes within the tryptophan-like material and the humic and fulvic-like material after storage. The most extreme change was seen with Pachena NOM which showed a tryptophan-like increase from 10% to 72% and a decrease of humic and fulvic-like from 85% to 16%. The DOM did not remain stable and the quality of the sample changed during the storage procedure. This could be attributed to the fractionation method used to collect the NOM, alternate storage methods should be considered.

Fluorescence quenching results in Chapter 4 do not agree with either EC_{50} determined for lead Nordic Reservoir NOM or voltammetry results and show an increased predicted binding capacity as DOC is increased instead of no dose dependence. Fluorescence quenching measurements for copper agree with predictions using tryptophan as a model system but lead, nickel and zinc display excessive quenching and disagreed with the theoretical equilibrium model. Additionally, copper fluorescence quenching was confirmed by inter-method comparison with copper ISE. Irving-William series did not agree with the binding strength order suggested

by fluorescence quenching and does not support the use of fluorescence quenching for the other metals nickel, zinc and lead. Fluorescence quenching seems to be a viable technique for copper speciation in marine systems but not for the other metal cations tested.

Objective 2: Assess salinity dependence and NOM concentration dependence to determine their affect on binding capacity for lead with NOM.

Lead speciation results for Nordic Reservoir NOM determined by anodic stripping voltammetry qualitatively agree with the observed lead toxicity results in Chapter 5. Both the EC_{50} values determined by toxicity tests and the binding capacities determined by voltammetry show little variation when DOC is increased. This did not agree with the hypothesis that an increased DOC concentration would result in an increased binding capacity. The lack of dose dependence can be attributed to DOC-DOC interactions due to salting out effects and salt induced colloid formation. Lack of dose dependence in marine systems is valuable information and can be implemented in the BLM.

Binding capacities were determined for two different organic matter concentrations and three different salinities completed in Chapter 5. No significant differences were found within the NOM sources comparing salinities and concentrations. This agreed with the third hypothesis that salinity would not affect binding capacity and is another valuable piece of information that can be implemented within the BLM. A statistically significant difference was found when comparing the different sources of NOM to each other. The NOM with a lower humic and fulvic-like fraction was found to be significantly different from the NOM with the higher humic and fulvic-like fraction. The percent of fluorophore fraction was compared to the binding capacity to determine any potential trends. A strong trend was found for the humic and fulvic

acid-like fraction, a slight trend for the tryptophan-like fraction and no trend for the tyrosine like fraction. This also agrees with the first hypothesis that NOM protection is source dependent. A quality factor may be needed within the BLM. However, the NOM collection method and storage may have influenced the results.

Objective 3: Transformation/dissolution experiments will be completed to determine solubility of two copper compounds, copper and cuprous oxide, and ensure that they are within appropriate limits and regulations. A solubility model will be used to compare to experimental results, and conclusions will be made on which ones can effectively describe the experimental results obtained.

Copper solubility models were used to estimate copper solubility in Chapter 2. The original copper solubility model which included all the precipitates was identical to the tenorite only precipitation because of the insolubility of the tenorite precipitate. The tenorite precipitation underestimates the copper solubility by half estimating 22 ppb. However, it is possible that the tenorite precipitate is not at equilibrium and may be a reasonable precipitate to use for modeling. Copper hydroxide solid seriously overestimates copper solubility by a factor of 12 estimating 600 ppb. The malachite precipitate overestimates copper solubility by a factor of 3 estimating 150 ppb. Ultimately, the experimental data point was placed between the tenorite precipitation model and the malachite precipitation model still leaving questions about how to optimize the modeling of copper solubility. This disagreed with the hypothesis that the models would agree with the measured data. There is a need for an accurate copper solubility model to be used for risk assessment and implemented in the BLM.

6.2 Future Work

Precipitation of copper solids from supersaturated solutions should be completed to accompany the transformation/dissolution experiments in Chapter 2 to get a complete picture of copper solubility in marine systems.

Additional experiments need to be completed for the fluorescence quenching modeling in Chapter 4 to confirm the presence of dynamic quenching. Stern-Volmer plots can be used to determine whether the quenching is solely one type of quenching (static or dynamic) or a combination of the two. If the plot is linear then further analysis needs to be completed to differentiate static quenching from dynamic quenching. This can be done using two possible methods. The first would be to complete the fluorescence quenching experiments at a higher temperature. The second method to differentiate static from dynamic quenching would be to examine the absorption spectra of tryptophan. Dynamic quenching only affects the excited state of the fluorophore which should result in no change to the absorption spectra. Static quenching occurs due to the formation of complex and can result in changes to the absorption spectra. Individually or in combination these experiments should be done to ensure that the quenching that is being viewed is dynamic.

There is a direct voltammetric method for copper, lead and zinc but not for nickel. Binding capacity was determined for Nordic Reservoir NOM with lead and was attempted with zinc. To complete these set of experiments and get a full understanding of the metal binding capacity with Nordic Reservoir NOM, copper should be completed as well.

Appendix A: Matlab Code for Transformation/Dissolution Modeling

```
clear; figure(1); clf
ClT=0.5;
PCO2=10^(-3.5);
CuT=5e-5;
SO4T=1e-2;
pHplot=[7.5:0.05:8.5]';

% model calc0.
c=0;
for i=1:size(pHplot,1)

[species,names]=Cumodel_highIS_Cl_open_ppte_malachite(CuT,pHplot(i),PC
O2,ClT, SO4T, 0); % flag=1 at end no malachite
    c=c+1;
    for j=1:size(species,2)
        txt=[names(j,:),'(c)=species(:,j);'];  eval(txt)
    end
end


Cusolidhydroxide=CuT-(2*malachite+tenorite+CuOH2s);
species=[]; species_summary=[]; malachite=[]; tenorite=[]; CuOH2s=[];


c=0;
for i=1:size(pHplot,1)

[species,names]=Cumodel_highIS_Cl_open_ppte_malachite(CuT,pHplot(i),PC
O2,ClT,SO4T,0); % flag=1 at end no malachite
    c=c+1;
    for j=1:size(species,2)
        txt=[names(j,:),'(c)=species(:,j);'];  eval(txt)
    end
  end

Cusolidmalachite=CuT-(2*malachite+tenorite+CuOH2s);  malachite=[];
tenorite=[]; CuOH2s=[];

c=0;
for i=1:size(pHplot,1)

[species,names]=Cumodel_highIS_Cl_open_ppte(CuT,pHplot(i),PCO2,ClT,SO4
T,0); % flag=1 at end no malachite
    c=c+1;
    for j=1:size(species,2)
        txt=[names(j,:),'(c)=species(:,j);'];  eval(txt)
    end
    species_summary(i,:)=species;species=[]; species_summary=[];

end
```

```
Cusolidtenorite=CuT-(2*malachite+tenorite+CuOH2s);

forRachael=[pHplot species_summary];

save forRachael.txt forRachael -ascii

h=plot(pHplot,
(Cusolidtenorite)*63500000,pHplot,(Cusolidmalachite)*63500000,pHplot,(
Cusolidhydroxide)*63500000,'linewidth',2);
set(gca,'linewidth',2)
set(gca,'fontsize',12)
xlabel('pH','fontsize',12)
ylabel('sum of soluble Cu species (ppb)','fontsize',12)

legend('tenorite','malachite','Cu(OH)_2')

hold on

plot(8.01,49.8,'ko','markersize',8,'markerfacecolor','b','linewidth',2
)

%end
%axis([5 8 -7.8 -5.5])

% Carrayrou  et al AIChE journal 2002, 48, 894-904.
% implement their method using thier notation
% try HFO ppte as an example calc and at fixed pH

function
[II,GG]=Cumodel_highIS_Cl_open_ppte_malachite(CuT,pH,PCO2,ClT,SO4T,fla
g)

warning('off')

[KSOLUTION,KSOLID,ASOLUTION,ASOLID,SOLUTIONNAMES,SOLIDNAMES]=get_equil
ib_defn(flag);

%CuT=3.9592e-7;

%pH=[6:0.1:9]; % fixed pH
numpts=size(pH,2);
Ncp=size(ASOLID,1);
solid_summary=zeros(numpts,Ncp);

for i=1:size(SOLIDNAMES,1)
    txt=[SOLIDNAMES(i,:),'=zeros(numpts,1);']; eval(txt)
end

for i=1:size(pH,2)
```

```matlab
    H=10.^(-1*pH(i)); Ka1=10^(-6.3); Ka2=10.^(-10.3); Kh=10.^(-1.47);
    CT=Kh*PCO2+(Kh*PCO2*Ka1)./H+(Kh*PCO2*Ka1*Ka2)./(H.^2);
    CTrun(i)=CT;

    % adjust for fixed pH


[Ksolution,Ksolid,Asolution,Asolid]=get_equilib_fixed_pH(KSOLUTION,KSO
LID,ASOLUTION,ASOLID,pH(i));

    Asolid_SI_check=Asolid; Ksolid_SI_check=Ksolid;

    % number of different species
    Nx=size(Asolution,2); Ncp=size(Asolid,1); Nc=size(Asolution,1);

    % initial guess
    Cu_guess=[-5.5]; CuOH2s_guess=0.1*CuT;  CuCO3s_guess=0.1*CT;
    guess=[10.^Cu_guess CT./10 CuOH2s_guess CuCO3s_guess];
iterations=1000; criteria=1e-19;
    T=[CuT CT ClT SO4T];

    % calculate species using NR

    solids=zeros(1,Ncp);

    if i==1;
[species,err,SI]=NR_method_solution(Asolution,Asolid,Ksolid,Ksolution,
T',[guess(1:Nx)]',iterations,criteria); end
    if i>1;

[species,err,SI]=NR_method_solution(Asolution,Asolid,Ksolid,Ksolution,
T',[species(2:Nx+1)],iterations,criteria);
    end

    for qq=1:Ncp

        [Y,I]=max(SI);

        if Y>1.000000001
            Iindex(qq)=I;
            Asolidtemp(qq,:)=Asolid_SI_check(I,:);
            Ksolidtemp(qq,:)=Ksolid_SI_check(I,:);
            solidguess(qq)=T(I)*0.5;
          % solidguess(qq)=min(T)*0.015;
           if i>1;
                %if max(solids)>0
                txt=['solidguess(qq)=',SOLIDNAMES(I,:),'(i-1);'];
eval(txt);
                %end
            end
```

```matlab
            guess=[species(2:Nx+1)' solidguess];

[species,err,SItst,solids]=NR_method(Asolution,Asolidtemp',Ksolidtemp,
Ksolution,T',guess',iterations,criteria);
            for q=1:size(solids,1);
                txt=[SOLIDNAMES(Iindex(q),:),'(i)=solids(q);'];
eval(txt)
            end
        end

        Q=Asolid*log10(species(2:Nx+1)); SI=10.^(Q+Ksolid); Ifirst=I;

    end

    Q=Asolid*log10(species(2:Nx+1)); SI=10.^(Q+Ksolid);
    SI_summary(i,:)=SI;

    species_summary(i,:)=species;
    mass_err_summary(i,:)=(err(1));

    Asolidtemp=[]; Ksolidtemp=[];

end

for i=1:size(species_summary,2)
    txt=[SOLUTIONNAMES(i,:),'=species_summary(:,i);']; eval(txt)
end

II=[species_summary tenorite malachite CuCO3s CuOH2s];
GG=strvcat(SOLUTIONNAMES,'tenorite','malachite','CuCO3s','CuOH2s');

end

% -------------------- NR method solids present

function
[species,err,SI,solids]=NR_method(Asolution,Asolid,Ksolid,Ksolution,T,
guess,iterations,criteria)

Nx=size(Asolution,2); Ncp=size(Asolid,2); Nc=size(Asolution,1);
X=guess;

for II=1:iterations

    Xsolution=X(1:Nx); Xsolid=[]; if Ncp>0; Xsolid=X(Nx+1:Nx+Ncp); end

     logC=(Ksolution)+Asolution*log10(Xsolution); C=10.^(logC); % calc
species

    if Ncp>0;
```

```
        Rmass=Asolution'*C+Asolid*Xsolid-T;
    end


    if Ncp==0; Rmass=Asolution'*C-T; end % calc residuals in mass
balance

    Q=Asolid'*log10(Xsolution); SI=10.^(Q+Ksolid);
    RSI=ones(size(SI))-SI;

      % calc the jacobian

      z=zeros(Nx+Ncp,Nx+Ncp);

      for j=1:Nx;
           for k=1:Nx;
                      for i=1:Nc;
z(j,k)=z(j,k)+Asolution(i,j)*Asolution(i,k)*C(i)/Xsolution(k); end
           end
    end

    if Ncp>0;
    for j=1:Nx;
           for k=Nx+1:Nx+Ncp;
                 t=Asolid';
                       z(j,k)=t(k-Nx,j);
           end
    end
    end

    if Ncp>0
    for j=Nx+1:Nx+Ncp;
           for k=1:Nx
                       z(j,k)=-1*Asolid(k,j-Nx)*(SI(j-Nx)/Xsolution(k));
           end
    end
    end

    if Ncp>0
    for j=Nx+1:Nx+Ncp
        for k=Nx+1:Nx+Ncp
            z(j,k)=0;
        end
    end
    end

    R=[Rmass; RSI]; X=[Xsolution; Xsolid];

    deltaX=z\(-1*R);
    %deltaX=-1*inv(z)*(R);
```

```
        one_over_del=max([1, -1*deltaX'./(0.5*X')]);
        del=1/one_over_del;
        X=X+del*deltaX;

    %X=X+deltaX;

        tst=sum(abs(R));
        if tst<=criteria; break; end

end

logC=(Ksolution)+Asolution*log10(Xsolution); C=10.^(logC); % calc
species
RSI=ones(size(SI))-SI;

if Ncp>0; Rmass=Asolution'*C+Asolid*Xsolid-T; end % calc residuals in
mass balance
if Ncp==0; Rmass=Asolution'*C-T; end % calc residuals in mass balance

err=[Rmass];

species=[C];
solids=Xsolid;

end

% ----------- NR method just solution species

function
[species,err,SI]=NR_method_solution(Asolution,Asolid,Ksolid,Ksolution,
T,guess,iterations,criteria)

Nx=size(Asolution,2); Ncp=size(Asolid,1); Nc=size(Asolution,1);
X=guess;

for II=1:iterations

    Xsolution=X(1:Nx);

        logC=(Ksolution)+Asolution*log10(Xsolution); C=10.^(logC); % calc
species

    Rmass=Asolution'*C-T;

    Q=Asolid*log10(Xsolution); SI=10.^(Q+Ksolid);
    RSI=ones(size(SI))-SI;

     % calc the jacobian

     z=zeros(Nx,Nx);
```

```
        for j=1:Nx;
            for k=1:Nx;
                        for i=1:Nc;
z(j,k)=z(j,k)+Asolution(i,j)*Asolution(i,k)*C(i)/Xsolution(k); end
            end
     end

     R=[Rmass]; X=[Xsolution];

     deltaX=z\(-1*R);
     %deltaX=-1*inv(z)*(R);
      one_over_del=max([1, -1*deltaX'./(0.5*X')]);
      del=1/one_over_del;
      X=X+del*deltaX;

     %X=X+deltaX;

      tst=sum(abs(R));
      if tst<=criteria; break; end

end

logC=(Ksolution)+Asolution*log10(Xsolution); C=10.^(logC); % calc
species
RSI=ones(size(SI))-SI;

Q=Asolid*log10(Xsolution); SI=10.^(Q+Ksolid);
RSI=ones(size(SI))-SI;

Rmass=Asolution'*C-T;

err=[Rmass];

species=[C];

end

% ----- equilib definition ---------------

function
[KSOLUTION,KSOLID,ASOLUTION,ASOLID,SOLUTIONNAMES,SOLIDNAMES]=get_equil
ib_defn(flag);

logKw=-13.75;
logKh1=-7.55;
logBh21=-5.59202
logBh22=-10.7463;
logBh34=-22.33122;
pKa1=5.97;
```

```
pKa2=9.53;
logKCuCO3=5.73;
logKCuCO32=9.23;
logKCuHCO3=1.03;
logKCuCl=-0.2;
logKCuSO4=0.7737;
logKHSO4=1.1781;

KSOLUTION=[...
     0
     0
     0
     0
     0
     logKw
     logKh1
     logBh21
     logBh22
     logBh34
     pKa2
     pKa2+pKa1
     logKCuCO3
     logKCuCO32
     logKCuHCO3
     logKCuCl
     logKCuSO4
     logKHSO4];

ASOLUTION=[...
   %H      M      CO3   Cl    SO4
    1       0      0     0     0
    0       1      0     0     0
    0       0      1     0     0
    0       0      0     1     0
    0       0      0     0     1
   -1       0      0     0     0
   -1       1      0     0     0
   -1       2      0     0     0
   -2       2      0     0     0
   -4       3      0     0     0
    1       0      1     0     0
    2       0      1     0     0
    0       1      1     0     0
    0       1      2     0     0
    1       1      1     0     0
    0       1      0     1     0
    0       1      0     0     1
    1       0      0     0     1];
```

```
SOLUTIONNAMES=strvcat('H','Cu','CO3','Cl','SO4','OH','CuOH','Cu2OH','C
u2OH2','Cu3OH4','HCO3','H2CO3','CuCO3aq','CuCO32aq','CuHCO3','CuCl','C
uSO4','HSO4');


    % -------------- solid values

    logKsp=-18.7;
    logKcuoh2s=-logKsp+2*logKw;
    logKCuCO3s=11.5;
    logKmalachite=33.18+2*logKw;
    logKmalachite=32.0+2*logKw;
    logKtenorite=20.48+2*logKw;
    if flag==1; logKmalachite=1; end
    logKcuoh2s=-10;
    %logKCuCO3s=1;
    logKtenorite=-100;
    %logKmalachite=1;

    KSOLID=[...
    logKtenorite
    logKmalachite
    logKcuoh2s
    logKCuCO3s];

    ASOLID=[...
     -2       1    0      0    0
     -2       2    1      0    0
     -2       1    0      0    0
      0       1    1      0    0];

 SOLIDNAMES=strvcat('tenorite','malachite','CuOH2s','CuCO3s');

end

% ----------- for fixed pH ----------------

function
[Ksolution,Ksolid,Asolution,Asolid]=get_equilib_fixed_pH(KSOLUTION,KSO
LID,ASOLUTION,ASOLID,pH)

    [N,M]=size(ASOLUTION);
    Ksolution=KSOLUTION-ASOLUTION(:,1)*pH;
    Asolution=[ASOLUTION(:,2:M)];
    [N,M]=size(ASOLID);
    Ksolid=KSOLID-ASOLID(:,1)*pH;
    Asolid=[ASOLID(:,2:M)];
end
```

Appendix B: Matlab Interpolations for corrected logK values

B.1 Copper logK Interpolations
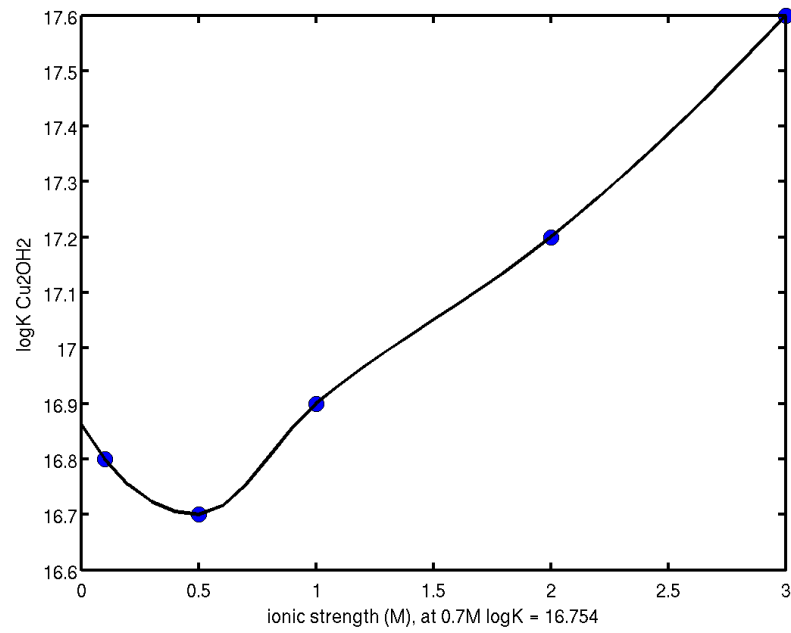
Figure B.1: Interpolation of Cu$_2$(OH)$_2$.
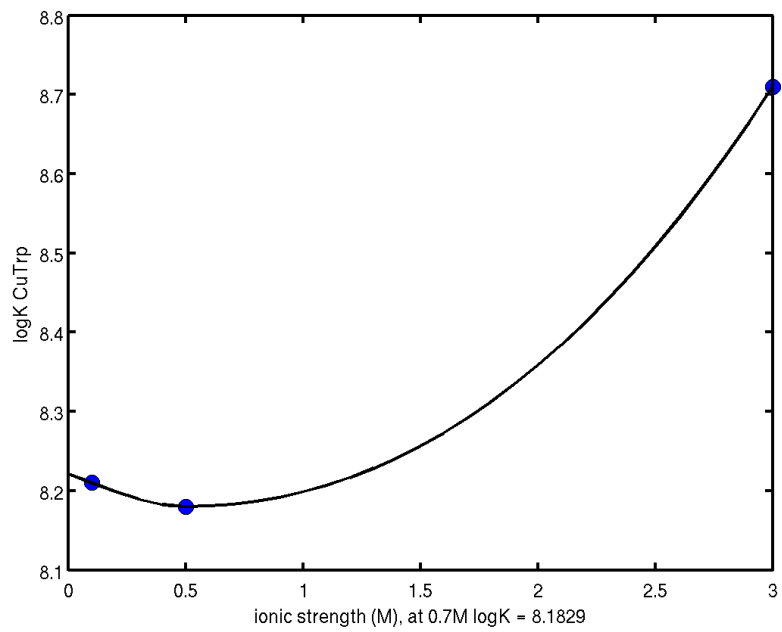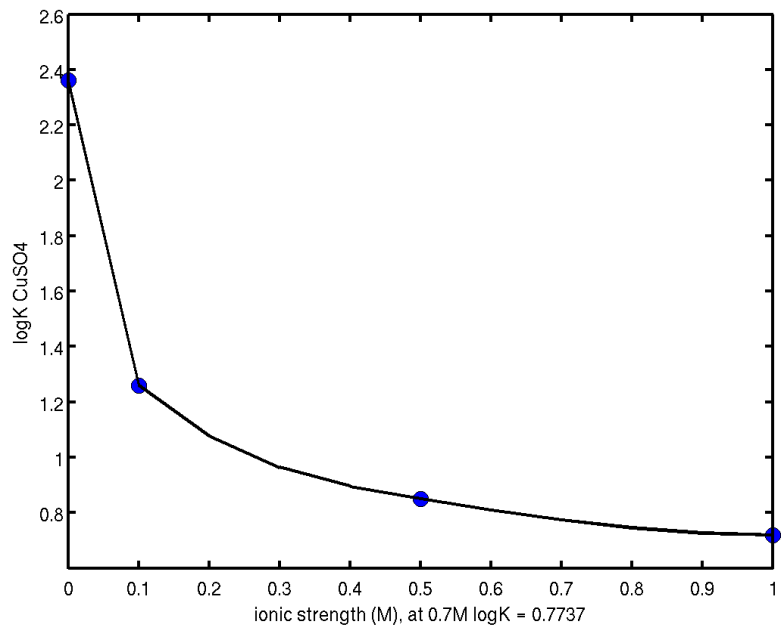
Figure B.2: Interpolation of CuTrp.

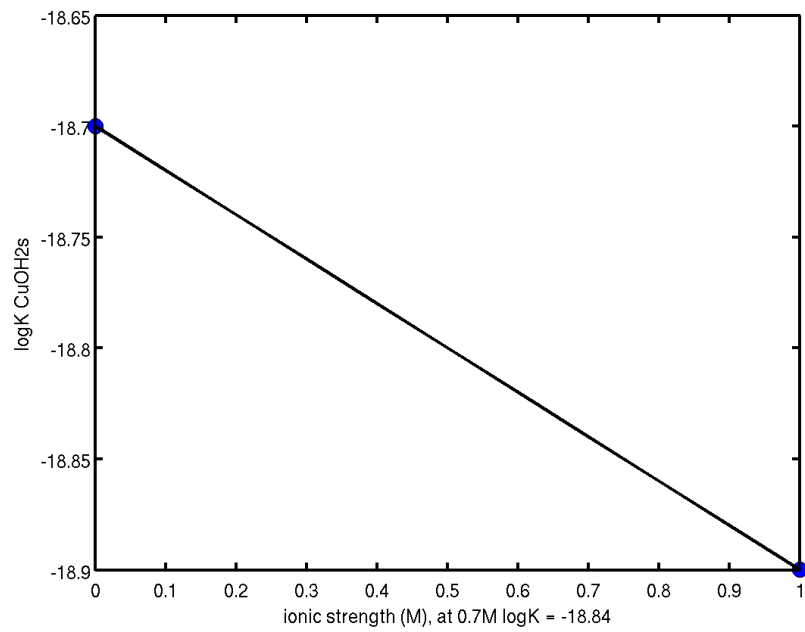**Figure B.3: Interpolation of CuSO₄.**

115

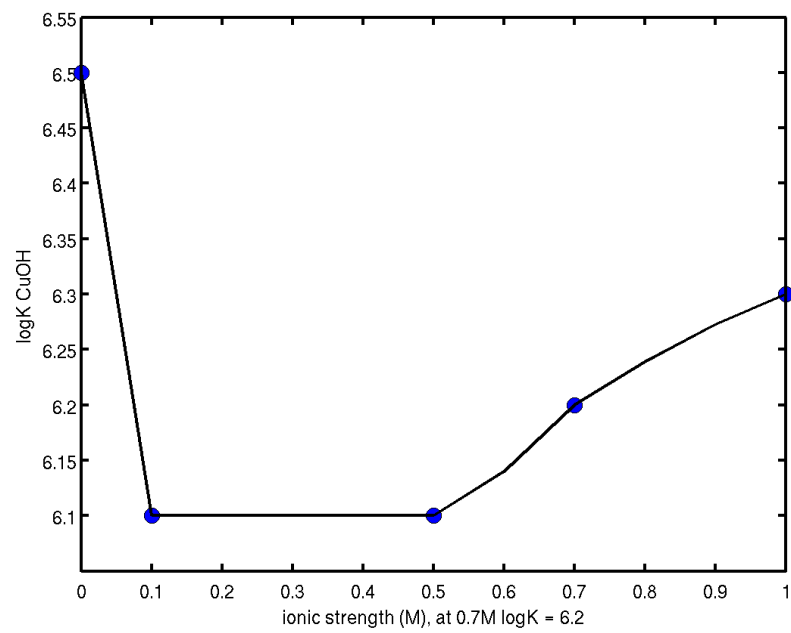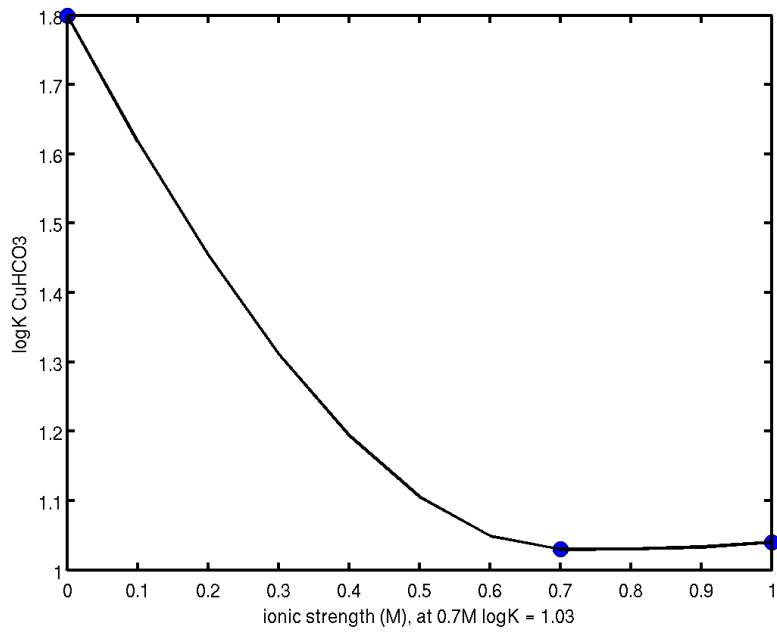**Figure B.4: Interpolation of solid Cu(OH)$_2$.**

Figure B.5: Interpolation of CuOH.

Figure B.6: Interpolation of CuHCO$_3$.
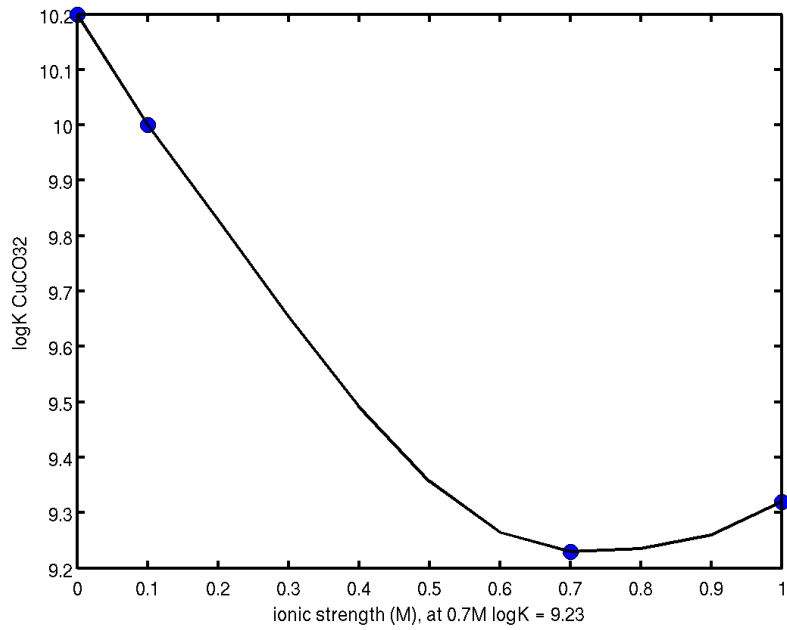
Figure B.6: Interpolation of Cu(CO$_3$)$_2$.
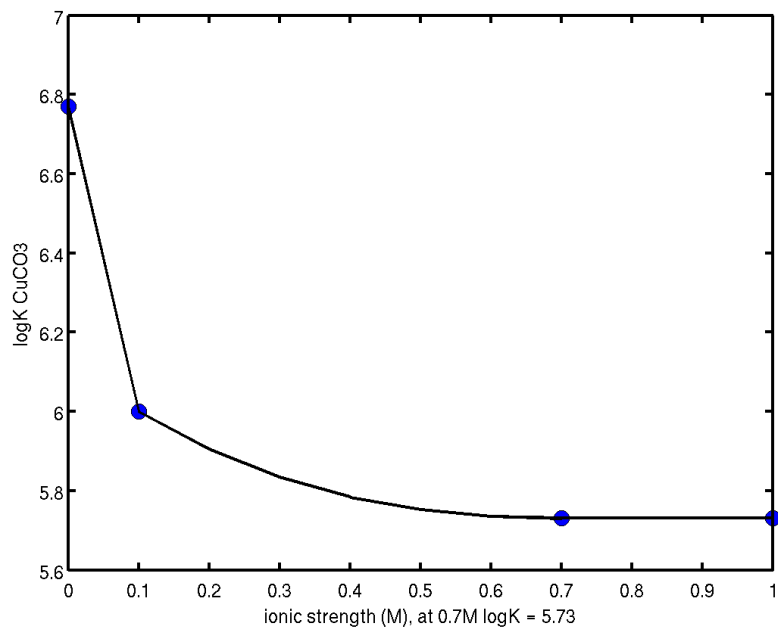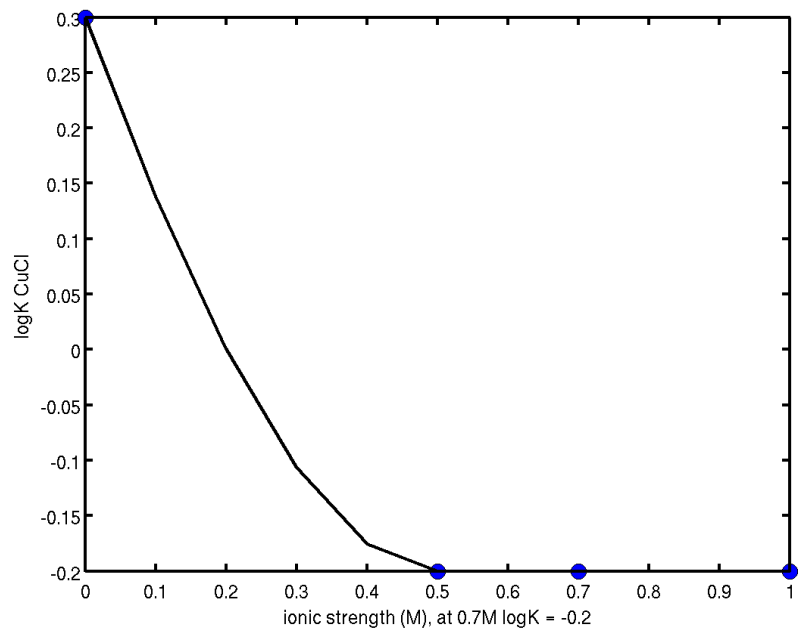
Figure B.7: Interpolation of CuCO$_3$.
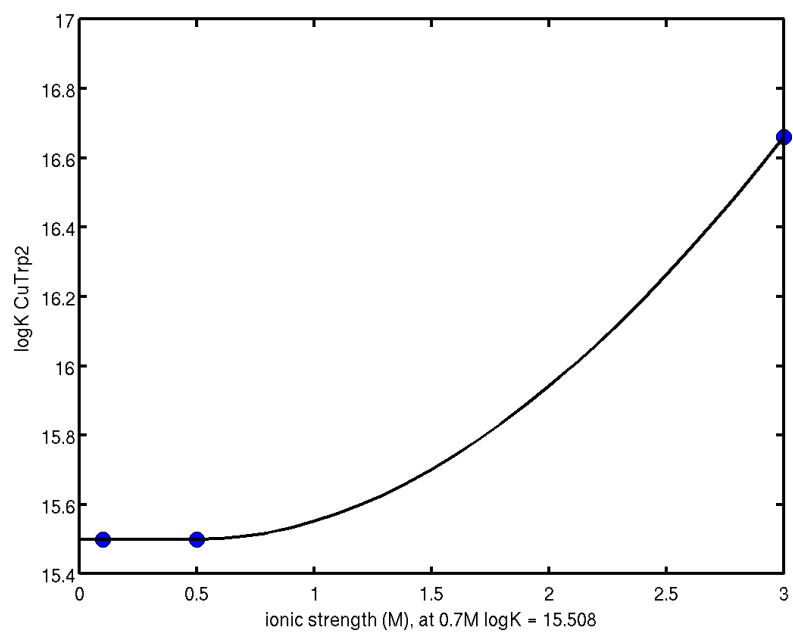

Figure B.9: Interpolation of CuCl.

Figure B.10: Interpolation of Cu(Trp)$_2$.

B.2 Acid and Ion logK Interpolations
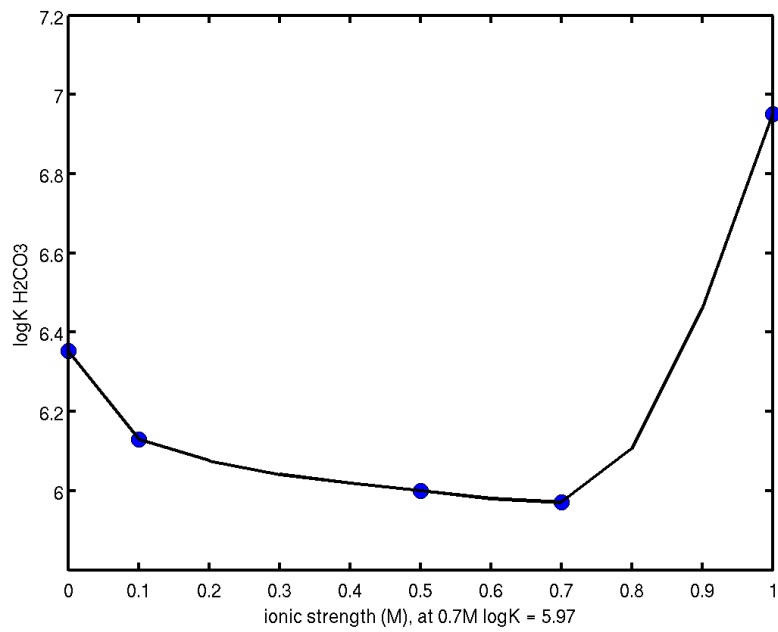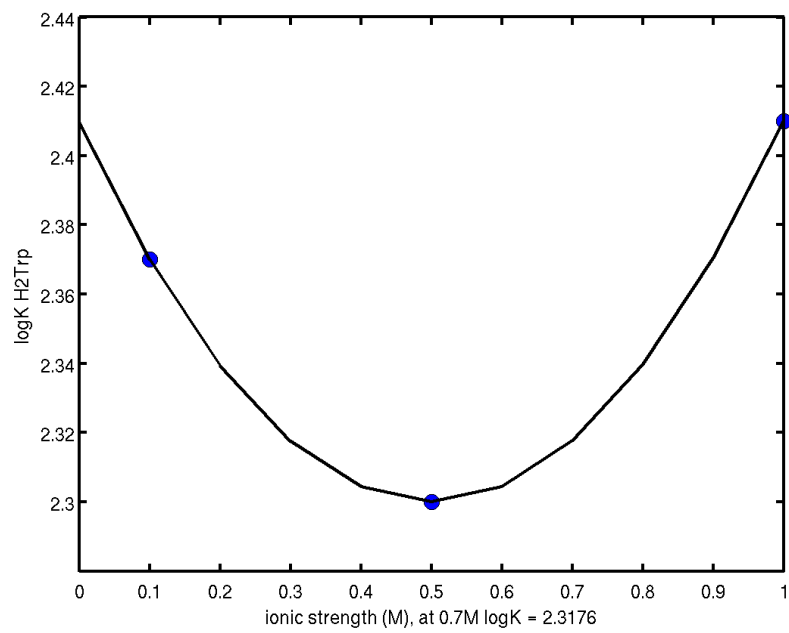
Figure B.11: Interpolation of H$_2$CO$_3$.
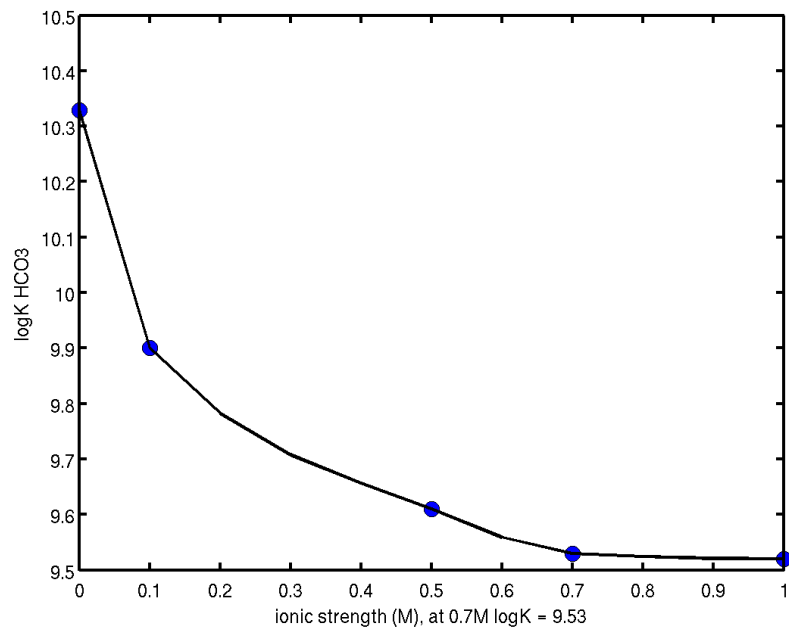

Figure B.12: interpolation of H$_2$Trp.

120
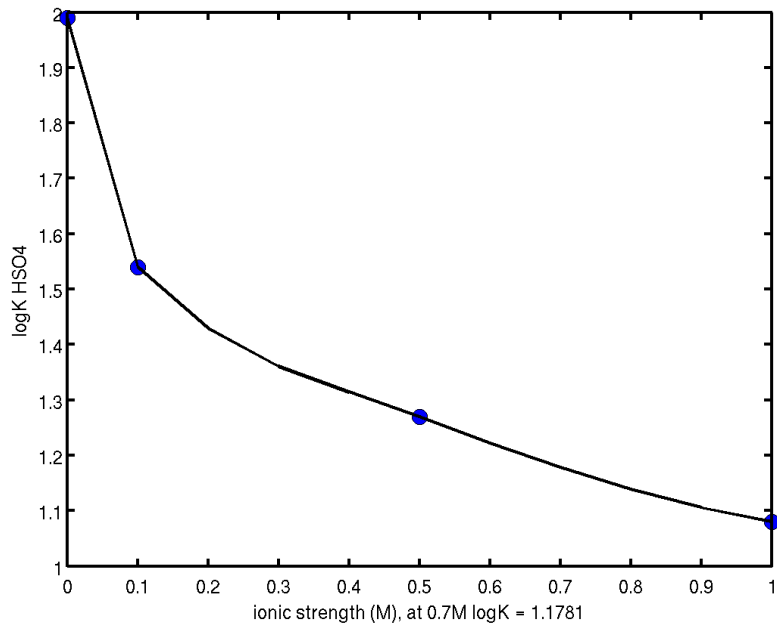
Figure B.13: Interpolation of HCO$_3$.

Figure B.14: Interpolation HSO$_4$.

121

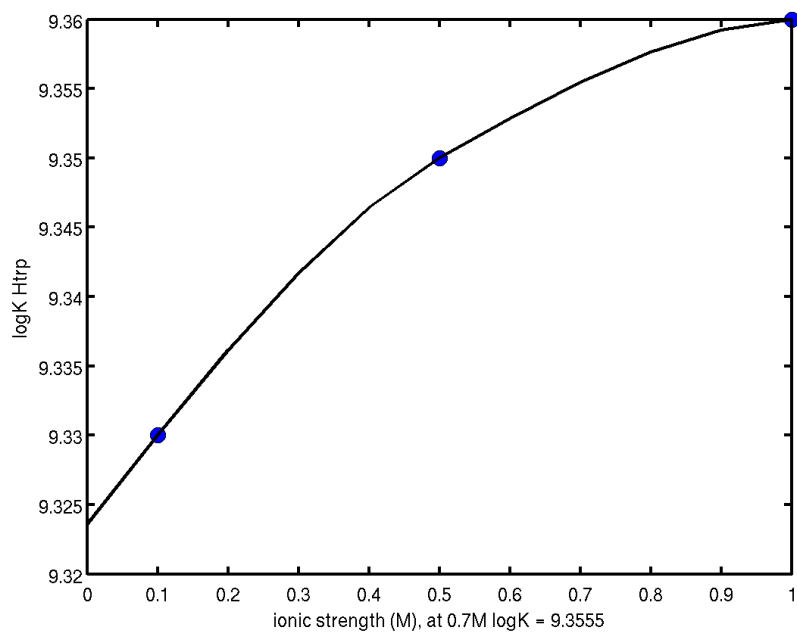**Figure B.15: Interpolation of HTrp.**
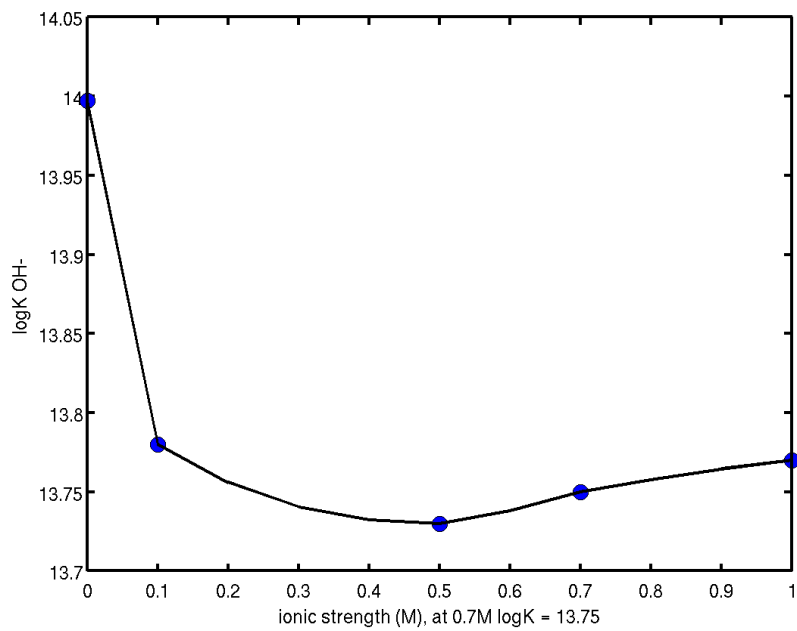
Figure B.16: Interpolation of OH-.

B.3 Lead logK Interpolations
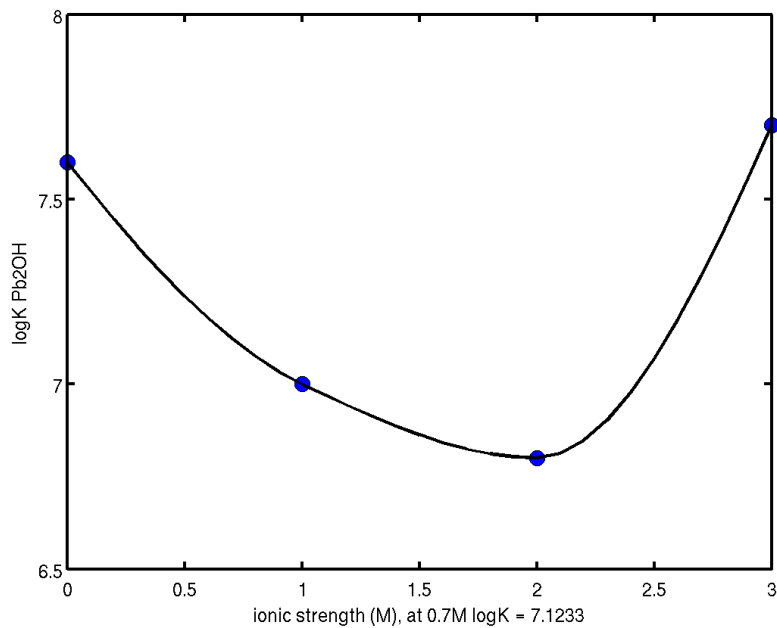
Figure B.17: Interpolation of Pb$_2$OH.
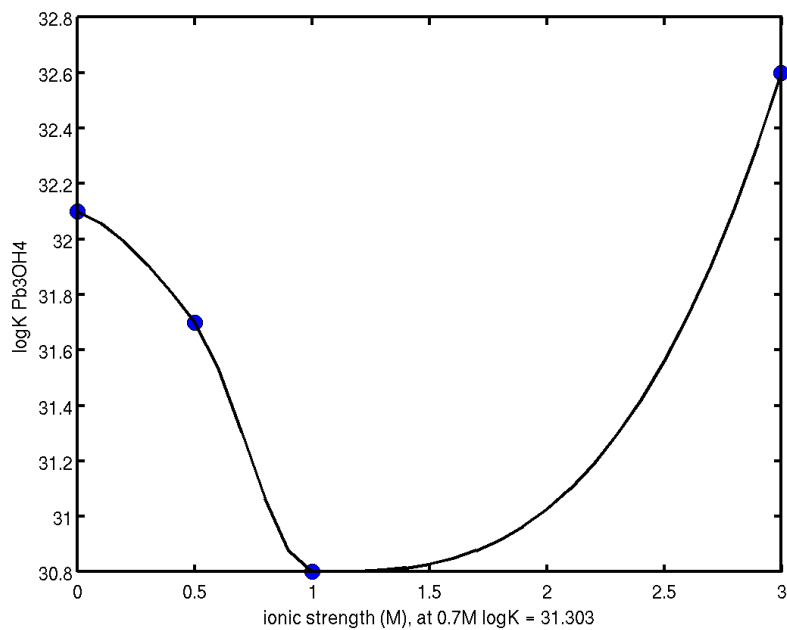
Figure B.18: Interpolation of Pb$_3$OH$_4$.
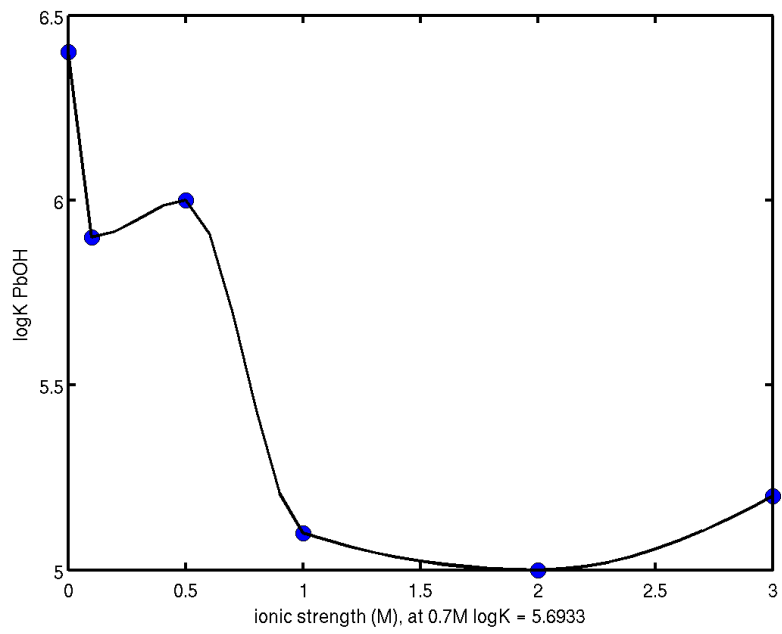
Figure B.19: Interpolation of PbOH.
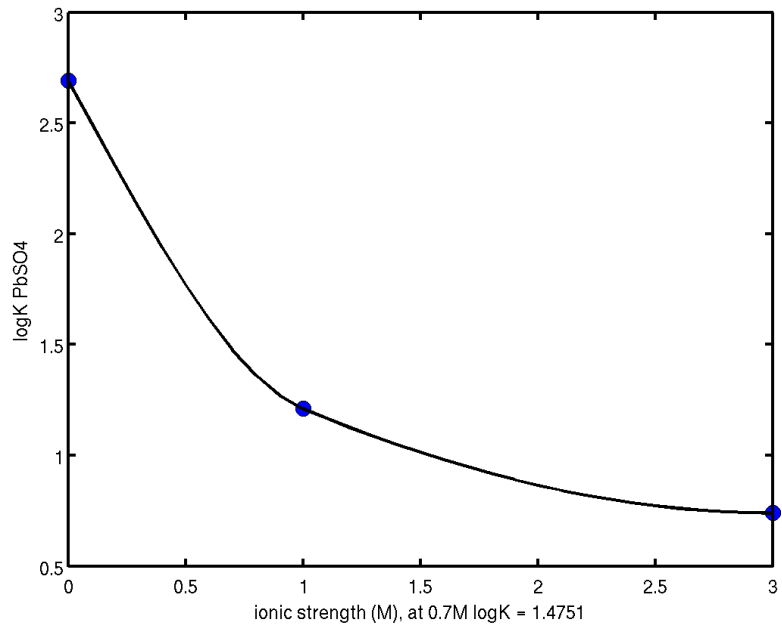
Figure B.20: Interpolation of PbSO$_4$.
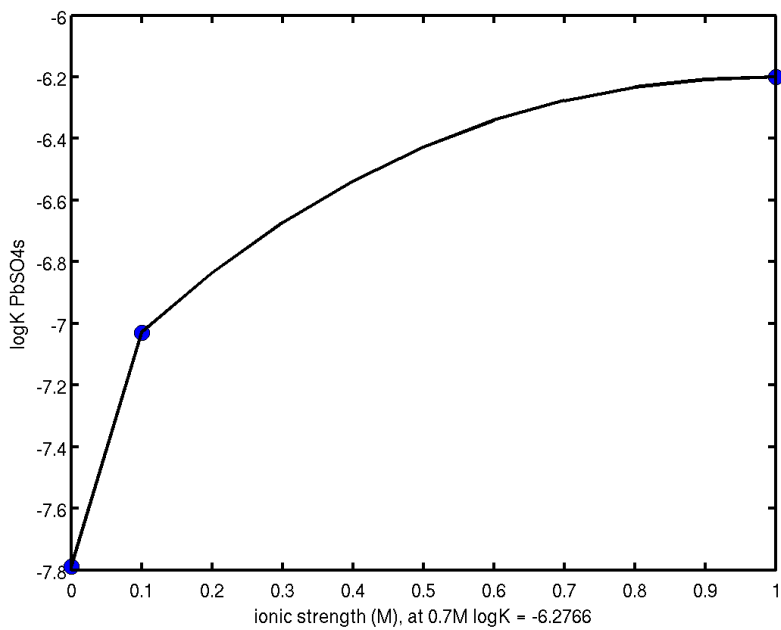
Figure B.21: Interpolation of solid PbSO$_4$.
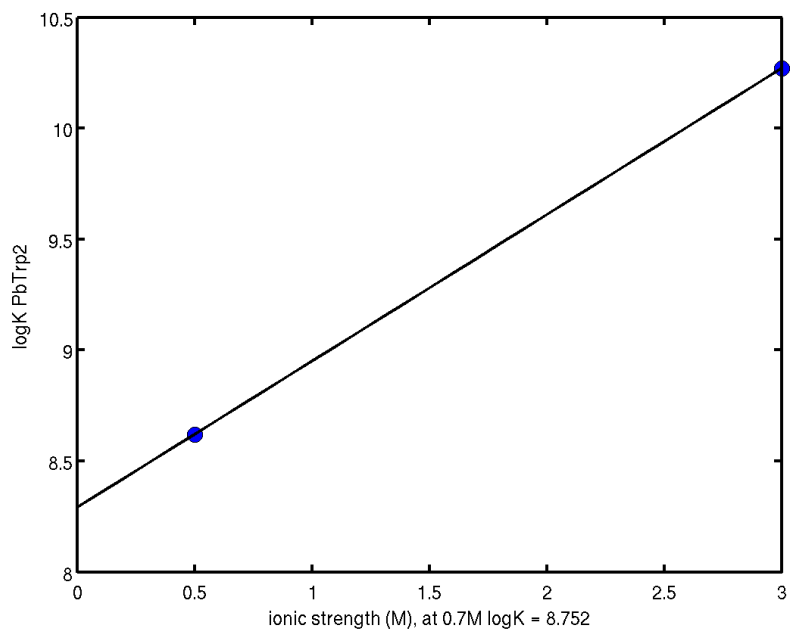
Figure B.22: Interpolation for Pb(Trp)$_2$.
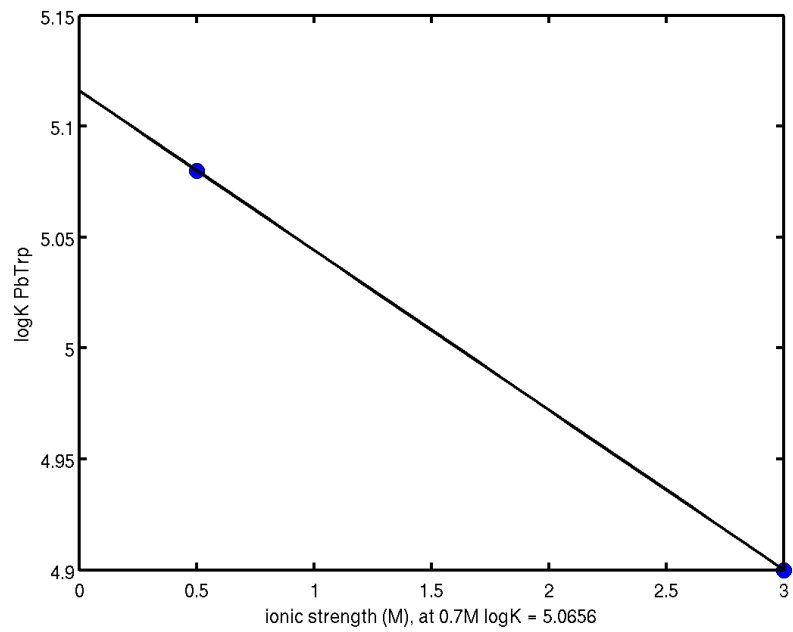
Figure B.23: Interpolation of PbTrp.
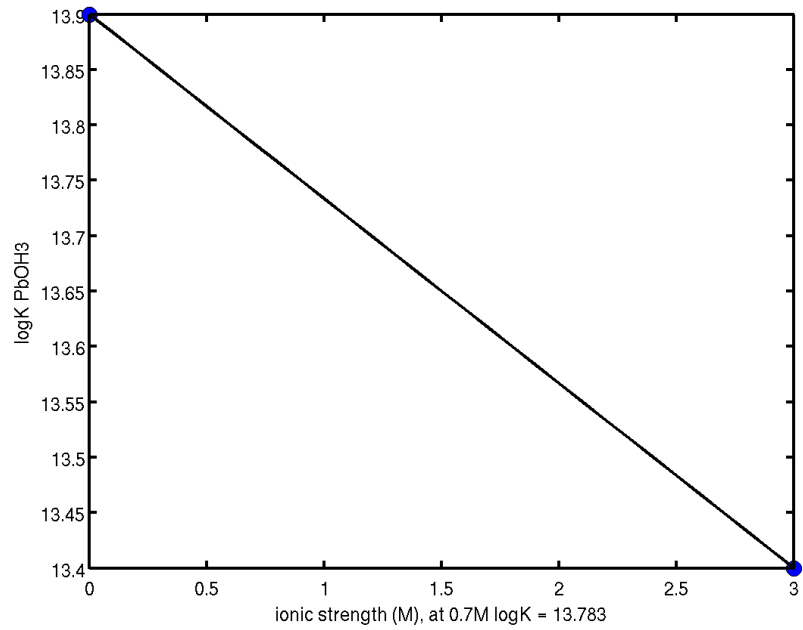
Figure B.24: Interpolation of Pb(OH)₃.

126
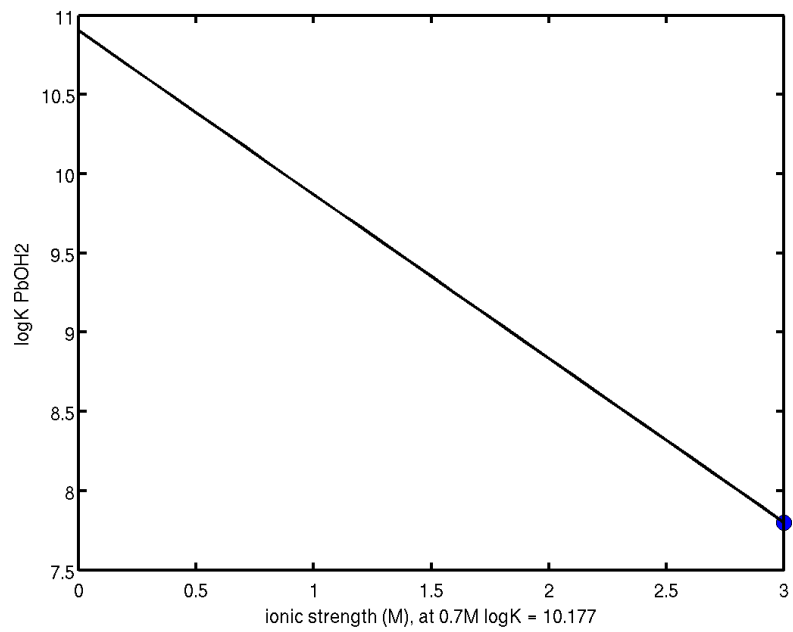
Figure B.25: Interpolation of Pb(OH)₂.
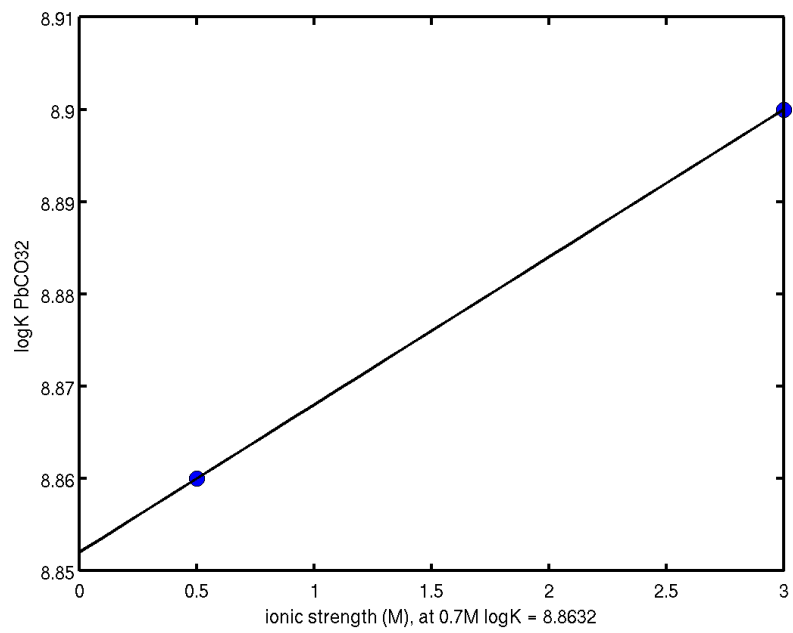
Figure B.26: Interpolation of Pb(CO₃)₂.

127
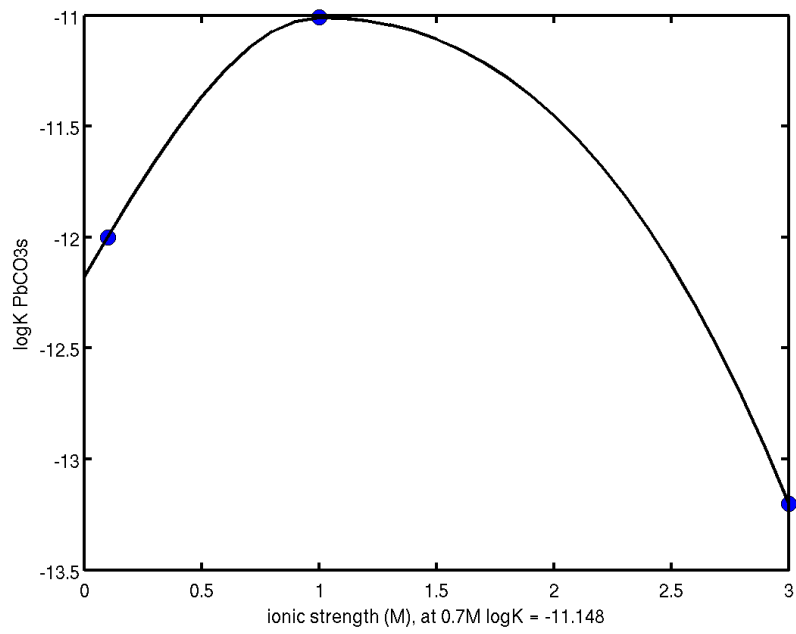
Figure B.27: Interpolation of solid PbCO$_3$.
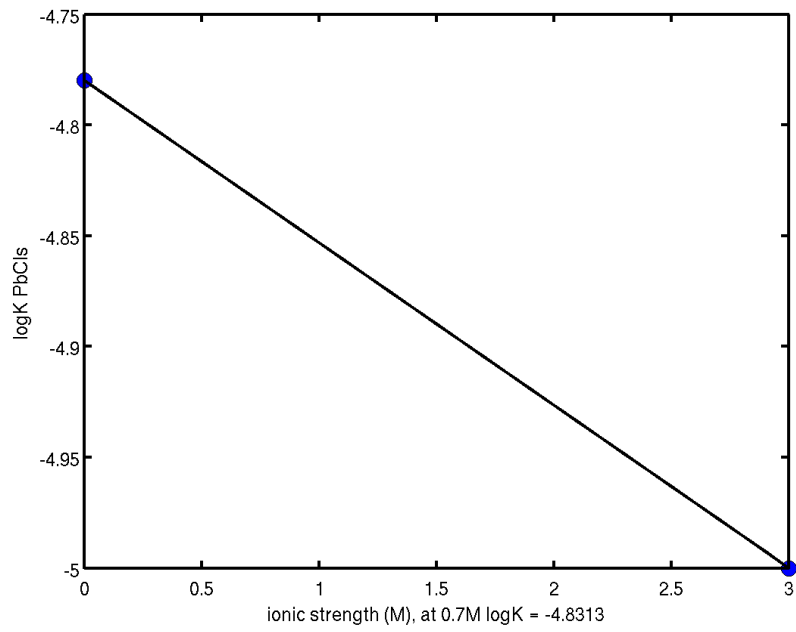
Figure B.28: Interpolation of solid PbCl.
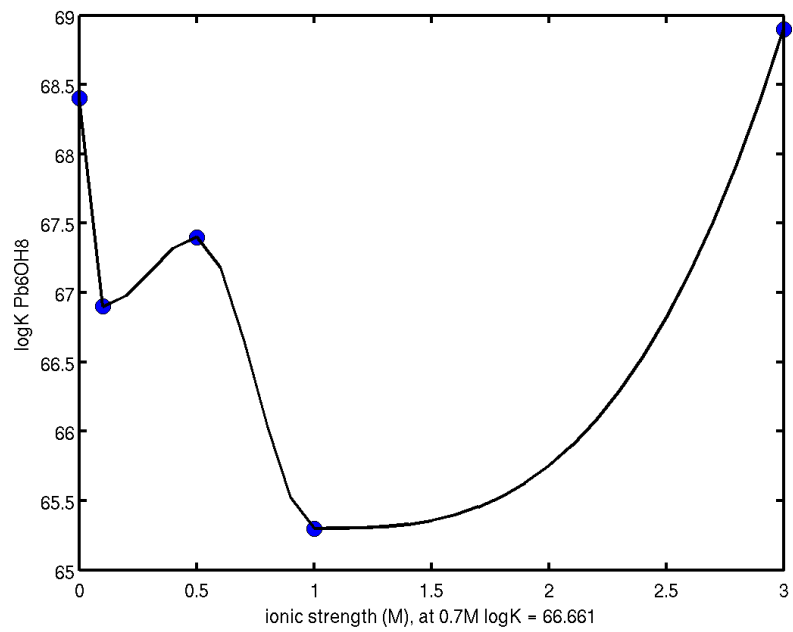
Figure B.29: Interpolation Pb$_6$(OH)$_8$.

B.4 Zinc logK Interpolations
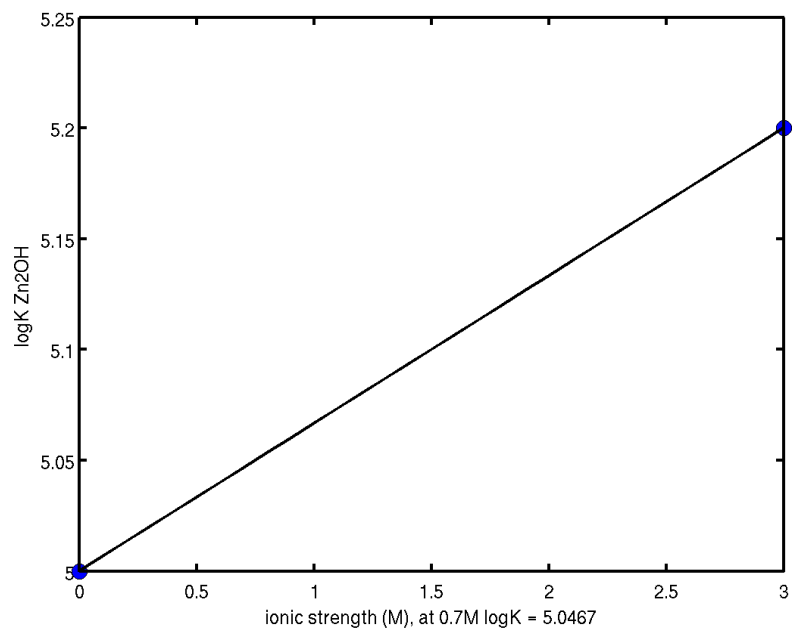
Figure B.30: Interpolation of Zn$_2$OH.
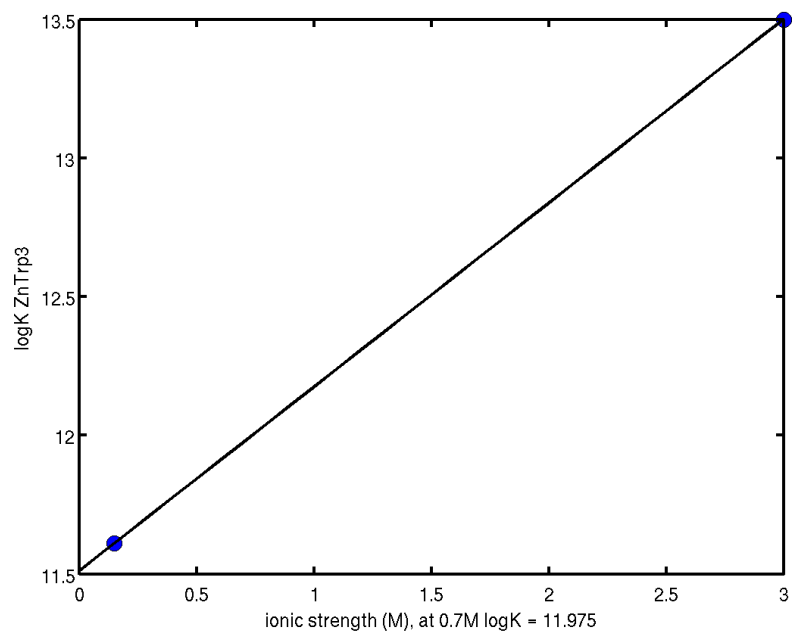
Figure B.31: Interpolation of Zn(Trp)₃.
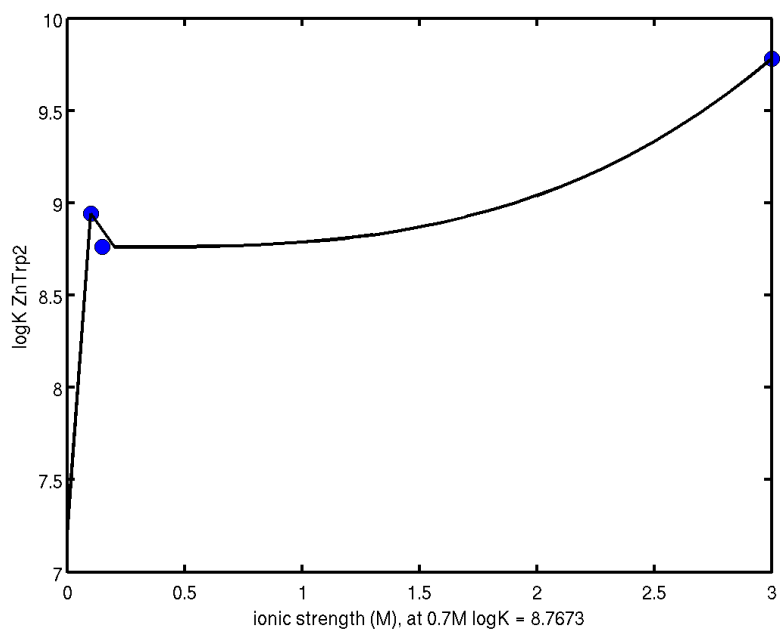
Figure B.32: Interpolation of Zn(Trp)₂.

130
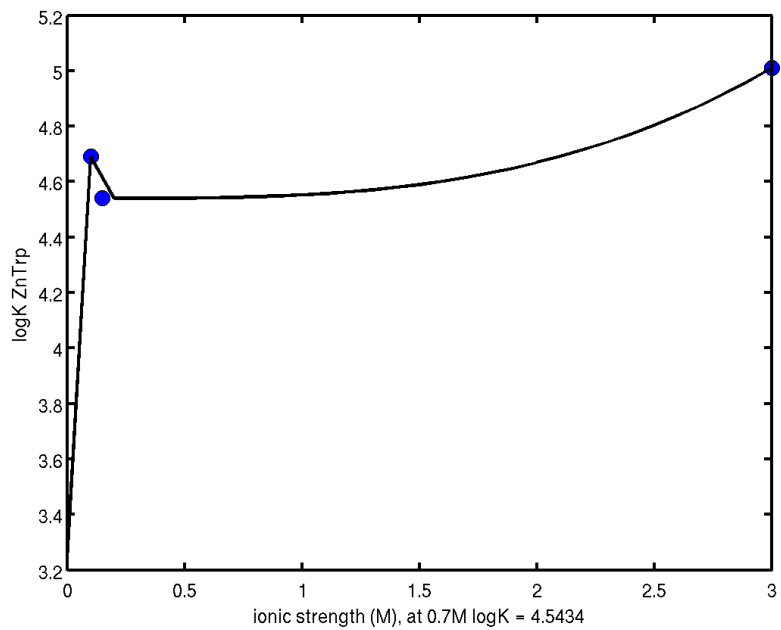
Figure B.33: Interpolation of ZnTrp.
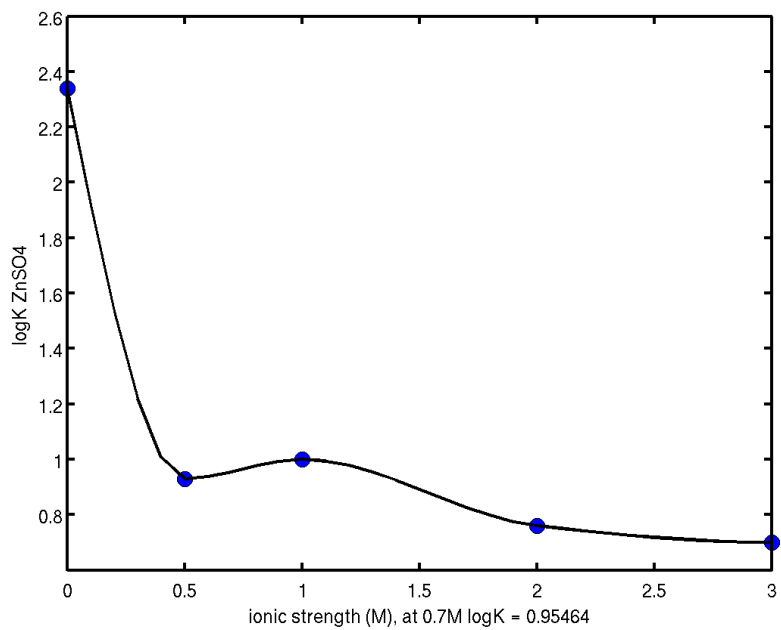
Figure B.34: Interpolation of ZnSO$_4$.

131
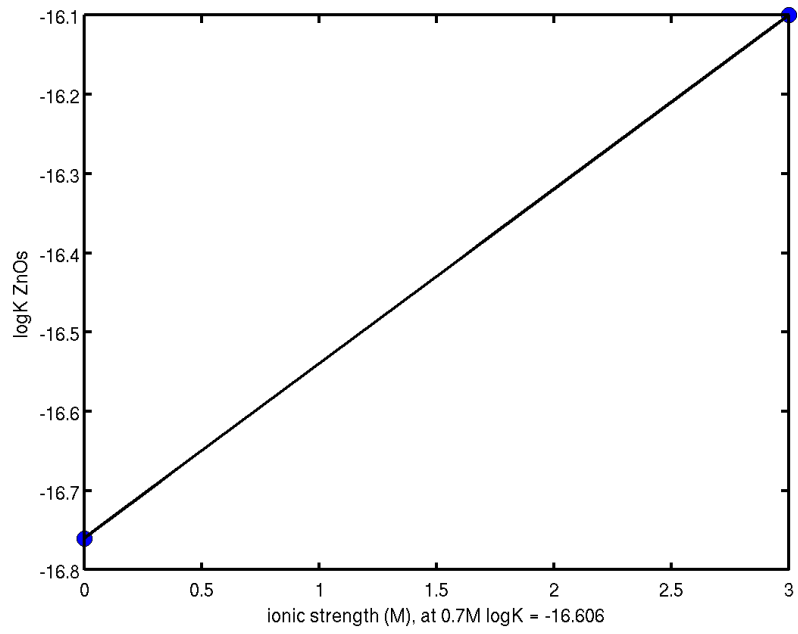
Figure B.35: Interpolation of solid ZnO.
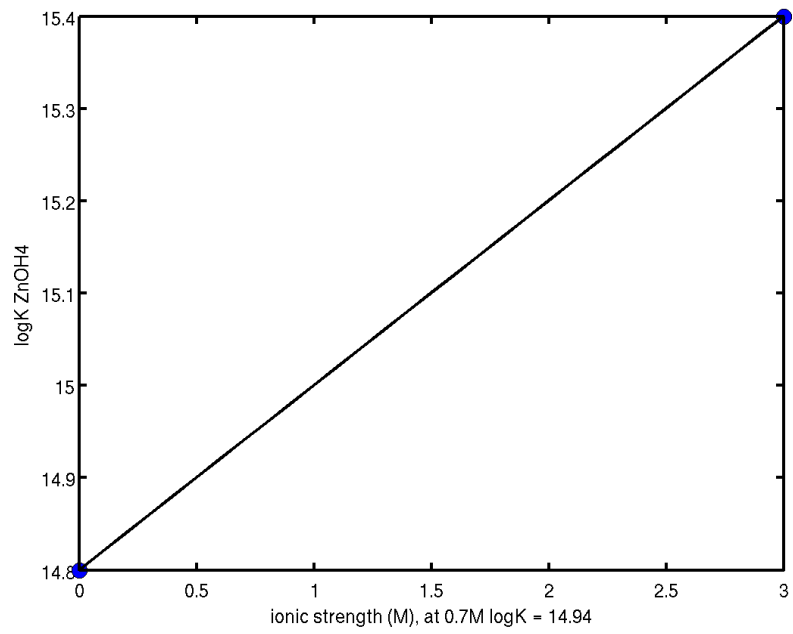
Figure B.36: Interpolation of Zn(OH)₄.
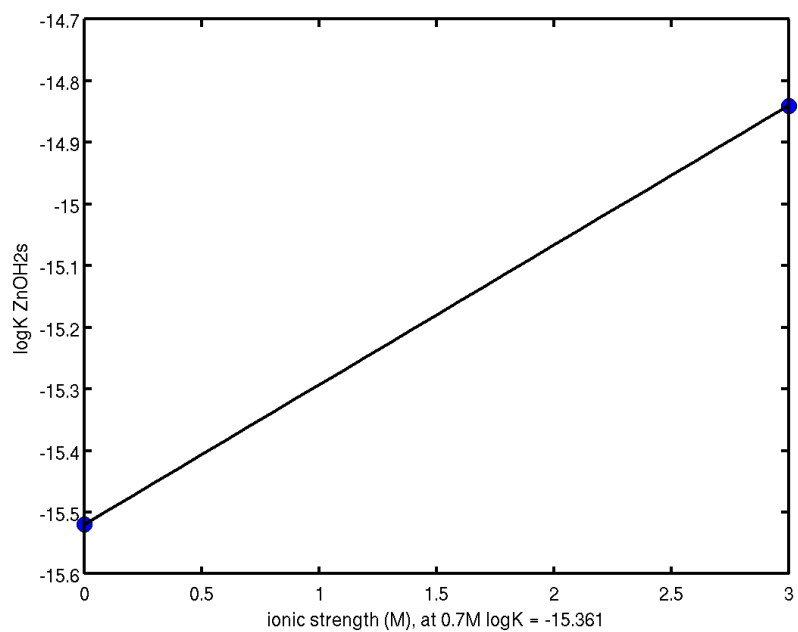
Figure B.37: Interpolation of solid Zn(OH)$_2$.
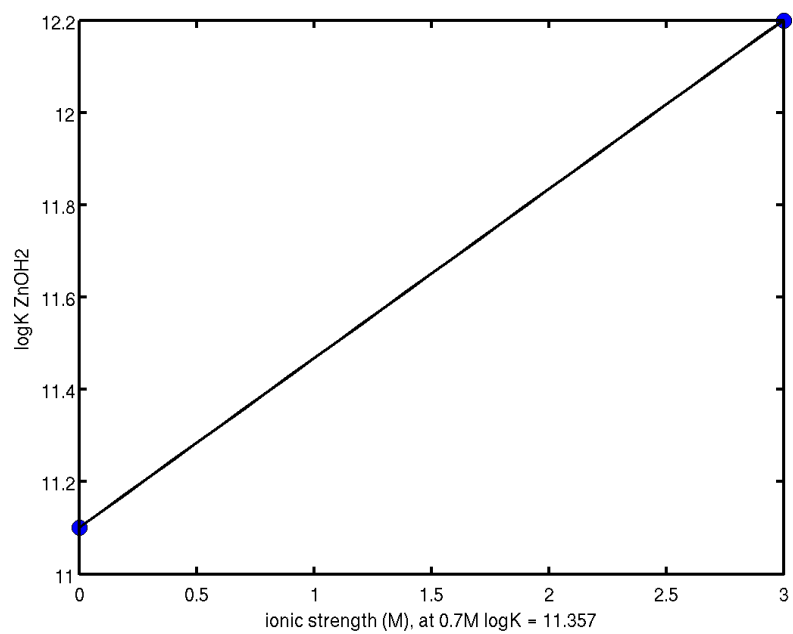
Figure B.38: Interpolation of Zn(OH)$_2$.

133
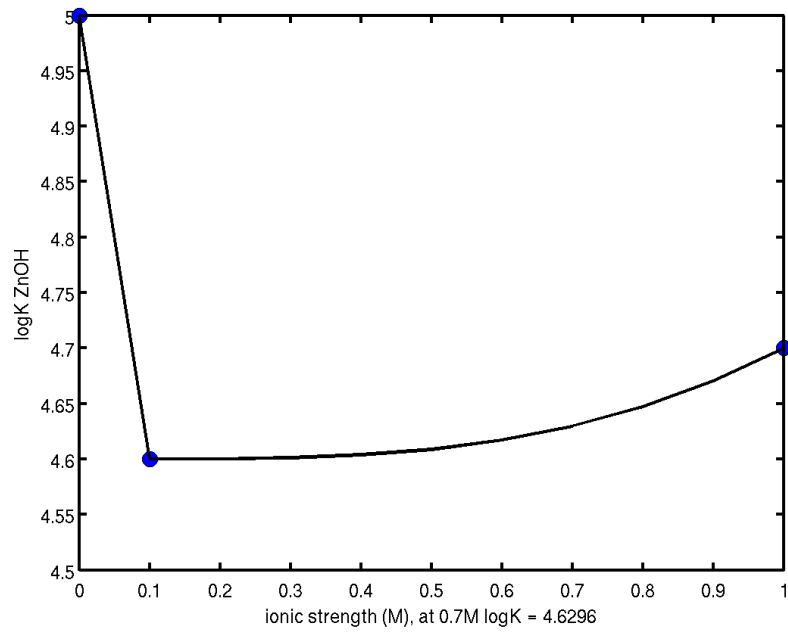
Figure B.39: Interpolation of ZnOH.

B.5: Nickel logK Interpolations
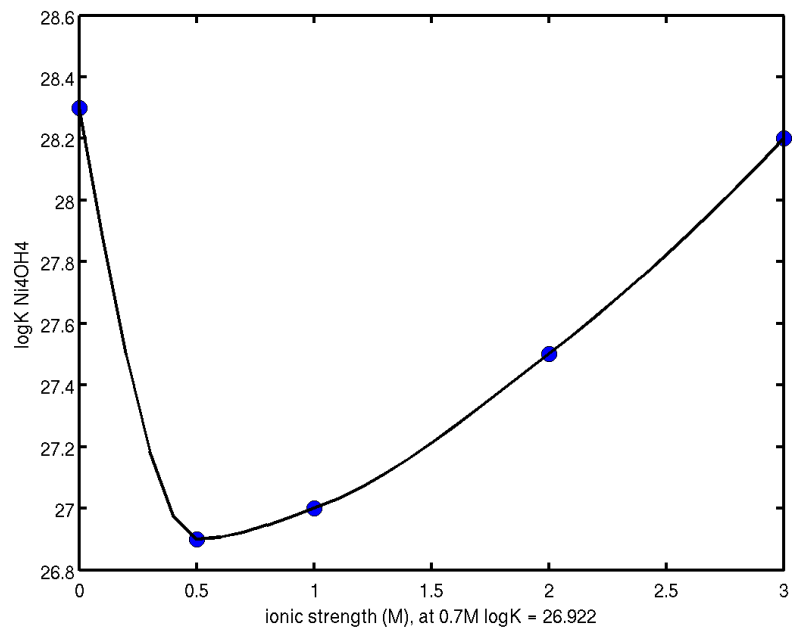
Figure B.40: Interpolation of Ni$_4$(OH)$_4$.
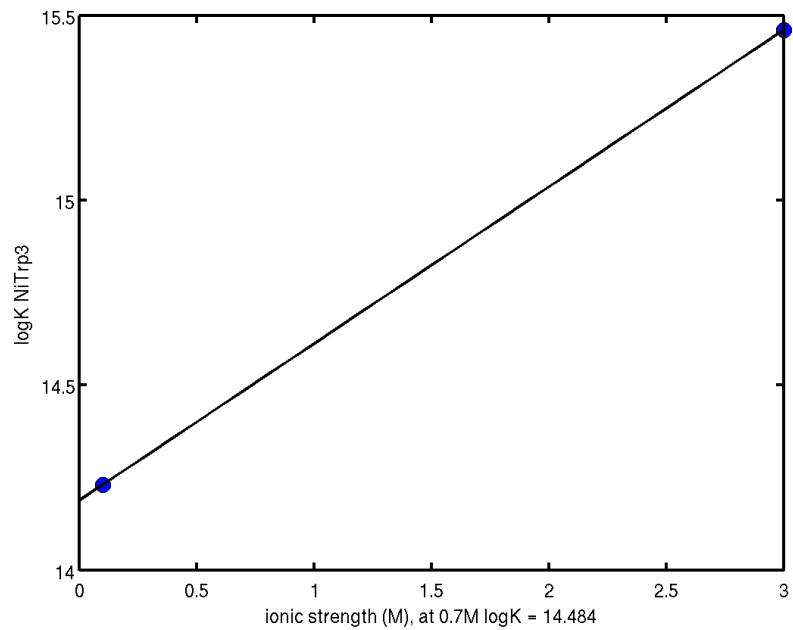
Figure B.41: Interpolation of Ni(Trp)₃.
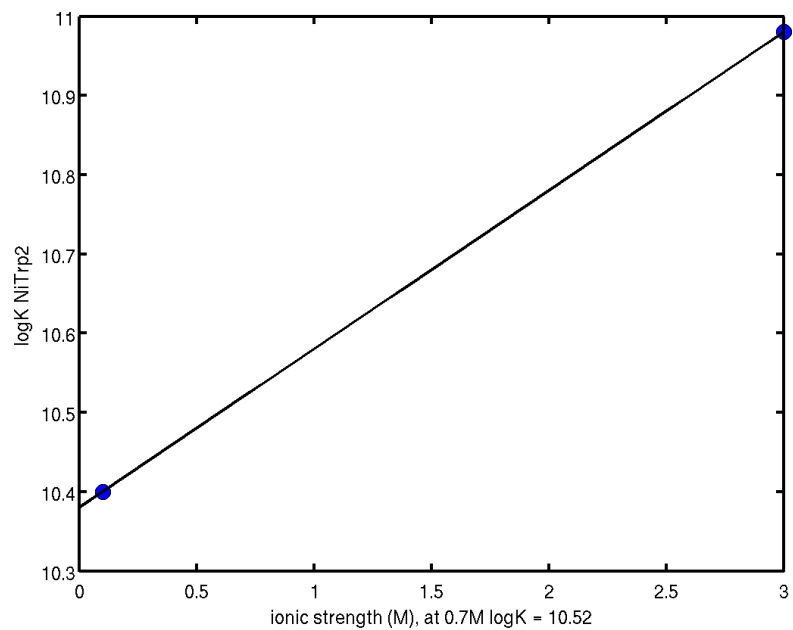
Figure B.42: Interpolation of Ni(Trp)₂.

135
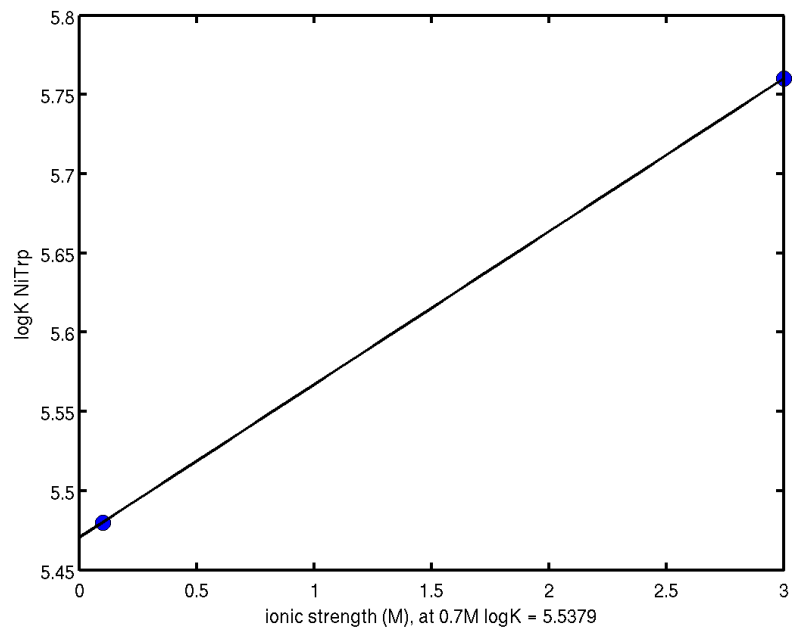
Figure B.43: Interpolation of NiTrp.
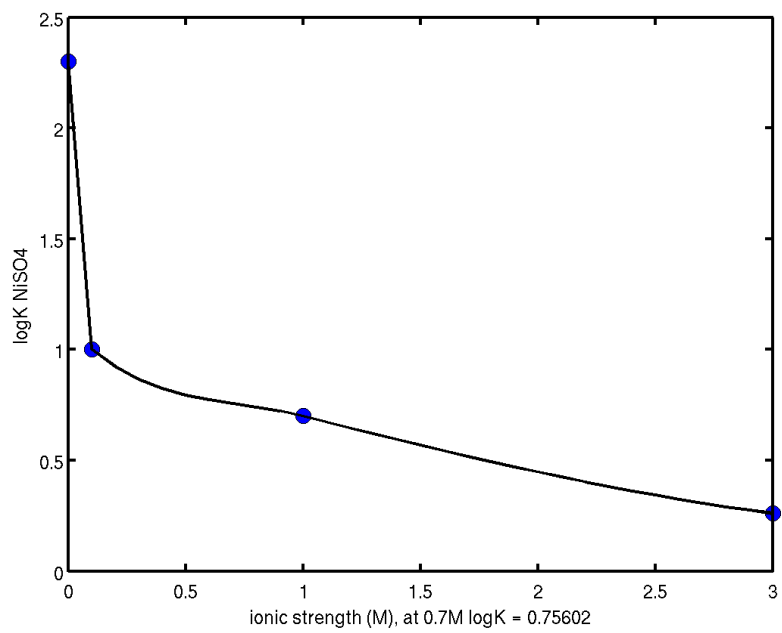
Figure B.44: Interpolation of NiSO$_4$.
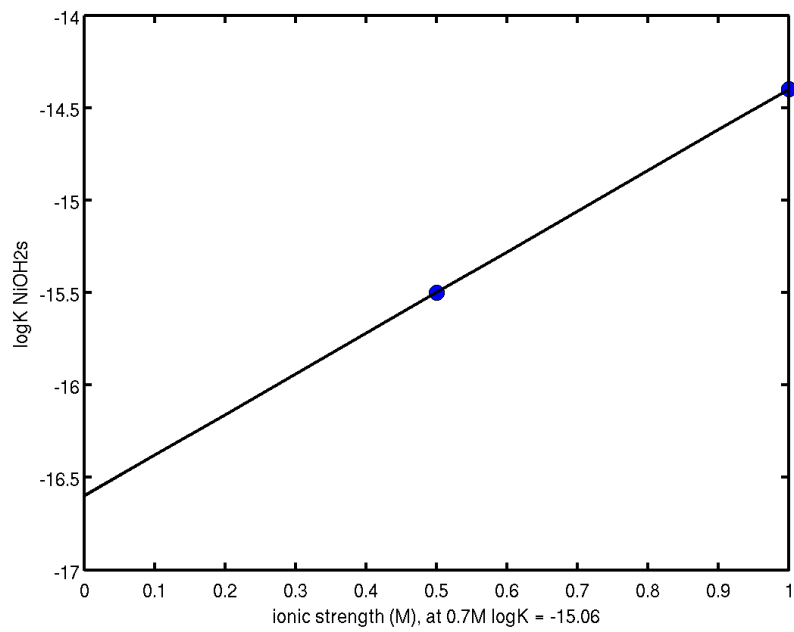
Figure B.45: Interpolation of solid Ni(OH)$_2$.
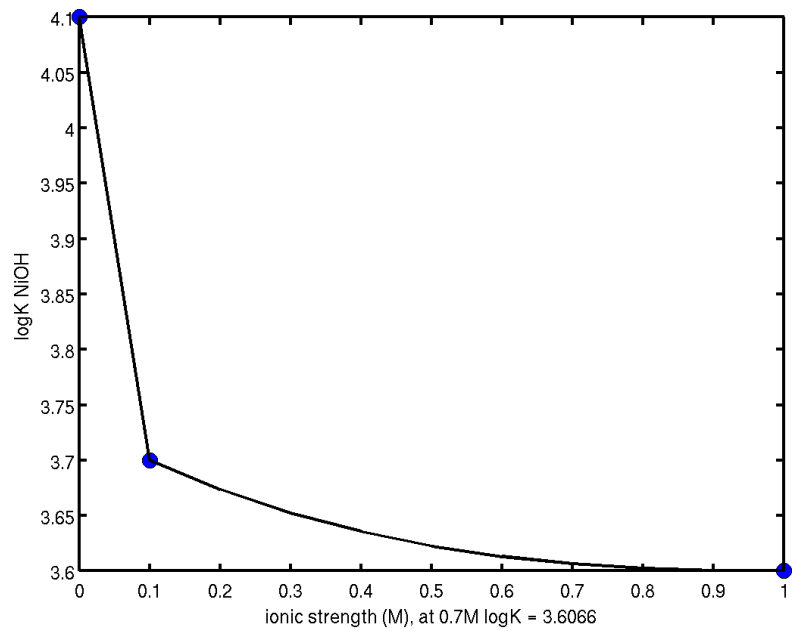
Figure B.46: Interpolation of NiOH.

137
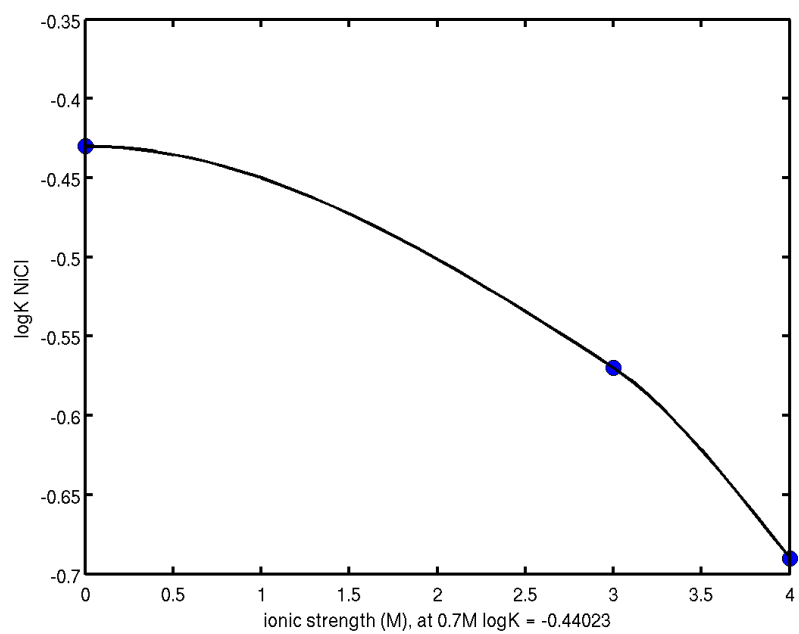
Figure B.47: interpolation of NiCl.

Appendix C: Matlab Code for Theoretical Fluorescence Modeling

C.1 Matlab Code for Lead

```
function GG=for_Rachael_vCuT_fixedpH_10uM_Trp2_Pb

clear; figure(1); clf; figure(2); clf

ClT=0.5;
PCO2=10^(-3.5);
NaHCO3=200; %mg/L from recipe
NaHCO3AW=100; %g/mol
DIC=((NaHCO3*1e-3)/NaHCO3AW);
PbTppb=[1:25:600];
PbT=(PbTppb*1e-6)/207.21;
TrpT=10e-6;
SO4T=1e-2;

pH=7.82;

% model calc no ppte

c=0;

for i=1:size(PbT,2)


[species,names]=Cumodel_highIS_Cl_DIC_Trp_ppte(PbT(i),pH,DIC,ClT,TrpT,
SO4T,3);

    % flag=2 malachite only
    % flag=1 tenorite only
    % flag=3 no ppte

    c=c+1;
    for j=1:size(species,2)
        txt=[names(j,:),'(c)=species(:,j);'];  eval(txt)
    end
    species_summary(i,:)=species;
end

%PbBound=PbTrp2+PbTrp;
%FreePb=PbT-PbBound;
%FreeTryp=TrpT-PbBound;

%K=log10(PbBound./(FreePb.*FreeTryp))
%plot(PbTppb,K,'ko')
%k=waitforbuttonpress

figure(1)
```

```matlab
h=plot(PbTppb,HTrp*1e6,PbTppb,H2Trp*1e6,PbTppb,Trp*1e6,PbTppb,PbTrp*1e
6,PbTppb,PbTrp2*1e6,'linewidth',2);
legend('HTrp','H2Trp','Trp','PbTrp','PbTrp2')
xlabel('Pb_T (ppb)','fontsize',12)
ylabel('species (\mumol/L)','fontsize',12)
set(gca,'linewidth',2)
set(gca,'fontsize',12)
title('Solubility','fontsize',12)

%%
 data=[0    9.9009900990099  33.8164251207729 78.3410138248848
      137.931034482759 206.349206349206 290.780141843972 372.822299651568
      528.619528619529
167.6157 158.1005 159.3358 150.547 142.0638 130.6604 116.9886 114.4316
109.40378];


MT=data(1,:)*1000/207.21; % ppb conc of metal
F1=data(2,:); %trp

figure(2); h=plot(MT,F1,'ko','markersize',8);
set(h(1),'markerfacecolor','b');
figure(2); hold on; plot(PbT*(1e9),HTrp*1.6785e7,'b','linewidth',2)
xlabel('Pb_T (nM)','fontsize',12)
ylabel('Fluorescence (arb)','fontsize',12)
set(gca,'linewidth',2,'fontsize',12)
title('Lead Quenching','fontsize',12)
%%



end

function
[II,GG]=Cumodel_highIS_Cl_DIC_Trp_ppte(CuT,pH,DIC,ClT,TrpT,SO4T,flag)

warning('off')

[KSOLUTION,KSOLID,ASOLUTION,ASOLID,SOLUTIONNAMES,SOLIDNAMES]=get_equil
ib_defn(flag);

%CuT=3.9592e-7;

%pH=[6:0.1:9]; % fixed pH
numpts=size(pH,2);
Ncp=size(ASOLID,1);
solid_summary=zeros(numpts,Ncp);

for i=1:size(SOLIDNAMES,1)
    txt=[SOLIDNAMES(i,:),'=zeros(numpts,1);']; eval(txt)
```

```matlab
end

for i=1:size(pH,2)
    %H=10.^(-1*pH(i)); Ka1=10^(-6.3); Ka2=10.^(-10.3); Kh=10.^(-1.47);
    %CT=Kh*PCO2+(Kh*PCO2*Ka1)./H+(Kh*PCO2*Ka1*Ka2)./(H.^2);
    CT=DIC;
    CTrun(i)=CT;

    % adjust for fixed pH


[Ksolution,Ksolid,Asolution,Asolid]=get_equilib_fixed_pH(KSOLUTION,KSO
LID,ASOLUTION,ASOLID,pH(i));

    Asolid_SI_check=Asolid; Ksolid_SI_check=Ksolid;

    % number of different species
    Nx=size(Asolution,2); Ncp=size(Asolid,1); Nc=size(Asolution,1);

    % initial guess
    Cu_guess=[-10.5]; CuOH2s_guess=0.1*CuT;  CuCO3s_guess=0.1*CT;
    guess=[10.^Cu_guess CT./10 CuOH2s_guess CuCO3s_guess];
iterations=1000; criteria=1e-16;
    T=[CuT CT ClT TrpT SO4T]; guess=T./10;

    % calculate species using NR

    solids=zeros(1,Ncp);

    if i==1;
[species,err,SI]=NR_method_solution(Asolution,Asolid,Ksolid,Ksolution,
T',[guess(1:Nx)]',iterations,criteria); end
    if i>1;

[species,err,SI]=NR_method_solution(Asolution,Asolid,Ksolid,Ksolution,
T',[species(2:Nx+1)],iterations,criteria);
    end

    for qq=1:Ncp

        [Y,I]=max(SI);

        if Y>1.000000001
            Iindex(qq)=I;
            Asolidtemp(qq,:)=Asolid_SI_check(I,:);
            Ksolidtemp(qq,:)=Ksolid_SI_check(I,:);
            solidguess(qq)=T(I)*0.5;
          % solidguess(qq)=min(T)*0.015;
            if i>1;
                %if max(solids)>0
```

```
                    txt=['solidguess(qq)=',SOLIDNAMES(I,:),'(i-1);'];
eval(txt);
                %end
            end
            guess=[species(2:Nx+1)' solidguess];

[species,err,SItst,solids]=NR_method(Asolution,Asolidtemp',Ksolidtemp,
Ksolution,T',guess',iterations,criteria);
              for q=1:size(solids,1);
                  txt=[SOLIDNAMES(Iindex(q),:),'(i)=solids(q);'];
eval(txt)
              end
        end

        Q=Asolid*log10(species(2:Nx+1)); SI=10.^(Q+Ksolid); Ifirst=I;

    end

    Q=Asolid*log10(species(2:Nx+1)); SI=10.^(Q+Ksolid);
    SI_summary(i,:)=SI;

    species_summary(i,:)=species;
    mass_err_summary(i,:)=(err(1));

    Asolidtemp=[]; Ksolidtemp=[];

end

for i=1:size(species_summary,2)
    txt=[SOLUTIONNAMES(i,:),'=species_summary(:,i);']; eval(txt)
end

II=[species_summary PbCl2s PbCO3s PbSO4s];
GG=strvcat(SOLUTIONNAMES,'PbCl2s','PbCO3s','PbSO4s');

end

% -------------------- NR method solids present

function
[species,err,SI,solids]=NR_method(Asolution,Asolid,Ksolid,Ksolution,T,
guess,iterations,criteria)

Nx=size(Asolution,2); Ncp=size(Asolid,2); Nc=size(Asolution,1);
X=guess;

for II=1:iterations

    Xsolution=X(1:Nx); Xsolid=[]; if Ncp>0; Xsolid=X(Nx+1:Nx+Ncp); end
```

```
        logC=(Ksolution)+Asolution*log10(Xsolution); C=10.^(logC); % calc
species

    if Ncp>0;
        Rmass=Asolution'*C+Asolid*Xsolid-T;
    end


    if Ncp==0; Rmass=Asolution'*C-T; end % calc residuals in mass
balance

    Q=Asolid'*log10(Xsolution); SI=10.^(Q+Ksolid);
    RSI=ones(size(SI))-SI;

      % calc the jacobian

      z=zeros(Nx+Ncp,Nx+Ncp);

      for j=1:Nx;
            for k=1:Nx;
                        for i=1:Nc;
z(j,k)=z(j,k)+Asolution(i,j)*Asolution(i,k)*C(i)/Xsolution(k); end
            end
    end

    if Ncp>0;
    for j=1:Nx;
            for k=Nx+1:Nx+Ncp;
                t=Asolid';
                        z(j,k)=t(k-Nx,j);
            end
    end
    end

    if Ncp>0
    for j=Nx+1:Nx+Ncp;
            for k=1:Nx
                        z(j,k)=-1*Asolid(k,j-Nx)*(SI(j-Nx)/Xsolution(k));
            end
    end
    end

    if Ncp>0
    for j=Nx+1:Nx+Ncp
        for k=Nx+1:Nx+Ncp
            z(j,k)=0;
        end
    end
    end
```

```
        R=[Rmass; RSI]; X=[Xsolution; Xsolid];

        deltaX=z\(-1*R);
        %deltaX=-1*inv(z)*(R);
          one_over_del=max([1, -1*deltaX'./(0.5*X')]);
          del=1/one_over_del;
          X=X+del*deltaX;

        %X=X+deltaX;

          tst=sum(abs(R));
          if tst<=criteria; break; end

end

logC=(Ksolution)+Asolution*log10(Xsolution); C=10.^(logC); % calc
species
RSI=ones(size(SI))-SI;

if Ncp>0; Rmass=Asolution'*C+Asolid*Xsolid-T; end % calc residuals in
mass balance
if Ncp==0; Rmass=Asolution'*C-T; end % calc residuals in mass balance

err=[Rmass];

species=[C];
solids=Xsolid;

end

% ----------- NR method just solution species

function
[species,err,SI]=NR_method_solution(Asolution,Asolid,Ksolid,Ksolution,
T,guess,iterations,criteria)

Nx=size(Asolution,2); Ncp=size(Asolid,1); Nc=size(Asolution,1);
X=guess;

for II=1:iterations

    Xsolution=X(1:Nx);

      logC=(Ksolution)+Asolution*log10(Xsolution); C=10.^(logC); % calc
species

    Rmass=Asolution'*C-T;

    Q=Asolid*log10(Xsolution); SI=10.^(Q+Ksolid);
    RSI=ones(size(SI))-SI;
```

```matlab
    % calc the jacobian

    z=zeros(Nx,Nx);

    for j=1:Nx;
        for k=1:Nx;
                for i=1:Nc;
z(j,k)=z(j,k)+Asolution(i,j)*Asolution(i,k)*C(i)/Xsolution(k); end
        end
    end

    R=[Rmass]; X=[Xsolution];

    deltaX=z\(-1*R);
    %deltaX=-1*inv(z)*(R);
     one_over_del=max([1, -1*deltaX'./(0.5*X')]);
     del=1/one_over_del;
     X=X+del*deltaX;

    %X=X+deltaX;

     tst=sum(abs(R));
     if tst<=criteria; break; end

end

logC=(Ksolution)+Asolution*log10(Xsolution); C=10.^(logC); % calc
species
RSI=ones(size(SI))-SI;

Q=Asolid*log10(Xsolution); SI=10.^(Q+Ksolid);
RSI=ones(size(SI))-SI;

Rmass=Asolution'*C-T;

err=[Rmass];

species=[C];

end



% ----- equilib definition ----------------

function
[KSOLUTION,KSOLID,ASOLUTION,ASOLID,SOLUTIONNAMES,SOLIDNAMES]=get_equil
ib_defn(flag);
```

```
logKw=-13.75;
logKh1=-8.0567;
logBh2=-17.3233;
logBh3=-27.4667;
logBh21=-6.6267;
logBh34=-23.6966;
logBh68=-43.3392;
pKa1=5.97;
pKa2=9.53;
logKPbCO32=8.8632;
logKPbCO3=5.284224;
logKPbHCO3=2.182954;
logKPb2CO3=6.832248;
logKPb3CO3=7.994746;
logKPbCl=0.89;
logKPbCl2=1.2;
logKPbCl3=1.15;
logKPbTrp=5.05656;
pKa1Trp=2.3176;
pKa2Trp=11.6731;
logKPbTrp2=8.752;
logKHSO4=1.1781;
logKPbSO4=1.4751;


KSOLUTION=[...
        0
        0
        0
        0
        0
        0
        logKw
        logKh1
        logBh2
        logBh3
        logBh21
        logBh34
        logBh68
        pKa2
        pKa2+pKa1
        logKPbCO32
        logKPbCO3
        logKPbHCO3
        logKPb2CO3
        logKPb3CO3
        logKPbCl
        logKPbCl2
        logKPbCl3
        logKPbTrp
```

```
        pKa2Trp
        pKa1Trp+pKa2Trp
        logKPbTrp2
        logKHSO4
        logKPbSO4];

    ASOLUTION=[...
        %H      M      CO3    Cl   Trp SO4
         1      0      0      0    0    0
         0      1      0      0    0    0
         0      0      1      0    0    0
         0      0      0      1    0    0
         0      0      0      0    1    0
         0      0      0      0    0    1
        -1      0      0      0    0    0
        -1      1      0      0    0    0
        -2      1      0      0    0    0
        -3      1      0      0    0    0
        -1      2      0      0    0    0
        -4      3      0      0    0    0
        -8      6      0      0    0    0
         1      0      1      0    0    0
         2      0      1      0    0    0
         0      1      2      0    0    0
         0      1      1      0    0    0
         1      1      1      0    0    0
         0      2      1      0    0    0
         0      3      1      0    0    0
         0      1      0      1    0    0
         0      1      0      2    0    0
         0      1      0      3    0    0
         0      1      0      0    1    0
         1      0      0      0    1    0
         2      0      0      0    1    0
         0      1      0      0    2    0
         1      0      0      0    0    1
         0      1      0      0    0    1];

    SOLUTIONNAMES=strvcat('H','Pb','CO3','Cl','Trp','SO4','OH','PbOH','PbO
    H2','PbOH3','Pb2OH','Pb3OH4','Pb6OH8','HCO3','H2CO3','PbCO32aq','PbCO3
    ','PbHCO3','Pb2CO3','Pb3CO3','PbCl','PbCl2','PbCl3','PbTrp','HTrp','H2
    Trp','PbTrp2','HSO4','PbSO4');

     %Try
        % -------------- solid values

        logKsp=-14.9;
        %logKPboh2s=-logKsp+2*logKw;
        logKPbCO3s=-11.1479;
        logKPbSO4s=-6.2766
```

147

```matlab
        logKPbCl2s=-4.8313;

        logKPboh2s=-10;
        logKPbCO3s=1;
        %logKtenorite=-100;
        %logKmalachite=1;

        KSOLID=[...
        logKPbCl2s
        logKPbSO4s
        logKPbCO3s];

        ASOLID=[...
        0       1    0      2    0   0
         0      1    0      0    0   1
         0      1    1      0    0   0];

    SOLIDNAMES=strvcat('PbCl2s','PbSO4s','PbCO3s');


end

% ----------- for fixed pH ----------------

function
[Ksolution,Ksolid,Asolution,Asolid]=get_equilib_fixed_pH(KSOLUTION,KSO
LID,ASOLUTION,ASOLID,pH)

    [N,M]=size(ASOLUTION);
    Ksolution=KSOLUTION-ASOLUTION(:,1)*pH;
    Asolution=[ASOLUTION(:,2:M)];
    [N,M]=size(ASOLID);
    Ksolid=KSOLID-ASOLID(:,1)*pH;
    Asolid=[ASOLID(:,2:M)];

end
```

C.2 Matlab Code for Copper

```matlab
function GG=for_Rachael_vCuT_fixedpH_10uM_Trp

clear; figure(1); clf; figure(2); clf

ClT=0.5;
PCO2=10^(-3.5);
NaHCO3=200; %mg/L from recipe
NaHCO3AW=100; %g/mol
DIC=(NaHCO3*1e-3)/NaHCO3AW;
CuTppb=[1:25:900];
```

```
CuT=(CuTppb*1e-6)/63.5;
TrpT=10e-6;
SO4T=1e-2;

pH=7.81;

logKw=-13.75;
logKh1=-7.55;
logBh21=-5.59202
logBh22=-10.7463;
logBh34=-22.33122;
pKa1=5.97;
pKa2=9.53;
logKCuCO3=5.73;
logKCuCO32=9.23;
logKCuHCO3=1.03;
logKCuCl=-0.2;
logKCuTrp=8.1829;
pKa1Trp=2.317;
pKa2Trp=9.3555;
logKCuTrp2=15.5084;
logKCuHTrp=2.47;
logKCuSO4=0.7737;
logKHSO4=1.1781;

KSOLUTION=[...
      0
      0
      0
      0
      0
      0
      logKw
      logKh1
      logBh21
      logBh22
      logBh34
      pKa2
      pKa2+pKa1
      logKCuCO3
      logKCuCO32
      logKCuHCO3
      logKCuCl
      logKCuTrp
      pKa2Trp
      pKa2Trp+pKa1Trp
      logKCuTrp2
      logKCuHTrp
      logKCuSO4
      logKHSO4];
```

149

```
ASOLUTION=[...
    %H     M     CO3   Cl   Trp   SO4
     1     0     0     0    0     0
     0     1     0     0    0     0
     0     0     1     0    0     0
     0     0     0     1    0     0
     0     0     0     0    1     0
     0     0     0     0    0     1
    -1     0     0     0    0     0
    -1     1     0     0    0     0
    -1     2     0     0    0     0
    -2     2     0     0    0     0
    -4     3     0     0    0     0
     1     0     1     0    0     0
     2     0     1     0    0     0
     0     1     1     0    0     0
     0     1     2     0    0     0
     1     1     1     0    0     0
     0     1     0     1    0     0
     0     1     0     0    1     0
     1     0     0     0    1     0
     2     0     0     0    1     0
     0     1     0     0    2     0
     1     1     0     0    1     0
     0     1     0     0    0     1
     1     0     0     0    0     1];

SOLUTIONNAMES=strvcat('H','Cu','CO3','Cl','SO4','Trp','OH','CuOH','Cu2
OH','Cu2OH2','Cu3OH4','HCO3','H2CO3','CuCO3aq','CuCO32aq','CuHCO3','Cu
Cl','CuTrp','HTrp','H2Trp','CuTrp2','CuHTrp','CuSO4','HSO4');

 Try
    % -------------- solid values

    logKsp=-18.7;
    logKcuoh2s=-46.34;
    logKCuCO3s=12.9089;
    logKmalachite=33.18+2*logKw;
    logKmalachite=32.0+2*logKw;
    logKtenorite=20.8648+2*logKw;
    if flag==1; logKmalachite=1; end
    if flag==2; logKtenorite=-100; end
    if flag==3; logKtenorite=-100; logKmalachite=1; end

    logKcuoh2s=-10;
    logKCuCO3s=1;
    logKtenorite=-100;
    logKmalachite=1;
```

```
    KSOLID=[...
    logKtenorite
    logKmalachite
    logKcuoh2s
    logKCuCO3s];

    ASOLID=[...
     -2      1     0         0    0    0
     -2      2     1         0    0    0
     -2      1     0      0    0    0
      0      1     1      0    0    0];

 SOLIDNAMES=strvcat('tenorite','malachite','CuOH2s','CuCO3s');
```

C.3 Matlab Code for Zinc

```
ClT=0.5;
PCO2=10^(-3.5);
NaHCO3=200; %mg/L from recipe
NaHCO3AW=100; %g/mol
DIC=((NaHCO3*1e-3)/NaHCO3AW);
ZnTppb=[1:25:600];
ZnT=(ZnTppb*1e-6)/65.39;
TrpT=10e-6;
SO4T=1e-2;

pH=7.82;

logKw=-13.75;
logKh1=-9.1204;
logBh2=-16.1433;
logBh3=-28.8547;
logBh4=-40.06;
logBh21=-8.7033;
pKa1=5.97;
pKa2=9.53;
logKZnCl=-0.4;
logKZnTrp=4.5434;
pKa1Trp=2.3176;
pKa2Trp=9.3555;
logKZnTrp2=8.7673;
logKZnTrp3=11.9747;
logKZnCO3=3.3;
logKZnCO32=5.3;
logKZnHCO3=0.85;
logKZn2CO3=4.635591;
logKZnSO4=0.9546;
logKHSO4=1.1781;
```

```
KSOLUTION=[...
    0
    0
    0
    0
    0
    0
    logKw
    logKh1
    logBh2
    logBh3
    logBh4
    logBh21
    pKa2
    pKa2+pKa1
    logKZnCl
    logKZnTrp
    pKa2Trp
    pKa2Trp+pKa1Trp
    logKZnTrp2
    logKZnTrp3
    logKZnCO3
    logKZnCO32
    logKZnHCO3
    logKZn2CO3
    logKZnSO4
    logKHSO4];

ASOLUTION=[...
    %H      M      CO3    Cl    Trp    SO4
    1       0      0      0     0      0
    0       1      0      0     0      0
    0       0      1      0     0      0
    0       0      0      1     0      0
    0       0      0      0     1      0
    0       0      0      0     0      1
    -1      0      0      0     0      0
    -1      1      0      0     0      0
    -2      1      0      0     0      0
    -3      1      0      0     0      0
    -4      1      0      0     0      0
    -1      2      0      0     0      0
    1       0      1      0     0      0
    2       0      1      0     0      0
    0       1      0      1     0      0
    0       1      0      0     1      0
    1       0      0      0     1      0
    2       0      0      0     1      0
    0       1      0      0     2      0
```

152

```
      0     1     0     0   3     0
      0     1     1     0   0     0
      0     1     2     0   0     0
      1     1     1     0   0     0
      0     2     1     0   0     0
      0     1     0     0   0     1
      1     0     0     0   0     1];

SOLUTIONNAMES=strvcat('H','Zn','CO3','Cl','Trp','SO4','OH','ZnOH','ZnO
H2','ZnOH3','ZnOH4','Zn2OH','HCO3','H2CO3','ZnCl','ZnTrp','HTrp','H2Tr
p','ZnTrp2','ZnTrp3','ZnCO3','ZnCO32','ZnHCO3','Zn2CO3','ZnSO4','HSO4'
);

 Try
     % ------------- solid values

     logKsp=-16.26;
     logKZnOH2s=-42.8613;
     logKZnCO3s=-12.2089;
     logKZnOs=-16.606;

     %logKZnOH2s=-10;
     %logKZnCO3s=1;
     %logKtenorite=-100;
     %logKmalachite=1;

     KSOLID=[...
     logKZnOs
     logKZnOH2s
     logKZnCO3s];

     ASOLID=[...
      0        1     0      0   0   0
      -2       1     0      0   0   0
      0        1     1      0   0   0];

 SOLIDNAMES=strvcat('ZnOs','ZnOH2s','ZnCO3s');
```

C.4 Matlab Code for Nickel

```
function GG=for_Rachael_vCuT_fixedpH_10uM_Trp2_Ni

ClT=0.5;
PCO2=10^(-3.5);
NaHCO3=200; %mg/L from recipe
NaHCO3AW=100; %g/mol
DIC=((NaHCO3*1e-3)/NaHCO3AW);
NiTppb=[1:100:800];
NiT=(NiTppb*1e-6)/58.71;
```

```
TrpT=10e-6;
SO4T=1e-2;

pH=7.82;

logKw=-13.75;
logKh1=-10.1434;
logBh2=-17.4195;
logBh3=-30.4547;
logBh44=-28.0779;
pKa1=5.97;
pKa2=9.53;
logKNiCl=-0.4402;
logKNiTrp=5.5379;
pKa1Trp=2.3176;
pKa2Trp=9.53;
logKNiTrp2=10.52;
logKNiTrp3=14.4845;
logKNiCO3=3.57;
logKNiHCO3=1.59;
logKNiSO4=0.756;
logKHSO4=1.1781;


KSOLUTION=[...
        0
        0
        0
        0
        0
        0
        logKw
        logKh1
        logBh2
        logBh3
        logBh44
        pKa2
        pKa2+pKa1
        logKNiCl
        logKNiTrp
        pKa2Trp
        pKa2Trp+pKa1Trp
        logKNiTrp2
        logKNiTrp3
        logKNiCO3
        logKNiHCO3
        logKNiSO4
        logKHSO4];

ASOLUTION=[...
```

```
    %H      M      CO3    Cl    Trp    SO4
     1      0      0      0     0      0
     0      1      0      0     0      0
     0      0      1      0     0      0
     0      0      0      1     0      0
     0      0      0      0     1      0
     0      0      0      0     0      1
    -1      0      0      0     0      0
    -1      1      0      0     0      0
    -2      1      0      0     0      0
    -3      1      0      0     0      0
    -4      4      0      0     0      0
     1      0      1      0     0      0
     2      0      1      0     0      0
     0      1      0      1     0      0
     0      1      0      0     1      0
     1      0      0      0     1      0
     2      0      0      0     1      0
     0      1      0      0     2      0
     0      1      0      0     3      0
     0      1      1      0     0      0
     1      1      1      0     0      0
     0      1      0      0     0      1
     1      0      0      0     0      1];

SOLUTIONNAMES=strvcat('H','Ni','CO3','Cl','Trp','SO4','OH','NiOH','NiO
H2','NiOH3','Ni4OH4','HCO3','H2CO3','NiCl','NiTrp','HTrp','H2Trp','NiT
rp2','NiTrp3','NiCO3','NiHCO3','NiSO4','HSO4');


% Try
    % -------------- solid values

    logKsp=-15.2;
    logKNiOH2s=-42.56;
    logKNiCO3s=-12.6089;

    %logKZnOH2s=-10;
    %logKZnCO3s=1;
    %logKtenorite=-100;
    %logKmalachite=1;

    KSOLID=[...
    logKNiOH2s
    logKNiCO3s];

    ASOLID=[...
    -2      1      0      0     0      0
     0      1      1      0     0      0];

 SOLIDNAMES=strvcat('NiOH2s','NiCO3s');
```

155

Appendix D: SIMPLISMA Script

```
% test SIMPLISMA

function II=MiamiJimbo_SIMPLISMA

clear; figure(1); close; figure(2); close; figure(3); close;
figure(4); close

data=getdata; enddata=400; startdata=180;

wavelength=data(startdata:enddata,2);
data=data(startdata:enddata,2:8); data=data';

n=2; % number of components
%data2=[]; % for second derivative.  not required.
offset=50; % value 1-15 depending on necessary correction factor
varlist=[wavelength]'; % wavelengths in real spectra

[purspec,purint,purity_spec]=simplisma(data,varlist,offset,n);

figure(1); close

conc=[0    24.390243902439 33.8164251207729 78.3410138248848
      137.931034482759 206.349206349206 290.780141843972 372.822299651568
      528.619528619529];

figure(1);
plot(wavelength,purspec(1,:),wavelength,purspec(2,:),'linewidth',2)
set(gca,'linewidth',2,'fontsize',12)
xlabel('wavelength (nm)','fontsize',12)
ylabel('pure spectra intensity (arb)','fontsize',12)
axis([340 520 0 15e-3])

figure(2); close; figure(2);
h=plot(conc,purint(:,1),'bo',conc,purint(:,2),'go','markersize',8)
set(h(1),'markerfacecolor','b'); set(h(2),'markerfacecolor','g')
set(gca,'linewidth',2,'fontsize',12)
xlabel('added Cu (ppb)','fontsize',12)
ylabel('flurophore concentration (arb)','fontsize',12)
axis([0 250 1.5e4 6e4])
end

function II=getdata

data=[...];

II=data;

end
```

Appendix E: Competitive Ligand Exchange Method by Anodic Stripping Voltammetry

Competitive ligand exchange experiments were completed on the voltammeter for copper with the natural organic matter from Luther Marsh in artificial seawater and the competitive ligand, salicylaldoxime (SA). In this technique, SA, which has a known competition strength, is allowed to equilibrate for 5 minutes with the natural ligands present in the sample and a range of dissolved copper. This procedure was completed by following the Kogut and Voelker (2001) method.

Data analysis for the result was completed following Kogut and Voelker (2001). The data points directly corresponding to the binding of the Cu-SA were fit and the binding capacity was calculated by using the equation for the line, setting the y=0 and solving for x. The height signal from each copper addition was divided by the slope of the above line to solve for the concentration of Cu-SA species. The copper total (CuT) was rearranged to solve for the total copper reacting with the natural ligand (CuT*) and was solved for using CuT*=[CuT]-[Cu-SA]. Free copper is calculated by the use of the equation k=[Cu-SA]/[Cu][SA]. The chosen k was for $Cu(SA)_2$ instead of $CuSA^+$ because the Cu-SA+ is only important at low SA concentrations 1 µM and 2.5 µM. Anything over it becomes insignificant relative to the $Cu(SA)_2$ complex (Buck and Bruland 2005) k=15.78. There are two unknown variables; one is [Cu] which we plan on solving for the other is [SA]. So to solve for SA we use mass balance for the system.

SA-total=[Cu-SA]+[SA]. SA-total is the 25µM SA initially added, which translates to 25000nM. The equation can be rearranged to [SA]=SA-total- 2[Cu-SA]. Now with our SA values for each point we can solve for Cu2+; $[Cu2+] =[Cu-SA]/k[SA]^2$. The results are plotted Figure 5.

Figure B.1 (a) shows the increasing copper additions vs. the height of the peak for the Cu-SA compound measured by the voltammeter. The first part of the graph has a small slope because the natural organic matter has a stronger binding strength than the copper-SA complex and is out competing it. Once the binding capacity for the natural organic matter is full, the SA can start to fully compete for the copper resulting in a much steeper slope. The linearization of the steeper copper-SA complex allows for the determination of binding capacity for the copper

binding ligands (Buck and Bruland, 2005). From our experimental results, it can be seen that binding capacity from trial one and two is 30.2 nM and 40.7 nM, respectively.

Figure B.1 (b) displays the bound copper vs. the free copper. In this process the concentration of the CuSA is subtracted because it is not a natural aspect of the system. By removing this concentration the results are now directly correlated to the natural sample and provide a graphical estimation between the free copper and the copper bound to the natural organic matter (Buck and Bruland, 2005).
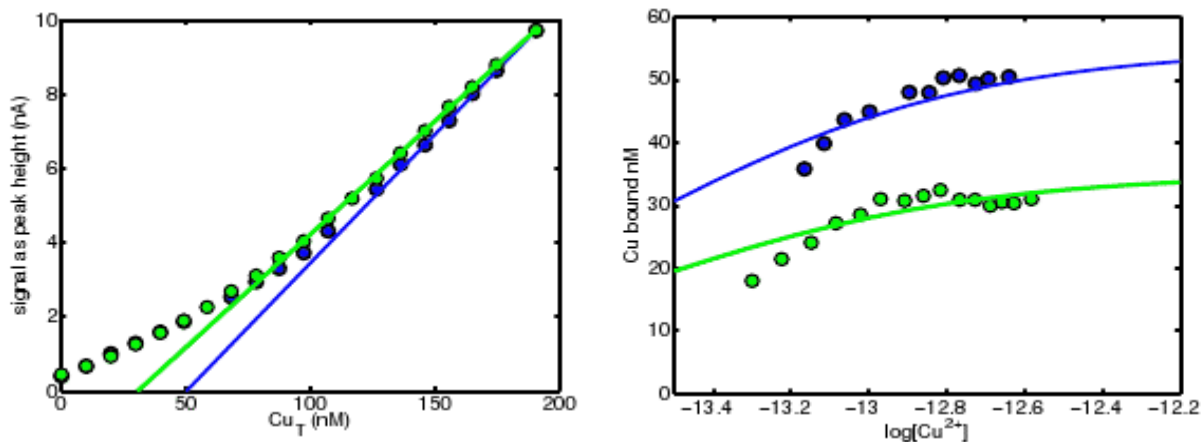
Figure B.1: Competitive ligand exchange results for copper and natural organic matter isolate, Luther Marsh. Figure B.1(a) shows the increase of the Cu-SA peak height with increasing total copper concentration. Figure B.1(b) graphically displays free copper vs. copper bound to the Luther Marsh organic matter (Natural ligand logK value of 13.6).

References

Buck, K.N. and Bruland K.W. Copper speciation in San Francisco bay: A novel approach using multiple analytical windows. *Mar. Chem.* **96**, 185-198. (2005).

Kogut M.B. and Voelker B.M. Strong copper binding behavior of terrestrial humic substances in seawater. *Environ. Sci. Technol.,* **35**, 1149-1156. (2001).

Appendix F: Determination of Binding Capacity with Zinc

Electrochemically labile zinc was measured by adapting the method of Sánchez-Marín et al. (2011) to include the zinc peak. Square wave anodic stripping voltammetry (SWASV) was used with a deposition potential of -1.5 V, a deposition time of 30 seconds, equilibration time of 5 seconds, voltage scanning (-1.5 to -0.8V), amplitude of 25 mV, frequency of 25 Hz, and a scan increment of 2mV. The resultant current measurements at the peak potential for zinc were recorded after additions from 0 to 700 ppb. NOM samples were dissolved in OECD seawater and pH was kept constant +/-0.02 throughout the titration.

The current measurements at the peak potential versus the metal added should result in a low slope for the initial data followed by steeper slope linear response at higher total metal as seen in Chapter 4 and Chapter 5. Figures E.1 and E.2 displays the voltammetric results of zinc addition versus peak height for Inshore Brazil and Nordic Reservoir at 2 mg C/L. These graphs do not follow the expected shape and are linear. This resulted in the inability to determine the binding capacity for zinc with the Inshore Brazil and Nordic Reservoir NOM.
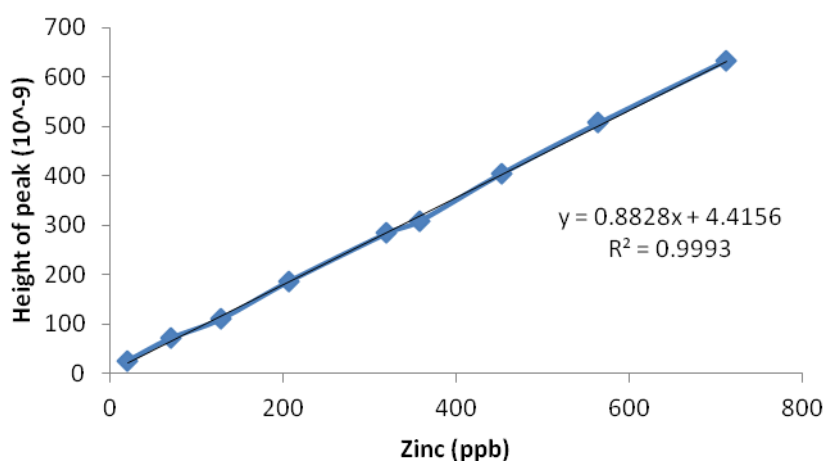
Figure E.1: Zinc speciation for 2 mg C/L Inshore Brazil measured by Anodic stripping voltammetry (ASV). Voltammetric results zinc addition (ppb) vs. height of lead peak.
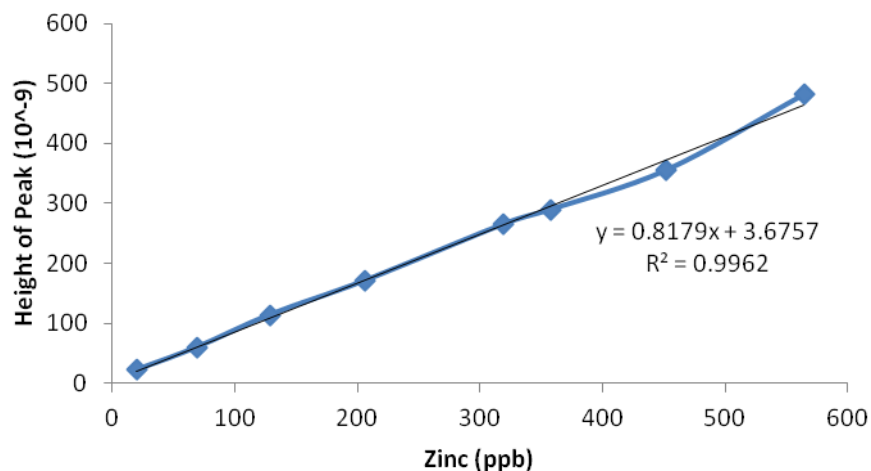
Figure E.2: Zinc speciation for 2 mg C/L Nordic Reservoir measured by Anodic stripping voltammetry (ASV). Voltammetric results zinc addition (ppb) vs. height of lead peak.

Voltammetric techniques detect strong ligand binding. The ligand (NOM) prevents the metal from accumulating at the mercury drop and being measured. The zinc binding is linear which indicates that the zinc binding to the NOM is not strong enough for this technique to prove useful for determination of binding capacity.

References

OECD Environment, Health and Safety Publications Series on Testing and Assessment. No. 29 "Guidance Document on Transformation/Dissolution of Metals and Metal Compounds in Aqueous Media" ENV/JM/MONO(2001)9. April (2001).

Sanchez-Marin, P., Bellas, J., Mubiana, V.K., Lorenzo, J.I., Blust, R., Beiras, R. Pb Uptake by the marine mussel Mytilus sp. Interactions with dissolved organic matter. *Aqua. Tox*. **102**. 48-57. (2011).

Appendix G:

Are salinity and DOC two variables that determine toxicity of Pb and Zn to blue mussel and sea urchin embryos?

Sunita R. Nadella [1, 2 *], Margaret Tellis[1,2] , Rachael Diamond [3], Scott Smith [3], Chris M. Wood[1,2].

1. Dept. of Biology
    McMaster University
    Hamilton, ON. L8S4K1
    Canada

2. Bamfield Marine Sciences Centre
    100 Pachena Road
    Bamfield, BC V0R 1B0
    Canada

3. Dept. of Chemistry
    Wilfrid Laurier University
    University Avenue West
    Waterloo, ON. N2L3C5
    Canada

*Corresponding Author:
                Sunita R. Nadella
                Dept. of Biology
                1280 Main Street West, McMaster University
                Hamilton, ON. L8S4K1
                Canada
                Phone: 905 525 9140 ext.26389
                FAX: 905 522 6066
                Email: nadellsr@mcmaster.ca

Introduction:

Anthropogenic sources historically related to industrial activity, waste disposal and vehicular emissions contribute toxic levels of trace metals like Cu, Pb and Zn into the marine environment. Assessing aquatic pollution in terms of chemical analysis of the contaminants present is not considered adequate as it does not provide information about the toxic effects of the contaminant on organisms. A more useful approach would be to derive comprehensive data on environmentally realistic pollutant levels that integrate biological factors such as survival and bioaccumulation.

The freshwater biotic ligand model (BLM) has successfully incorporated the above approach of predicting toxicity associated with metal accumulation on or in the organism, such that lethality occurs when a critical tissue concentration of the metal is reached (LA50; Niyogi and Wood, 2004). The BLM framework assumes that a particular amount of metal bound to the "toxic sites" is critical to toxicity (the lethal accumulation-50% or LA50 parameter). In practice, the LA50 value is often an assumed value derived from iterative modeling but Niyogi and Wood (2004) have specified the importance of measured values. Critical body residues (CBR), based on whole body concentrations, have been sometimes suggested as a more toxicologically relevant means of predicting toxicity as compared to water concentrations for a variety of organic contaminants and metals (McCarty and Mackay,1993; Adams et al. 2011; McCarty et al., 2011; Sappington et al. 2011;). Recently Rosen et al. (2008) explored the use of the CBR approach for Cu in embryo-larval stages of *Mytilus galloprovincialis* and *Stronglylocentrotus purpuratus*

and found whole body Cu residues were a better predictor of toxicity than exposure water Cu concentrations.

Larval toxicity bioassays have therefore become important for regulatory and monitoring programs, largely because they are assumed to be good indicators of ecological damage to aquatic communities. Early life stages of aquatic invertebrates are considered more sensitive than adults as they respond to subtle chemical and physical changes in the environment (His et al. 1999). Investigation on early life stages is also particularly important since mortality during early life stages is the decisive factor regulating subsequent adult population size of benthic marine invertebrates (Gosselin & Qian 1997).

Sea urchin embryo-larval development has been studied since the late 19th century (Hertwig & Hertwig, 1887) and this life stage has been used to monitor pollutants in marine environments since the 1950s (Tabata, 1956; Okubo and Okubo, 1962). In particular, the early life stages of several different species of sea urchins have been shown to be sensitive to metals (Kobayashi, 1973; Phillips et al., 2003). Similarly, previous studies report that early life stages of freshwater mussels are more sensitive to contaminants than are adults (Yeager et al. 1994; Naimo 1995; Jacobson et al. 1997). This finding is also supported by field observations, as alarmingly few young mussels have been found in contaminated environments with diverse adult populations (Jacobson et al. 1997; Weinstein, 2001).

There is good reason to believe that metals like Cu, Zn and Pb will be very sensitive to the early life stages of these marine organisms because of their common

occurrence in municipal and industrial effluents (Ringwood,1992; Eisler, 1993;)as well as their known toxicity at elevated concentrations to marine organisms. Very recently, we examined Cu toxicity to various early life stages of the blue mussel *Mytilus trossolus* and we showed that the embryo-larval life stage is 10-100 fold more sensitive than either sperm or eggs alone (Fitzpatrick et al. 2008). A parallel study (Nadella et al. 2009), investigated the individual relative toxicities of four metals to mussel embryo-larval stages, demonstrating the following rank order of toxicity Cu>Zn>Ni >Cd. The toxicity of Cu (the most toxic metal) was further evaluated in relation to modifying factors like DOM from different NOM sources and salinity. While there was no additive effect of salinity changes on Cu toxicity, we clearly showed that different DOM's had varying protective effects and these were correlated with fluorescent properties of NOM sources.

Clearly these results disagree with modeling approaches like the BLM that generally assume that all DOMs have equivalent protective abilities. The results of several recent studies including ours now argue against this. Toxicity of both copper (De Schamphelaere et al. 2004) and Ag (Glover et al. 2005) toward the highly sensitive freshwater cladoceran *Daphnia magna*, for example, is highly dependent on both the concentration and the origin of the DOM that is present. Richards et al. (2001) showed that Luther Marsh NOM (LMN) was the most effective of three NOMs for protecting against mixed-metal toxicity to rainbow trout, similar to the effects seen with *D. magna* (Glover et al.2005).

The influence of NOM source appears to depend on differing species-dependent binding affinities of the metal for the biotic ligand. Furthermore, metals appear to bind to

distinct moieties within the NOM; consequently, NOM may have different protective abilities for the toxicity of different metals. Silver, for example, likely binds to nitrogen-containing groups (Sikora et al. 1988) and, possibly, to organic thiols (Kramer et al. 2002), whereas a metal, such as copper, tends to bind to carbon-containing moieties, such as phenolic groups (Lu and Allen 2002). Clearly, the influence of NOM source on metal toxicity is likely to depend on both the metal and the organism under investigation as well as on the nature of the NOMs themselves. The qualities of NOM responsible for this differential protection are yet to be established, but indications suggest that optical properties may correlate with ameliorative ability (De Schamphelaere et al. 2004), at least for copper.

The purpose of this study was to measure CBR and evaluate the effect of DOC on the toxicity of Zn which we found to be most toxic after Cu in the previous study (Nadella et al. 2009). We extended the study to include Pb as preliminary tests indicated the metal could be equally toxic like Zn. While the toxicity of Zn and to a lesser extent Pb has been explored in marine organisms (Conroy et al., 1996; Phillips et al., 1998; Novelli et al., 2003; Radenac et al., 2001) few studies have examined the influence of physico-chemical factors such as DOC or salinity on the ecotoxicity of these metals to marine organisms. Current chronic ambient water quality criteria (AWQC) for Zn and Pb in seawater are 81 µg L^{-1} (U.S. EPA 2006) and 8.1 µg L^{-1} (EPA 440/5-84-027) respectively. These values have been derived from data available in the 1980's and have not been adjusted for salinity and DOC. There is a clear need to revisit these criteria with modern approaches incorporating the influence of DOC and salinity, the two factors likely to be the most important variables affecting the toxicity of these metals. As AWQC

are not usually based on single organisms, we included two species of blue mussels-
Mytilus trossolus, Mytilus galloprovincialis and the sea urchin *Strongylocentrotus
purpuratus* to account for variations in sensitivity.

Methods:

Adult *Mytilus trossolus* were collected from natural intertidal populations in the Broken
Island Group, near Bamfield, B.C. *Mytilus galloprovincialis* adults were obtained
courtesy of Northwest Aquaculture Farm located on the Effingham Inlet in Barkley
Sound on the west coast of Vancouver Island. *Strongylocentrotus purpuratus* were
supplied by Westwind Sealab Supplies, Victoria B.C. In the laboratory, animals were
cleaned and transferred to aerated flowing seawater baths maintained at 11-13°C and
allowed to acclimate for 24 h. Representative seawater chemistry is given in Table 1.

Mytilus 48 h embryo test:

Embryo development was assessed using well-established protocols (ASTM 2004-E724).
Briefly, adult *Mytilus* were transferred to a 10 L filtered (0.20μm) seawater bath (15-20
adults/bath) maintained at 22-25°C. The thermal shock induced spawning, and
individuals releasing gametes were immediately moved to separate 250 ml beakers
containing 200 ml of filtered seawater, for isolation and collection of gametes. Egg
quality and sperm motility were assessed using a microscope at 200x magnification.
Subsequently, eggs from several individual females were pooled and homogenized by
gentle stirring. An aliquot of sperm solution pooled from several male individuals was

added to the eggs to initiate fertilization. A subsample of this mixture was periodically

observed until 80% or more of the eggs were fertilized. The test was initiated by adding

100 µl of fertilized embryos (approximately 600-1000 individuals) to each test vial

containing 10 ml of test solution. Test vials were incubated in a biological incubator

maintained at a constant temperature of 20ºC ±1 and a photoperiod of 16-h light: 8-h

dark. After 48 h, control test vials were examined to ensure more than 80% embryos

developed into normal D-shaped prodissoconch larvae. Tests in which control

development was less than 80% normal were discarded. The test was then terminated via

addition of 1 ml buffered formalin to each test vial to arrest development. Contents of

each test vial were observed microscopically on a Sedgewick-Rafter slide to determine

the percentage of embryos exhibiting normal development. At least 100 embryos in each

replicate were assessed.

Seaurchin 72 h embryo test:

Sea urchins were stimulated to spawn by injecting 1M KCl into the gonads, sperm

and eggs were collected separately (ASTM 2004-E1563) . After fertilization, 100 µl of

fertilized embryos were added to 10 ml of test solution and the gametes were incubated

in a biological incubator maintained at a constant temperature of 15ºC ±1 and a

photoperiod of 16-h light: 8-h dark. The test was terminated at 72 h by addition of 1%

formalin when 80% embryos were normal in control vials. Contents of each test vial were

observed microscopically to determine the percentage of embryos exhibiting normal

development. At least 100 embryos in each replicate were assessed.

Whole body residue determination:

Exposures for this test were modified slightly from the above procedure according to details from Rosen et al (2008). In order to obtain sufficient biomass and determine weight and tissue burden, test were conducted using larger water volumes (1L) with embryo concentrations of ~60 embryos ml^{-1}. After the appropriate exposure period, each beaker was gently homogenized with a Pasteur pipette and a 5 ml aliquot was removed and preserved with 500 µl of formaldehyde for EC50 determination.

The remainder of the sample was filtered through a pre-weighed 8µm polycarbonate filter (Whatman Nuclepore Track-Etch Membrane PC MB 47 MM 8.0 um). The filter was dried at ~ 25ºC until a constant weight was achieved and the mass was recorded. The filter was then digested with 100 µL of trace metal grade HNO_3 overnight. The next day 1 mL of de-ionized water was added and the sample stored for tissue Pb measurements.

Analytical Chemistry:

As per US EPA (2001) recommendations water chemistry parameters were measured in treatments critical to the toxicity tests.

Dissolved Pb and Zn concentrations were measured after passing samples through a 0.45um filter, using a method modified from Toyota et al. (1982). Briefly, the representative metal was precipitated from 1 ml of sample by adding 1µl of lanthanum oxide (10 mg La ml^{-1}) and 7.5 µl of 1M Na_2CO_3, which brought the pH of the sample to approximately 9.8. The solution was gently stirred in a hot water bath maintained at 80ºC for 30 min to allow flocculation of precipitate (largely lanthanum hydroxide). The solution was centrifuged at 5000 rpm for 15 min and the supernatant discarded. The

remaining precipitate was dissolved in 1 ml of 1N HNO_3 and Pb concentration was measured via graphite furnace atomic absorption spectroscopy (220, Varian, Palo Alto, CA. U.S.A.). Zn levels were measured via flame atomic absorption spectroscopy (220FS; Varian, Palo Alto, CA. U.S.A.). Fisher Scientific calibration standards were used after every run. Recovery was always ± 10% as determined from similarly processed Analytical Reference material TM15 (Environment Canada, Natural Water Research Institute). Measured values are reported in Tables 2 & 3.

Na^+, K^+, Ca^{2+}, and Mg^{2+} concentrations in seawater samples were determined by atomic absorption spectroscopy (Varian SpectrAA-1275FS) and Cl^- by coulometric titration on a chloridometer (CMT 10 Chloride Titrator; Radiometer, Copenhagen, Denmark; Cl^-). Reference standards were used for the measurement of all ions studied [Fisher Scientific and Radiometer (Copenhagen, Denmark)].Measured values are reported in Table1.

DOC in the samples was analysed after passing the sample through a 0.45um filter and measuring total organic carbon (TOC) using a Shimadzu TOC analyzer (5050A, Mandel Scientific). Organic Carbon Standards were prepared according to Shimadzu specifications.

Statistical Analysis:

An Environmental Toxicity Data Analysis Software Tox Calc[TM] package(Tidepool Scientific Software) was used to estimate EC50 and EC20 with 95% confidence intervals (CI),[employing the responses and measured toxicant concentration data from all concentrations].

Results:

Water Chemistry Parameters: key salinity variables (Na, Cl, Mg, Ca, pH) were measured for each test, details are listed in summary table 1.

Accurate concentrations of Pb, Zn and DOC were measured in all tests. EC50 values were calculated using measured metal concentrations.

Salinity series:

48h embryo-larval development tests over a range of salinities (15-32 ppt) were performed for *Mytilus galloprovincialis* and *Mytilus trossolus and Strongylocentrotus purpuratus* (Fig.1). Exposure to different salinities influenced embryo development. *S. purpuratus* was the most sensitive to salinity changes (Fig. 1C), with normal embryo development declining significantly (< 80% normal) at salinity levels lower than 30 ppt. Embryo development in *M. galloprovincialis* (Fig. 1B) and *M. trossolus* (Fig. 1A) was less sensitive with a salinity threshold of 25 ppt and 20 ppt.

Pb series:

Toxic effects:

In 48h embryo-larval toxicity tests over a range (nominally 3.2-1000 µg L^{-1}) of Pb concentrations for *Mytilus trossolus*, and *Mytilus galloprovincialis*, we determined an EC50 of 63 (36-94) µg L^{-1} for *M. gallprovicialis*, and 45 (22-72) µg L^{-1} for *M. trossolus*. EC20 values representing possible chronic thresholds were 19 (7-33) µg L^{-1} and 16 (5-30) µg L^{-1} for the two species respectively (Table 2).

72h embryo-larval toxicity tests over a nominal range (3.2-1000 µg L^{-1}) of Pb

concentrations in 100% seawater were completed with the sea urchin *S. purpuratus.* We

determined an EC50 of 74 (50-101) µg L^{-1} and EC 20 of 31 (16-46) µg L^{-1}, slightly, but

not significantly higher than for the two mussel species (Table 2).

DOC effects:

The addition of DOC (Marine Inshore and Nordic Reservoir) to test waters decreased the

toxicity of Pb moderately. However this protective effect did not show a dose-response

relationship with increasing DOC concentrations. Both types of DOC tested showed

similar responses with dissolved EC50 values for Pb ranging between 134 (98-169)-157

(141-172) µg L^{-1} with 2.1-10.5 mg L^{-1} added DOC, moderately increased from a control

EC 50 value of 63 µg L^{-1} for *M. galloprovincialis*. Similarly DOC showed marginal

protection from Pb toxicity to *M. trossolus* embryos with EC50 values ranging from 97

(90-105) to 117 (77-157) µg L^{-1} compared to control values of 45 µg L^{-1} (Table 2).

72h embryo-larval toxicity tests over a range of Pb concentrations in exposure water

spiked with a series of DOC concentrations (2-12 mg L^{-1}) were completed with the sea

urchin *S. purpuratus.*, to assess the protective effects, if any, of DOC against Pb toxicity.

However, Inshore DOC actually exacerbated Pb toxicity to the embryos, as indicated by a

decrease in the Pb EC50 from 74 (50-101) µg L^{-1} to between 46 and 57 µg L^{-1} when Pb

treatments were spiked with 2-12 mg/L DOC. Nordic Reservoir DOC proved toxic over

the whole concentration range (Table 2).

Salinity-DOC interactions:

The effect of salinity on Pb toxicity was investigated for *M. trossolus*, the more low-salinity tolerant of the two mussel species. 48h embryo-larval toxicity tests were performed over a range (nominally 3.2-1000 µg L^{-1}) of Pb concentrations in 100% SW and at 21 ppt. Salinity had no effect on Pb toxicity, with EC50 values of 67 (37-100) µg L^{-1} in 100% SW (33 ppt; Fig.2A) and 69 (34-19) µg L^{-1} at 21 ppt (Fig.2B).

Considering the moderate protective effect of DOC against Pb toxicity, this was investigated at a lower salinity for *M. trossolus*. Like in full strength seawater we observed a small protective effect at 21 ppt, for both Inshore DOC and Nordic Reservoir DOC. EC50 increased from 69 (34-19) µg L^{-1} to only 156 (97-222) µg L^{-1} in the presence of 6 mg C L^{-1} of Inshore DOC (Fig.2D) and 184 (111-277) with 6 mg C L^{-1} of Nordic Reservoir DOC (Fig.2C).

Tissue Burden:

Critical Body Residues (CBR) of Pb, based on whole body concentrations at 48 h of Pb exposure (Fig.3A) were determined for *M. galloprovincialis*, employing methods described in Rosen et al. (2008). A good correlation was observed between tissue burden and % mortality (r^2 = 0.88) for *M. galloprovincialis* embryos. An LA50 for Pb of 575 (251-1000) µg/g was determined from this relationship (Fig.3B).

In embryos of *S. purpuratus* whole body Pb accumulation increased in a dose-dependent manner after a 72h exposure to a range of Pb concentrations (Fig.4A), a good correlation was observed between tissue burden and % mortality (R^2 = 0.88). An LA50 of 316 (141-

741) µg g^{-1} was determined from this relationship (Fig.4B), which was not significantly different from the LA50 for Pb in *M. galloprovincialis* embryos.

Larval tissue weight served as an additional toxicity endpoint for both mussels and seaurchins. Larval weight reduced significantly for *M. galloprovincialis* at a measured Pb concentration of 74 µg L^{-1} (nominal Pb = 100 µg L^{-1}; Fig. 5A). For *S. purpuratus* larval weight was significantly lower at a measured Pb concentration of 82 µg L^{-1} (nominal Pb = 100 µg L^{-1}; Fig.5B) close to the EC50 value for normal development.

Zn Series:

Toxic effects:

In 48h embryo-larval toxicity tests over a nominal range (3.2-1000 µg L^{-1}) of Zn concentrations in 100% seawater for *Mytilus trossolus*, and *Mytilus galloprovincialis* we determined an EC50 of 172 (126-227) µg L^{-1} for *M. galloprovincialis*, and 135 (103-170) µg L^{-1} for *M. trossolus*. EC20 values representing possible chronic threshold were 101 (59-136) µg L^{-1} and 69 (44-92) µg L^{-1} for the two species respectively. Thus Zn was somewhat less toxic than Pb (Table 3).

In 72h embryo-larval toxicity tests over a nominal range (3.2-1000 µg L^{-1}) of Zn concentrations in 100% seawater with *S. purpuratus* it was observed that sea urchin embryos proved to have about the same sensitivity as mussel larvae, with EC50 values of 151 (129-177) µg L^{-1} (Table 3).

DOC effects:

48h embryo-larval toxicity tests over a range of Zn concentrations in exposure water spiked with a series of DOC concentrations (2-12 mg L^{-1}) were completed for *Mytilus trossolus*, and *Mytilus galloprovincialis*, to assess the protective effects, if any, of DOC against Zn toxicity. Surprisingly, the addition of DOC (Marine Inshore and Nordic Reservoir) to test waters had no significant effect on Zn toxicity. Both types of DOC tested showed similar responses with dissolved EC50 values for Zn ranging between 164 (118-219) - 239 (177-317) µg L^{-1} with 2.1-10.5 mg L^{-1} added DOC for *M. galloprovicialis*. For *M. trossolus* embryos, EC50 values ranging from 155 (119-192) to 184 (137-236) µg L^{-1} were measured (Table 3).

72h embryo-larval toxicity tests over a range of Zn concentrations in exposure water spiked with a series of DOC concentrations (2-12 mg L^{-1}) with the sea urchin *S. purpuratus.*, to assess the protective effects, if any, of DOC against Zn toxicity, revealed that Inshore DOC aggravated Zn toxicity to the embryos, as indicated by a decrease in the Zn EC50 to 101 (99-103) µg L^{-1}when Zn treatments were spiked with 2 mg/L DOC. Adding a higher concentration (12 mg L^{-1}) of the same DOC proved to further exacerbate toxicity to the embryos 77 µg L^{-1} . Nordic reservoir DOC was toxic to seaurchin embryos even in the absence of added Zn (Table 3).

Tissue Burden:

Whole body accumulation of Zn in embryos of *M. galloprovincialis* after a 48h exposure to a range of Zn concentrations increased significantly from controls initially at the

lowest Zn exposure concentration and then substantially at the two highest exposures

(Fig. 3C). Critical Body Residues of Zn (Rosen et al., 2008) in these embryos provided a

good correlation between tissue burden and % mortality ($R^2 = 0.95$). An LA50 of 759

(617-776) µg/g was determined from this relationship (Fig. 3D). Thus despite the

differences in toxicity, LA50 values were similar for Pb and Zn.

In embryos of *S. purpuratus,* after a 72 h exposure to a range of Zn concentrations, whole

body accumulation showed significant dose-dependent increases (Fig. 4C). We measured

an LA50 of 398 (347-575) µg/g ($R^2 = 0.82$) (Fig.4D). The CBR for Zn was thus

comparable to that for Pb in this species and less than that in mussel embryos.

Larval weight as in the case for Pb was equally sensitive to Zn exposures as a toxicity

endpoint both for mussels and seaurchins. A significant drop in weight comparable to

EC50 values for normal development in these embryos was observed at measured Zn

concentrations of 151 µg L^{-1} for *M. galloprovincialis* (nominal Zn =100 µg L^{-1}; Fig. 5C)

and 174 µg L^{-1} for *S. purpuratus* (nominal Zn =100 µg L^{-1}; Fig. 5D)

	33ppt Seawater (SW)	21ppt SW	1000 μg Pb L^{-1} 33ppt SW	12 mg C L^{-1} Marine Inshore DOC 100% SW
pH	7.5	7.4	7.7	7.6
Na (mM)	443 ± 0.47	277 ± 0.75	430± 1.5	486± 0.86
K (mM)	9.3 ± 2	5.4 ± 1	9.2± 1.4	9.3 ± 1
Ca (mM)	7.8 ± 0.9	4.8 ± 0.4	8.6 ± 0.6	8.8 ± 0.7
Mg (mM)	67 ± 5	43 ± 1.6	63 ± 5	69± 7
Cl (mM)	535 ± 5.29	323 ± 1.3	304 ± 3.1	543 ± 0.88

Table 1. Measured water chemistry parameters for representative test solutions.(means ± SEM).

Table 2. 48 h EC 50; EC20; EC10 and NOEC values for abnormal development in embryos of *M. galloprovincialis* , *M. trossolus* and *P. lividus* for Pb in the presence of a potential modifying factor (DOC).

Mytilus galloprovincialis	EC50 (µg/L)	EC20 (µg/L)	EC10 (µg/L)	NOEC (µg/L)
Pb	63 (36-94)	19 (7-33)	10 (3-20)	3.2
Inshore DOC (2.5 mg/L)	134 (98-169)	68 (39-94)	48 (24-70)	4.4
Inshore DOC (10.5 mg/L)	141 (99-182)	82 (43-113)	62 (27-91)	2.2
Nordic Reservoir DOC (2.1 mg/L)	153 (141-165)	85 (75-95)	63 (54-72)	12.2
Nordic Reservoir DOC (8.8 mg/L)	157 (141-172)	85 (71-99)	62 (49-75)	30
Mytilus trossolus				
Pb	45 (22-72)	16 (5-30)	9 (2-19)	3.4
Inshore DOC (1.4 mg/L)	97 (90-105)	65 (59-72)	53 (47-59)	4.3
Inshore DOC (10.1 mg/L)	109 (100-118)	80 (71-88)	68 (60-76)	11.8
Nordic Reservoir DOC (3.1 mg/L)	117 (77-157)	67 (31-96)	50 (19-76)	1.7
Nordic Reservoir DOC (11.2 mg/L)	108 (83-133)	57 (37-75)	40 (24-57)	0.7
Mytilus trossolus				
Pb (33ppt SW)	67 (37-100)	27 (10-46)	17 (5-32)	2.7
Pb (21 ppt)	70 (34-109)	30 (8-53)	19 (3-38)	
21 ppt SW+ Nordic Res DOC (7.3 mg/L)	174 (111-248)	48 (19-81)	25 (7-47)	9.7
21 ppt SW+ Inshore DOC (5.5 mg/L)	156 (97-222)	52 (20-86)	30 (9-55)	3
Paracentrotus lividus				
Pb	74 (50-101)	31 (16-46)	19 (8-31)	2.7
Inshore DOC (4.2 mg/L)	46(10-92)	17 (0.8-40)	10 (0.2-27)	2
Inshore DOC (10.3 mg/L)	57 (29-89)	27 (7-45)	18 (3-34)	1.5
Nordic Reservoir DOC (2.7&10.3 mg/L)	No survival			

Table 3. 48 h EC 50; EC20; EC10 and NOEC values for abnormal development in embryos of *M. galloprovincialis*, *M. trossolus* and *S. purpuratus* for Zn in the presence of a potential modifying factor (DOC).

Mytilus galloprovincialis	EC50 (µg/L)	EC20 (µg/L)	EC10 (µg/L)	NOEC (µg/L)
Zn	172 (126-227)	101 (59-136)	76 (38-108)	46
Inshore DOC (3 mg/L)	203 (138-290)	132 (59-180)	105 (36-150)	<98
Inshore DOC (9.6 mg/L)	239 (177-317)	167 (100-216)	138 (72-185)	111
Nordic Reservoir DOC (2 mg/L)	165 (80-279)	79 (19-137)	54 (8-102)	<51
Nordic Reservoir DOC (8.4 mg/L)	164 (118-219)	98 (57-133)	75 (37-107)	<56
Mytilus trossolus				
Zn	135 (103-170)	69 (44-92)	48 (28-68)	46
Inshore DOC (2.1 mg/L)	168 (113-232)	99 (48-140)	76 (30-112)	89
Inshore DOC (10.4 mg/L)	184 (137-236)	109 (65-144)	82 (42-115)	92
Nordic Reservoir DOC (3.1 mg/L)	184 (169-198)	102 (89-113)	75 (64-85)	58
Nordic Reservoir DOC (11.3 mg/L)	155 (119-192)	85 (56-112)	63 (37-87)	<49
Paracentrotus lividus				
Zn	151 (129-177)	125 (95-144)	114 (80-132)	109
Inshore DOC (2 mg/L)	101 (99-103)	88 (85-91)	82 (78-85)	<82
Inshore DOC (12 mg/L)	77	41	29	78
Nordic Reservoir DOC	**No survival**			

Table 4: Median effect concentration (EC50) values for embryo toxicity test compared to literature values. Exposure Pb concentrations are nominal.

Species	Pb µg L^{-1}	Exposure duration	Medium	pH	Temperature	Embryo toxicity test EC50 µg L^{-1}	Reference
Strongylocentrotus purpuratus	3.2-1000 Pb(NO$_3$)$_2$	72h	33ppt Filtered Seawater	7.6	15°C	74 (51-101) (measured)	Present study
Paracentrotus lividus	Pb(NO$_3$)$_2$	72h	35ppt Artificial Seawater	8	18°C	68 (57-80) (nominal)	Novelli et al. 2003, Env. Toxicol. Chem. 22,1295-1301.
Paracentrotus lividus	10-250 Pb(NO$_3$)$_2$	48h	34.3ppt Artificial Seawater	8.3	22°C	40* (nominal)	Radenac et al. 2001, Mar. Env. Res. 51, 151-166.
Paracentrotus lividus	10-1200 Pb(OCOCH$_3$)$_2$	48h	33ppt Filtered Seawater		21°C	482 (101) (nominal)	His et al. 1999, Water Res. 33,1706-1718.
Paracentrotus lividus	250-4000 Pb(NO$_3$)$_2$	48h	Artificial Seawater		20°C	509 (C.V.3.2) (measured)	Fernandez & Beiras, 2001, Ecotox. 10, 263-271.

*this value was calculated by Novelii et al 2003 using data from Radenac et al. 2001(EC50 = 250 µg L^{-1}). Endpoint measured was % larva reaching pluteus stage at 48h.

Figure Legends:

Figure 1. The influence of salinity on percent normal development in embryos of A.
M. trossolus, B. *M. galloprovincialis* and C. *S. purpuratus* in the absence of
added metals. Values are means ± SEM of 5 replicates.

Figure 2. The influence of salinity and two sources of DOC on toxic responses (%
abnormal development) of *M. trossolus* embryos exposed to various
concentrations of Pb during 48 h development tests. Values are means ±
SEM of 5 replicates.

Figure 3. A. Whole body accumulation of Pb in *M. galloprovincialis*. Values are
means ± SEM of 5 replicates.
B.LA50 concentrations for *M. galloprovincialis* calculated from tissue
accumulation relative to exposure Pb concentration.
C. Whole body accumulation of Zn in *M. galloprovincialis*. Values are
means ± SEM of 5 replicates.
D. LA50 concentrations for *M. galloprovincialis* calculated from tissue
accumulation relative to exposure Zn concentration.

Figure 4. A. Whole body accumulation of Pb in *S. purpuratus* Values are means ±
SEM of 5 replicates.
B. LA50 concentrations for *S. purpuratus* calculated from tissue
accumulation relative to exposure Pb concentration.
C. Whole body accumulation of Zn in *S. purpuratus* Values are means ±
SEM of 5 replicates.
D. LA50 concentrations for *S. purpuratus* calculated from tissue
accumulation relative to exposure Zn concentration.

Figure 5. Mean dry weight per embryo (Values are means ± SEM of 5 replicates)
relative to Pb exposures in A. *M. galloprovincialis* B. *S. purpuratus*
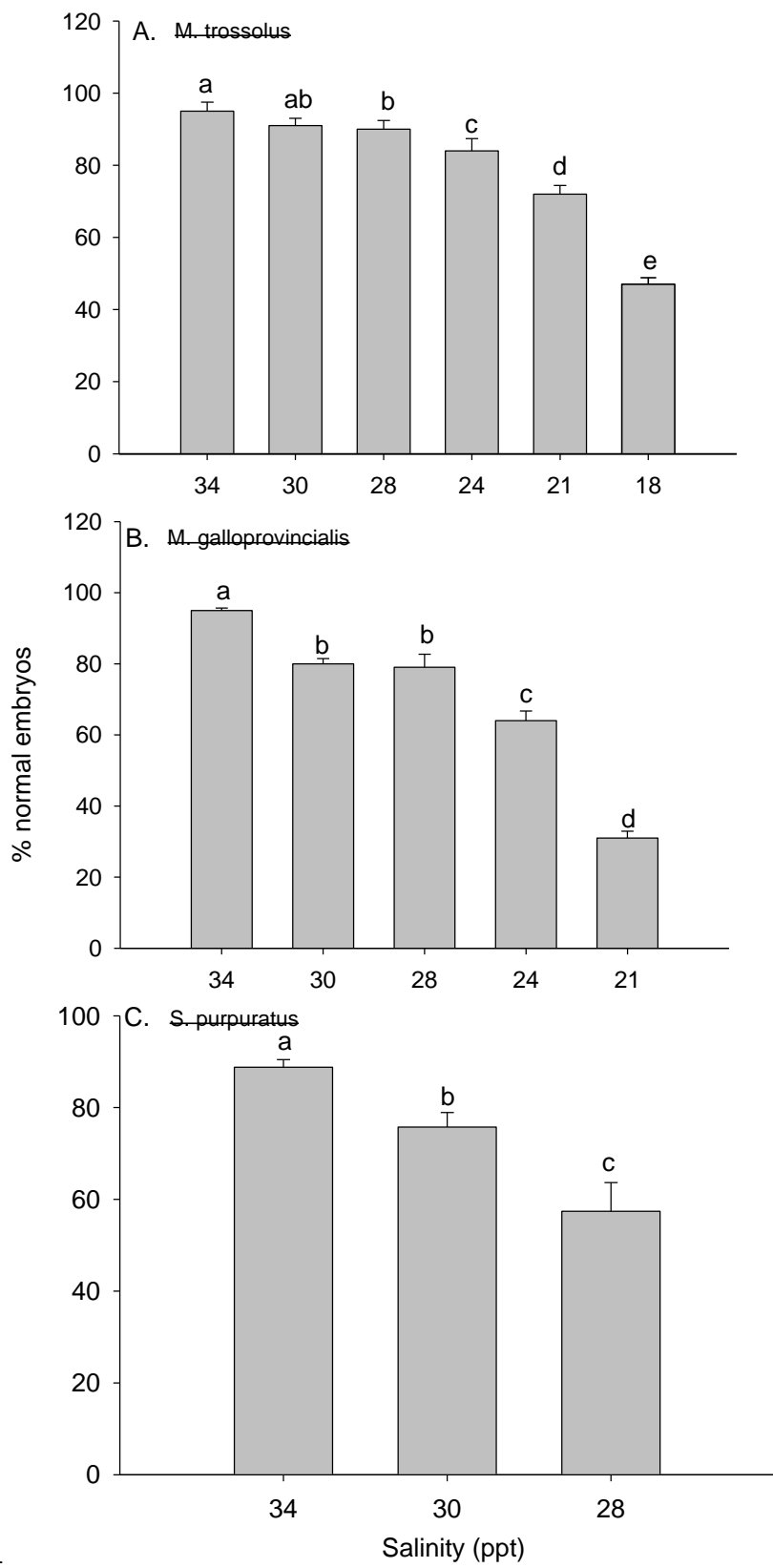relative to Zn exposures in C. *M. galloprovincialis* D. *S. purpuratus*
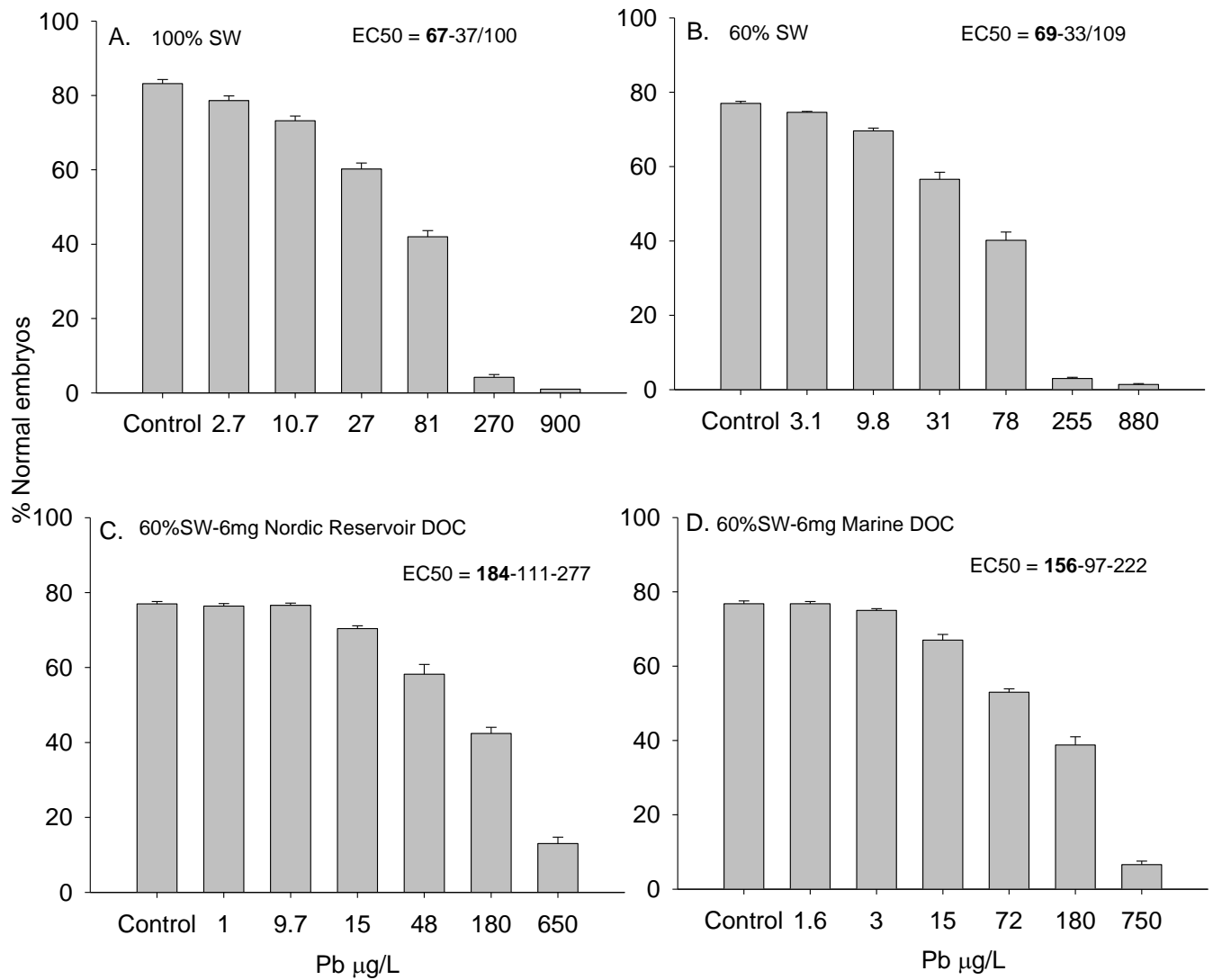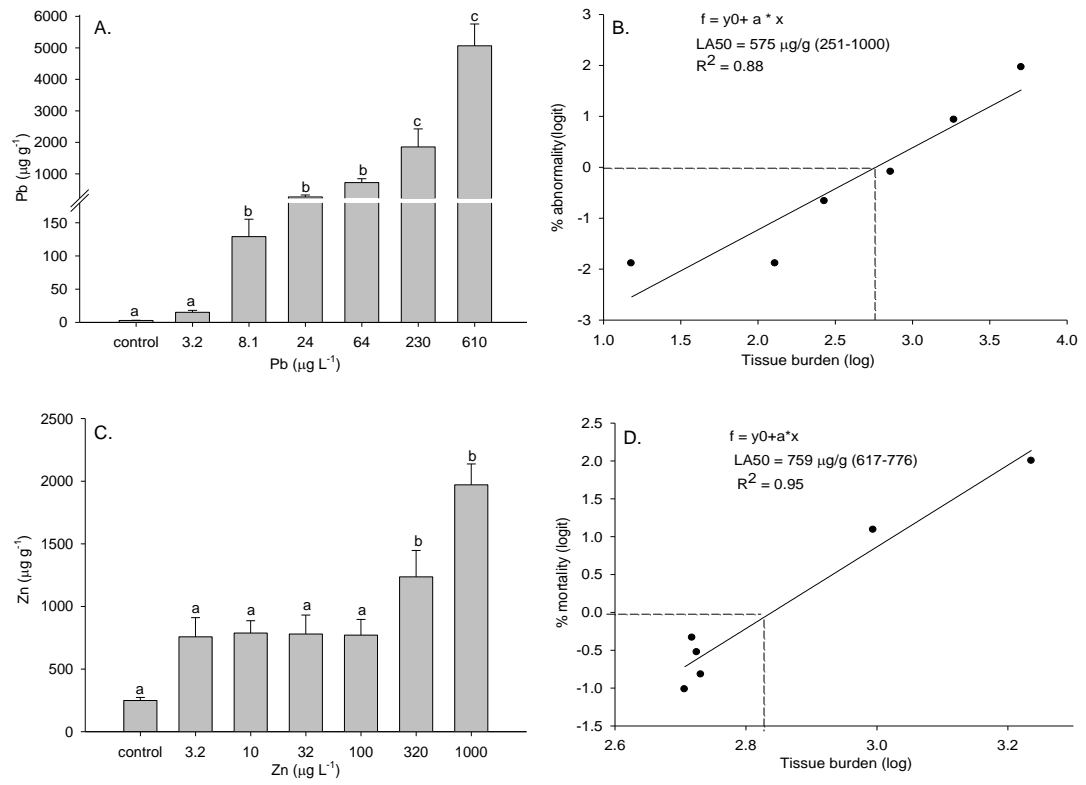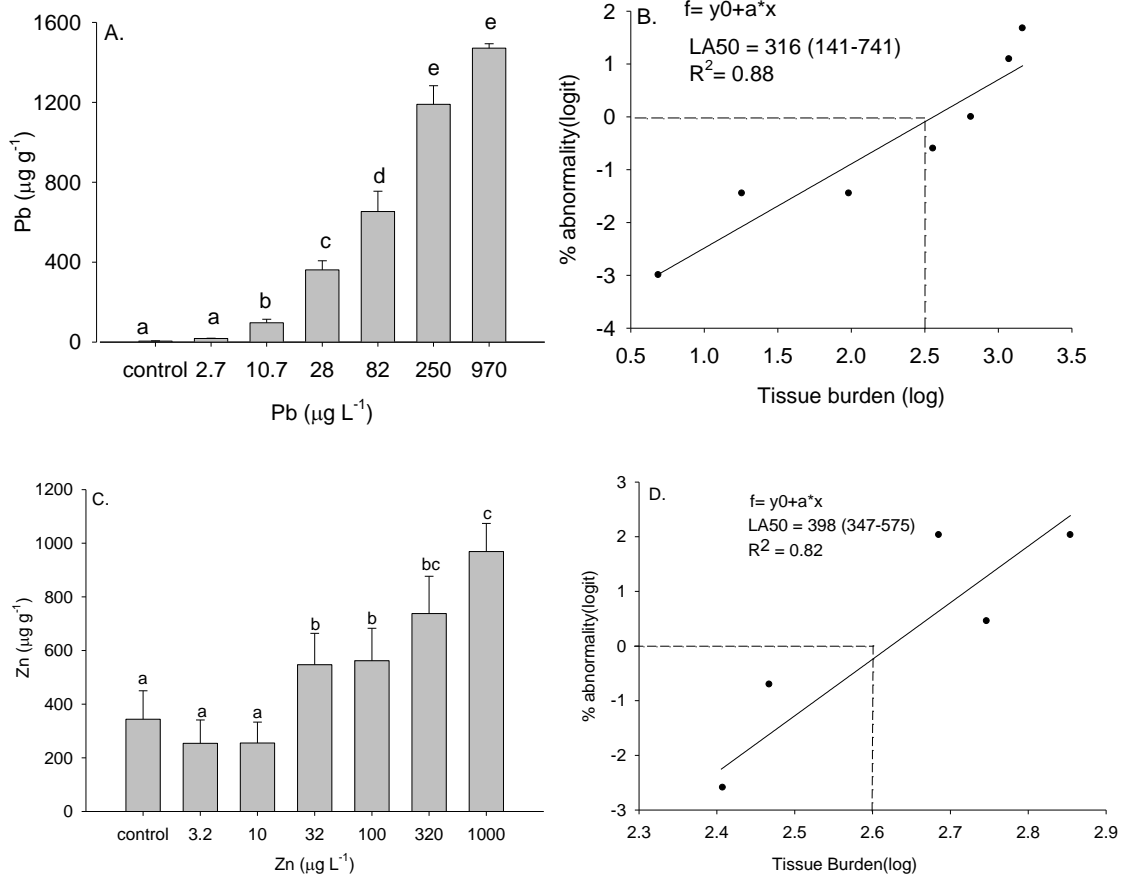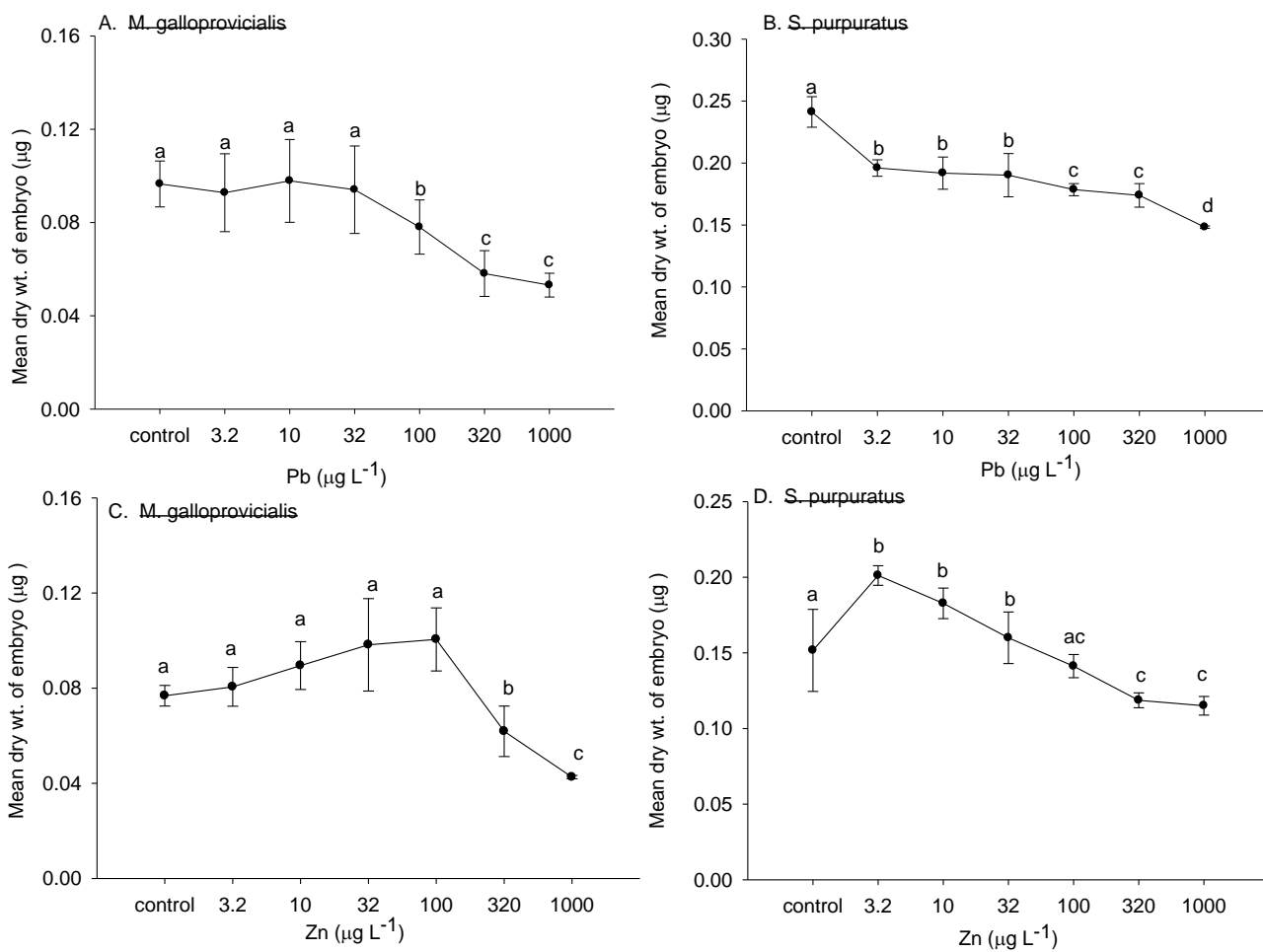
Fig. 1

183

Fig. 2

Fig. 3

Fig. 4

Fig. 5

187

Literature Cited:

Adams, W.J., Blust, R., Borgman, U., Brix, K.V., DeForest, D.K., Green, A.S., Meyer, J.S., McGeer, J.C., Paquin, P.R., Rainbow, P.S. and Wood, C.M. 2011

Utility of tissue residues for predicting effects of metals on aquatic organisms Integr. Env. Assess. 7, 75-98.

ASTM. 2004. Standard Guide for conducting static acute toxicity tests starting with embryos of four species of saltwater bivalve molluscs. E 724 -98.

ASTM. 2004. Standard Guide for conducting static acute toxicity tests with embryos echinoid embryos. E 1563 -98.

De Schamphelaere K.A.C., Vasconcelos F.M., Tack F.M.G., Allen H.E., Janssen C.R. 2004. Effect of dissolved organic matter source on acute copper toxicity to *Daphnia magna*. Environ. Toxicol. Chem. 23,1248–1255.

Eisler, R. 1993. Zinc hazards to fish, wildlife and invertebrate: a synoptic review. Biological Report 10. Washington D.C.: US Department of Interior, Fish and Wildlife Service.

Fitzpatrick, J.L., Nadella, S., Bucking, C.P., Balshine, S., Wood, C.M. 2008. The relative sensitivity of sperm, eggs and embryos to copper in the blue mussel (*Mytilus trossulus*). Comp. Biochem. Physiol. C 147, 441-449.

Glover C.N., Playle R.C., and Wood C.M. 2005. Heterogeneity of natural organic matter amelioration of silver toxicity to *Daphnia magna*: Effect of source and equilibration time. Environ. Toxicol. Chem. 24, 2934–2940.

Gosselin L.A., Qian P.Y. 1997. Juvenile mortality in benthic marine invertebrates. Mar Ecol Prog Ser 146, 265-282

Hertwig, O., Hertwig, R.1887. Uber den Befruchtungs- und Teilungs-vorgang des tierischen Eies unter dem Einfluss ausserer Agentien. Jena. Zeitsch. N.F. 13,120–241 and 477–510.

His, E., Beiras, R., Seaman, M.N.L.1999. The assessment of marine pollution-bioassays with bivalve embryos and larvae. In: Southward, A.I., Tyler, P.A., Young, C.M. (Eds.), Advances in Marine Biology, vol. 37. Academic Press, London, pp. 1–178.

Jacobson, P.J., Neves, R.J., Cherry, D.S., Farris, J.L. 1997. Sensitivity of glochidial stages of freshwater mussels (Bivalvia: Unionidae) to copper. *Environ Toxicol Chem* 16, 2384–2392.

Kobayashi, N. 1984. Marine ecotoxicological testing with echinoderms. In: Persoone, G., Jaspers, E., Claus, C. (Eds.), Ecotoxicological Testing for the Marine Environment, vol. 1. State University Ghent, Bredene, p. 798.

Kramer J.R.;Benoit G., Bowles K.C., Di Toro D.M., Herrin R.T., Luther G.W. III, Manolopoulos H, Robillard K.A., Shafer M.M., Shaw J.R. 2002. Environmental chemistry of silver. In Andren AW, Bober TW, eds, *Silver in the Environment: Transport, Fate, and Effects.* SETAC, Pensacola, FL, USA.

Lu, Y. and Allen, H.E. 2002. Characterization of copper complexation with natural dissolved organic matter (DOM)—Link to acidic moieties of DOM and competition by Ca and Mg. Water Res. 36, 5083–5101.

McCarty, L.S. and Mackay, D. 1993. Enhancing ecotoxicological modeling and assessment. Environ. Sci. Tech. 27, 1719-1728.

McCarty, L.S., Landrum, P.F., Luoma, S.N., Meador, J.P., Merten, A.A., Shephard, B.K., Van Wezel, A.P. 2011. Advancing environmental toxicology through chemical dosimetry: External exposures versus tissue residues. Integr. Env. Assess. 7, 7-27.

Nadella, S.R., Fitzpatrick, J.L., Franklin, N., Bucking, C., Smith, S. and Wood, C.M. 2009. Toxicity of dissolved Cu, Zn, Ni and Cd to developing embryos of the blue mussel (*Mytilus trossolus*). Comp. Biochem. Physiol. C. 149:340-348.

Naimo, T.J. 1995. A review of the effects of heavy metals on freshwater mussels. Ecotoxicology 4,341–362.

Niyogi, S.,Wood, C.M. 2004. The BLM, a flexible tool for developing site-specific water quality guidelines for metals. Env. Sci. Technol. 38:6177-6192.

Novelli, A.A., Losso, C., Ghetti, P.F. and Ghirardini, A.M. 2003. Toxicity of heavy metals using sperm cell and embryo toxicity bioassays with *Paracentrotus lividus* (Echinodermata: Echinoidea): comparisons with exposure concentrations in the lagoon of Venice, Italy. Env. Toxicol. Chem. 22, 1295-1301.

Okubo, K., Okubo, T. 1962. Study on the bioassay method for the evaluation of water pollution. II. Use of the fertilized eggs of sea urchins and bivalves. Bull. Tokai Reg. Fish. Res. Lab. 32, 131–140.

Phillips, B.M., Nicely, P.A., Hunt, J.W., Anderson, B.S., Tjeerdema, R.S., Palmer, S.E., Palmer, F.H., Puckett, H.M. 2003. Toxicity of cadmium–copper–nickel–zinc mixtures to larval purple sea urchins. Bull. Environ. Contam. Toxicol. 70, 592–599.

Richards, J.G., Curtis, P.J., Burnison, B.K., Playle, R.C. 2001. Effects of natural organic matter source on reducing toxicity to rainbow trout (*Oncorhynchus mykiss*) and on metal binding to their gills. Environ. Toxicol. Chem. 20, 1159–1166.

Ringwood, A.H. 1992. Comparative sensitivity of gametes and early developmental stages of a seaurchin (*Echinometra mathaei*) and a bivalve species (*Isognomon californicum*) during metal exposure. Arch. Environ. Contam. Toxicol. 22, 288-295.

Rosen, G., Ignacio, RD, Chadwick, BD, Ryan, A., Santore, RC 2008. Critical tissue Cu residues for marine bivalve (*M. galloprovincialis*) and echinoderm (*S. purpuratus*) embryonic development.Mar. Environ. Res. 66, 327-336.

Sappington, K.G., Bridges, T.S., Bradbury, S.P., Erickson, R.J., Hendriks, A.J., Lanno, R.P., Meador, J.P., Mount, D.R., Salazar, M.H. and Spry, D.J. 2011. Application of the tissue residue approach in ecological risk assessment. Integr. Env. Assess. 7, 116-140.

Sikora, F.J., and Stevenson, F.J. 1988. Silver complexation by humic substances: Conditional stability constants and nature of the reactive sites. *Geoderma* 42, 353–368.

Tabata, K. 1956. Systematic studies on toxic components in industrial wastes with reference to the tolerance of aquatic lives. III. On acute toxic components in water-extract liquor from bark. Bull. Tokai Reg. Fish. Res. Lab. 42, 17–21.

Toyota, Y., Okabe, S., Kanamori, S., Kitano, Y., 1982 . The determination of Mn, Fe, Ni, Cu and Zn in seawater by atomic absorption spectrometry after coprecipitation with lanthanum hydroxide. J. Oceanograph. Soc. Jap. 38, 357-361.

US EPA, 2001. Streamlined water-effect ratio procedure for discharges of copper: US Environmental Protection Agency. Office of Water, Washington, DC. EPA 822-R-01-05.

US EPA (2006) Short-term methods for estimating the chronic toxicity of effluents and receiving waters to west coast marine and estuarine organisms (http://www.epa.gov/nerleerd/westmethman.htm

Weinstein, J.E. 2001. Characterization of the acute toxicity of photoactivated fluoranthene to glochidia of the freshwater mussel *Utterbackia imbecillis*. Environ Toxicol Chem 20,412–419.

Yeager, M.M., Cherry, D.S., Neves, R.J. 1994. Feeding and burrowing behavior of juvenile rainbow mussels, *Villosa iris* (Bivalvia: Unionidae). J North Am Benthol Soc 13,217–222.